MOLECULAR MECHANISM OF PROTHROMBIN ACTIVATION BY VON WILLEBRAND FACTOR-BINDING PROTEIN

By

Heather K. Kroh

Dissertation

Submitted to the Faculty of the

Graduate School of Vanderbilt University

in partial fulfillment of the requirements

for the degree of

DOCTOR OF PHILOSOPHY

in

Pathology

May, 2010

Nashville, Tennessee

Approved:

Richard L. Hoover, Ph.D.

Albert H. Beth, Ph.D.

David Gailani, M.D.

D. Borden Lacy, Ph.D.

Samuel A. Santoro, M.D., Ph.D.

Munirathinam Sundaramoorthy, Ph.D.

For my father

ACKNOWLEDGEMENTS

I would like to recognize several people whose support during my time at Vanderbilt was instrumental for my development as a scientist. Most significantly, I am obliged to my dissertation advisor Paul E. Bock, Ph.D., who first provided me with the opportunity to work on numerous projects and gain experience as a research assistant in his lab. Through his encouragement and example, I was able to develop my enthusiasm for scientific research and make the decision to attend graduate school to pursue a doctorate. I am also grateful to the members of my thesis committee, Richard Hoover, Ph.D., Samuel Santoro, M.D., Ph.D., David Gailani, M.D., Al Beth, Ph.D., D. Borden Lacy, Ph.D., and Munirathinam Sundaramoorthy, Ph.D., for the time they dedicated to my project, as well as for the critical comments and suggestions which allowed me to refine my experiments. Particular appreciation goes to Peter Panizzi, Ph.D., who was responsible for much of my early technical training, and Ingrid Verhamme, Ph.D., who was always willing to discuss problematic results and analyses. I would also like to thank other past and present members of the lab—including Sarah Stuart, Karen Wiles, Malabika Laha, and Jonathan Creamer, Ph.D.—for their absolute support and assistance.

Personal thanks must go to my parents, Clarence and Sharon Kroh, for always giving me their love—and the ability to make my own decisions, the best gifts of all. Most of all, I owe unending gratitude to my husband, Jamie Cufr, for promising to support completely my decision to go back to school, whenever I decided that the time was right. The promise was kept.

Finally, I am grateful for financial support for this project from the National Institutes of Health (NIH) through NIH Grant R37 HL071544 from the National Heart, Lung, and Blood Institute and Training Grant 2-T32 HL07751.

TABLE OF CONTENTS

LIST OF TABLES

LIST OF FIGURES

CHAPTER I

INTRODUCTION

Initiation and Regulation of Blood Coagulation

Maintenance of the integrity of the circulatory system is critical after vessel injury. Hemostasis is controlled by several components of the vascular system, including endothelial cells, platelets, and protein coagulation factors in the blood and on cell surfaces. Damage to the endothelial cell layer disrupts the primarily non-reactive vessel lining and uncovers the subendothelium. This triggers an early primary hemostatic response through localization of platelets with the exposed collagen through a tethered interaction of the platelet receptor GP Ibα with collagen-bound von Willebrand factor (1). Even in the high shear environment found in arteries and capillaries, adhesion of the cells into a platelet plug at the site of injury can occur and lead to cellular activation and aggregation, stimulating further recruitment and expansion of the platelet mass (Fig. 1). The activated platelets serve as foundation for what is called the secondary phase of hemostasis, activation of the fluid-phase protein factors responsible for formation of a stabilizing fibrin clot (2). The characteristic balance between procoagulant and anticoagulant events is normally sustained by an overlapping system of enzyme-cofactor reactions, commonly described as a “waterfall” or “cascade” (3-4). Highly coordinated amplification and feedback responses within this system result in precise temporal and spatial control of coagulation.

Activation of coagulation factors is conventionally segregated into two branches, termed the intrinsic and extrinsic pathways, but the line of demarcation only exists for the initial activation steps of each system, with ultimate convergence of the pathways at the level of factor IX/factor X activation (Fig. 2) (5). Initiation of the intrinsic (or contact)

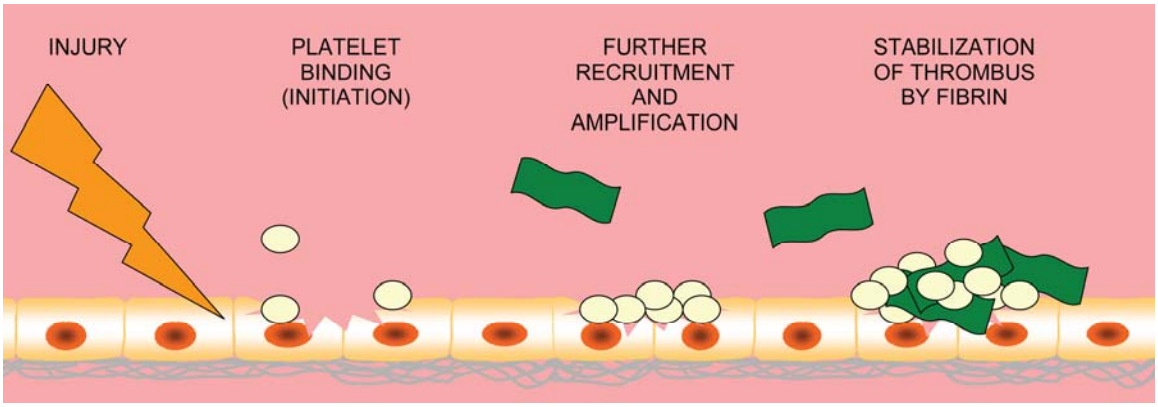

Figure 1. Ordered events in the formation of a blood clot. Initial injury to the endothelial cells exposes tissue factor and triggers binding of platelets (*yellow ovals*) to collagen in the subendothelium. Growth of the primary plug through platelet-platelet interactions helps propagate and amplify the extrinsic coagulation response, eventually resulting in fibrin deposition (*green*) to stabilize the final formed clot. (Adapted from (10))

system can occur upon negatively charged surfaces such as glass or collagen, and it involves activation of factor XII and binding of factor XI and prekallikrein to the surface by the cofactor high-molecular weight kininogen (HMWK). Factor XIIa subsequently cleaves factor XI to XIa, which activates factor IX, the enzyme responsible for production of factor Xa by the Xase complex on platelet membranes (6).

The fundamental contribution of the intrinsic system to normal induction of coagulation is considered to be minimal, compared to the involvement of the components of the extrinsic, or factor VIIa-tissue factor initiated, pathway. Factor VII is present in plasma in an inactive zymogen form, but it is thought to be converted to factor VIIa through cleavage of a single bond at Arg^{152} by a number of different proteases, including factor Xa (7). Even though 1-2% of factor VII exists in cleaved form in plasma (8), it does not elicit a coagulative response due to several factors. Activated factor VIIa has very little enzymatic activity in the absence of tissue factor, attributable to an incomplete structural shift to the enzyme conformation following proteolysis, and it only attains catalytic competence when bound to its tissue factor cofactor (9). Tissue factor

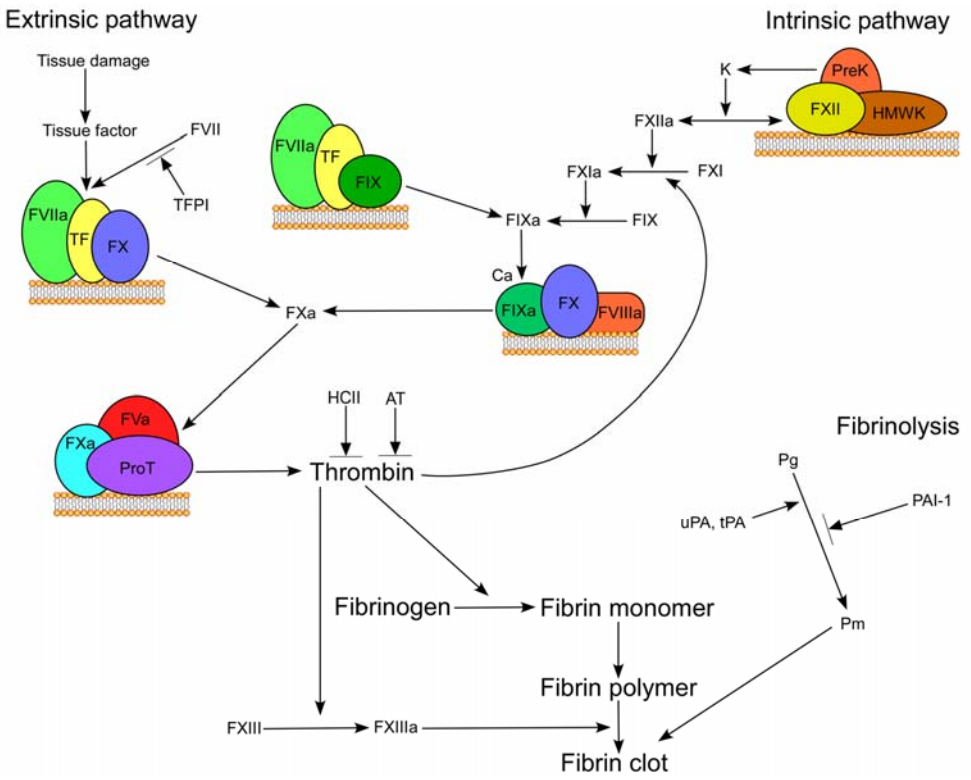

Figure 2. Schematic of extrinsic and intrinsic pathways of blood coagulation. After injury, tissue factor can complex with factor VII to initiate the extrinsic pathway to lead to thrombin production and fibrin formation. Factor XIIa in coordination with kallikrein and high-molecular weight kininogen mediate the procoagulant response through the intrinsic pathway.

itself is sequestered from the coagulation machinery in the vasculature, because it is only constitutively expressed in the cells within and surrounding the vessel walls, including vascular smooth muscle cells and fibroblasts (10). Factor VIIa and tissue factor can only form an active complex following damage to the blood vessel, restricting the extrinsic pathway response to just the required areas. Factor VIIa-tissue factor goes on to primarily activate factor X, which coordinates with factor VIIa-tissue factor to hydrolyze the necessary cleavage sites on factor IX. The two products of this “extrinsic” Xase complex, factor Xa and factor IXa, play subsequent roles in acceleration of factor Xa production through “intrinsic” factor Xase (factor IXa-factor VIIIa complex) and thrombin production by the prothrombinase complex (11).

Although small amounts of thrombin are produced during the initiation phase of coagulation, when only low concentrations of factor Xa and IXa are being produced (12), the majority of thrombin is generated in the propagation phase of coagulation once a sustainable cycle of factor Xa production is established. The inactive precursor of thrombin, prothrombin, associates with a large macromolecular complex called the prothrombinase complex, which contains factor Xa and its cofactor Va on the phospholipid surface of activated platelets. All three proteins involved in thrombin production by prothrombinase have specific domains which govern binding to the phospholipid surface of the platelet, regulating localization of the proteins to optimize complex activity. The enzyme factor Xa is responsible for cleaving two intramolecular bonds in prothrombin, after Arg^{320} and Arg^{271}, which results in formation and release of active thrombin. Factor V exists as a large single-chain glycoprotein that gains its cofactor function upon cleavage of three peptide bonds by enzymes such as thrombin and factor Xa (13). In contrast to the single-domain thrombin molecule, the zymogen prothrombin also contains two smaller domains which are lost upon physiological activation. Once thrombin is produced and liberated from the complex, it can bind its primary physiological substrate, the glycoprotein fibrinogen, and sequentially cleave off fibrinopeptides A and B. The resultant fibrin monomers associate and are cross-linked by the transglutaminase factor XIIIa into a covalent fibrin meshwork that stabilizes the forming clot (14).

The positive feedback reactions involved in the amplification of the coagulation response could easily become uncontrollable, if not for an equally efficient subset of plasma proteins responsible for diminishing or changing the activity of the procoagulant enzymes. An early regulator of coagulation is tissue factor pathway inhibitor (TFPI), which is found in the plasma and directly inhibits the factor VIIa-factor Xa complex, effectively stopping the extrinsic response (15). The serine proteinase inhibitor (serpin)

antithrombin is most important for directly inhibiting thrombin, and with assistance from glycosaminoglycans such as heparin or heparan sulfate, it forms an irreversible covalent complex with the protease (16-17). Heparin cofactor II, a homologous member of the serpin family, also specifically inhibits thrombin in a glycosaminoglycan-dependent manner (18). Other proteases have specific anticoagulant functions of their own, such as activated protein C (APC), which degrades the procoagulant cofactors Va and VIIIa to target thrombin generation (19). In addition to its anticoagulant activity, APC also exhibits anti-inflammatory and other cytoprotective effects through the endothelial protein C receptor (20). Further pathways for altering procoagulant activity rely on proteins that modulate thrombin specificity. One of the better characterized examples is the binding of thrombomodulin, a endothelial cell surface protein, to thrombin, which shifts the protease specificity of thrombin from procoagulant cleavage of fibrinogen to anticoagulant activation of protein C (21).

To enable healing of the vessel injury, the fibrinolytic system in blood is responsible for the dissolution of existing clots. The primary component of this system is the protease plasmin, which directly cleaves polymerized, insoluble fibrin into soluble degradation products that are easily cleared. Control of fibrinolysis, like coagulation, is achieved through proteolytic feedback and amplification reactions, with plasmin being activated from plasminogen by two physiological serine proteinases, tissue-type plasminogen activator and urokinase-type plasminogen activator. Fibrin itself serves as a cofactor for the generation of plasmin, because localization of both plasminogen and the activators to the fibrin clot must occur to initiate efficient plasmin production. Furthermore, fibrinolytic events can be suppressed through direct inhibition of plasmin activity, mediated by α_2-antiplasmin, or inhibition of the activators themselves by a serpin, plasminogen activator inhibitor-1 (22). Together, fibrinolysis and coagulation provide a web of extremely complex, but well-coordinated, protein- and cell-mediated

reactions which maintain the integrity of the circulatory system, despite its inherent vulnerability to damage and disease.

Serine Proteinases and Prothrombin Activation

All of the proteinases included in the procoagulant, anticoagulant, and fibrinolytic pathways are classified as members of the serine proteinase family of enzymes. The definitive characteristic of this family is the presence of a serine residue that functions as the catalytic nucleophile in the active site cleft of the enzyme. In coordination with two other residues, a conserved histidine and typically an aspartic acid, the serine serves as the functional center of the "catalytic triad" of the active site. While the serine proteinases play roles in a large number of physiological processes, from digestion to cell differentiation, they can be broadly categorized into groups which share similar protein folds, primarily the chymotrypsin-like enzymes and the subtilisin-type enzymes (23). The blood clotting enzymes have chymotrypsin-like conformations represented by two domains each containing a six-stranded, anti-parallel β-barrel, with the catalytic triad situated in the same orientation at the interface of the two domains.

Hydrolysis of proteinase substrates occurs through an ordered cycle of reactions controlled in large part by the nucleophilicity of Ser^{195} (chymotrypsinogen numbering). This residue attacks the carbonyl atom of the substrate amide bond to produce a covalent tetrahedral intermediate, with the imidazole group of His^{57} (stabilized by Asp^{102}) assisting in the reaction. Hydrogen bonding from the backbone amide atoms of Ser^{195} and Gly^{193} (the oxyanion hole) further stabilizes the intermediate. The amino portion of the substrate is released after receiving a proton from His^{57}, leaving an acyl-enzyme derivative, which is subsequently hydrolyzed through a second tetrahedral intermediate into the final product and the restored enzyme (24). Proper orientation of all of the residues involved in this mechanism relies on initial proteolytic activation of the zymogen

precursor of the enzyme, specifically formation of a new NH_2-terminus through cleavage of the Arg^{15}-Ile^{16} bond. The Ile^{16} α-ammonium group forms a salt bridge with the carboxylate side chain of Asp^{194} and hydrogen bonds to other residues of the activation domain of the enzyme, the portion containing the active site and substrate binding regions. This interaction induces the conformational changes needed to fully activate the proteinase and form the substrate specificity pocket (Fig. 3) (25). Induction of this structural transition by just peptides mimicking the NH_2-terminus (Ile-Val, Val-Val) has been measured for bovine trypsinogen covalently modified with *p*-guanidinobenzoate (26-27), verifying the importance of the NH_2-terminal dipeptide in the overall mechanism of serine proteinase activation.

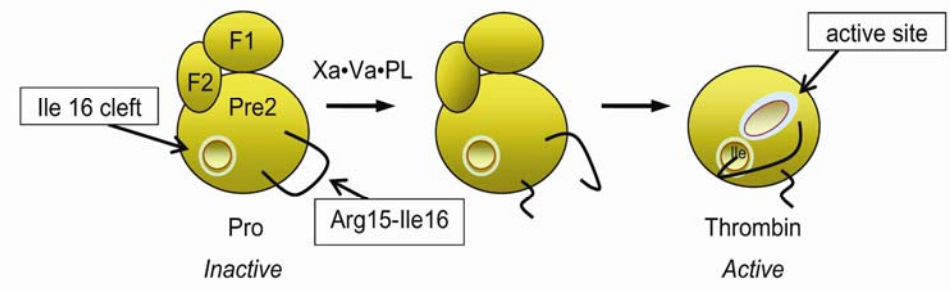

Figure 3. Formation of the active site of a proteinase. As a typical serine proteinase, thrombin is produced by cleavage of the Arg^{15}-Ile^{16} bond in prothrombin and insertion of the new NH_2-terminus into the NH_2-terminal binding cleft. The subsequent conformational changes within the activation domain generate the active site and a functional oxyanion hole.

The overall activity and efficiency of a proteinase is impacted by different physical attributes of the proteinase itself, not the least of which is the degree to which the substrate can access the active site. In the serine proteinase family, zymogens and their corresponding enzymes share almost all of their overall structure, with only a small region undergoing most of the conformational change required for proper substrate selectivity and proteolytic activity. Crystallographic comparisons of trypsinogen and

trypsin have detailed a disordered substrate-binding cleft in the zymogen that becomes defined after formation of the new NH_2-terminus (25, 28). Functional analysis of trypsinogen and chymotrypsinogen with active-site titrants also demonstrated much slower acylation rates, but similar deacylation rates, for the zymogens compared to the enzymes, consistent with rearrangement of the substrate-binding site being a primary step in activation, not significant shifts in the catalytic triad (29-30).

Additional residues within the proteinase also determine the specificity of substrate recognition and cleavage, including those which contact the substrate and residues which act at a distance through influencing the overall structure of the core of the protein. The concept of multiple individual subsite interactions which govern substrate recognition was first specified for the cysteine proteinase papain, with correlation between the amino acids on either side of the scissile bond for both the substrate and enzyme (31). The residues of the substrate are referred to as P4-P3-P2-P1-P1'-P2' (scissile bond at P1-P1'), with the corresponding enzyme subsites named as S4-S3-S2-S1-S1'-S2'. The primary specificity of the enzyme is determined by the interactions at the S1/P1 subsite, especially in members of the chymotrypsin-like serine proteinases, which exhibit a fairly restricted preference for substrates with particular amino acids at the P1 position (23). Specificity for certain residues at the P1 subsite allows classification of the serine proteinases into groups displaying trypsin, chymotrypsin, or elastase-like preferences, with the coagulation and fibrinolysis proteinases exhibiting the P1-Arg or Lys selection of trypsin. Trypsin-like proteinases also contain a deeply-pocketed substrate binding cleft with the Asp^{189} residue at the bottom, a characteristic that helps select for the basic residues at P1 and is not found in chymotrypsin (32). A large proportion of the residues responsible for specific active site recognition of substrates, as well as other critical functions such as stabilization of the catalytic domain or Asp^{102} of the catalytic triad, have been localized to the COOH-

terminal sequence (~50 amino acids) of many model serine proteinases, including trypsin and thrombin (33).

As one of the better characterized members of the chymotrypsin-like serine proteinases, thrombin shares many features with the prototypical proteinases, but it also displays a number of unique attributes which not only shape substrate specificity but ultimately alter the function of thrombin. Prothrombin, the zymogen precursor of thrombin, contains a primary catalytic domain and two smaller covalently attached domains called fragment 1 and fragment 2. Fragment 1 includes the NH_2-terminal portion of the sequence (to residue 155) and mediates binding of prothrombin to platelet membranes for processing by the prothrombinase complex. Proper folding and function of fragment 1 is regulated by the presence of ten γ-carboxyglutamic acid residues which bind Ca^{2+} and form the Gla domain, allowing both association with acidic phospholipids in the platelet membrane (primarily phospatidylserine) and stabilization of the domain structure. The fragment 2 domain extends to residue 271, sharing a very similar global kringle-like structure with fragment 1 including conserved disulfide bonds, but without the ability to bind calcium ions. After proteolytic cleavage at Arg^{320}, the catalytic domain of (pro)thrombin is composed of two disulfide linked peptide chains referred to as the A-chain and B-chain. The B-chain is homologous to the structure of trypsin, but neither trypsin nor elastase contains a portion equivalent to the thrombin A-chain (34). The catalytic triad of Ser^{195}, His^{57}, and Asp^{102} is found between the β-barrel structures of the B-chain, but the active site cleft is comparatively narrow and deep, due to several additional insertion loops not found in trypsin. These loops border the substrate-binding site and effectively narrow the substrate specificity of thrombin by blocking access to the catalytic machinery of the enzyme (35). Accessory contact sites are also present on parts of the thrombin molecule distant from the active site, in particular two electropositive regions on nearly opposite sides of thrombin called anion-binding

exosites I and II. These sites function as focal points for the allosteric regulation of thrombin activity and binding of numerous substrates, regulatory macromolecules, and inhibitors, affecting not only the immediate structure, but also the general substrate specificity of thrombin (36-37). Further allosteric control is exerted through the binding of a single sodium ion (Na^+), which directs the procoagulant/anticoagulant activities of thrombin through effects on both the exosites and the active site (38).

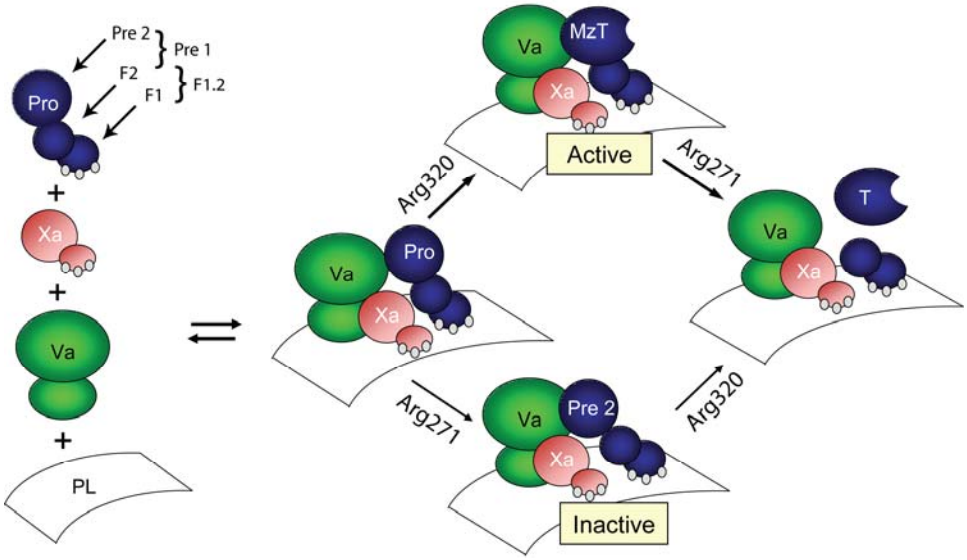

Figure 4. Schematic of alternative pathways for activation of prothrombin by the prothrombinase complex. Initial cleavage by factor Xa at Arg^{320} generates the active intermediate meizothrombin (MzT). Alternate cleavage at Arg^{271} produces inactive prethrombin 2 (Pre 2) and fragment 1.2.

The conventional pathway of activation of prothrombin to thrombin requires proteolysis of two essential bonds, Arg^{320}-Ile^{321} and Arg^{271}-Thr^{272}, by factor Xa in the prothrombinase complex, resulting in formation of the new Ile^{321} NH_2-terminus and release of the fragment 1 and 2 domains of the zymogen (Fig. 4). Detailed biochemical studies have been performed on the temporal and spatial requirements for proteolysis of prothrombin by the prothrombinase complex to determine the chronological order of

peptide bond cleavage. Early studies on bovine prothrombin had shown that in the absence of factor Va, the reaction order is through initial cleavage at Arg^{271}, creating a noncovalently bound fragment 1.2 species and the inactive catalytic domain, which is now called prethrombin 2 (39-41). Subsequent studies were confounded by the ability of thrombin to cleave additional bonds in prothrombin at Arg^{155} and Arg^{284}, producing the secondary feedback intermediates prethrombin 1 (prothrombin without fragment 1) and prethrombin 2' (prethrombin 2 lacking the first 13 residues) (42). Use of a reversible thrombin inhibitor eventually allowed qualitative evaluation of only the factor Xa-generated products, revealing meizothrombin, the proteolytically active product of initial cleavage at Arg^{320}, as the principal intermediate in the sequential formation of thrombin from prothrombin (43). Differences were observed with reactions performed with prethrombin 1, however, which showed evidence of intermediates from both proteolytic pathways during activation with factor Xa alone (44). Later reports focused on the individual components of the human prothrombinase complex to help reveal which pathway intermediate, meizothrombin or prethrombin 2, was physiologically relevant. Kinetic analysis in the presence and absence of factor Va indicated that the cofactor altered the rate limiting step in the overall reaction to favor initial cleavage at Arg^{320} (45). Similarly, addition of saturating concentrations of phospholipid membrane vesicles increased the rate of cleavage at Arg^{320} approximately 60-fold, compared to the 5-fold change in rate seen at Arg^{271}, supporting meizothrombin as the more pertinent intermediate (46).

More recent investigations have attempted to build a comprehensive model of the overall activation mechanism for prothrombin, with two opposing views at the forefront. Development of different recombinant prothrombin mutants that have one or both of the factor Xa cleavage sites modified to a non-cleavable Gln residue has allowed examination of the kinetics of proteolysis and product inhibition at each individual site.

The first model supports a sequential mechanism initiated by cleavage at Arg^{320} by a single form of prothrombinase complex, driven by differences in accessibility of the two cleavage sites in the prothrombin substrate. Generation of meizothrombin changes the structure of the substrate, facilitating subsequent cleavage at Arg^{271} through a mechanism termed conformational "ratcheting" (47-49). The second perspective espouses the existence of two interconverting conformational forms of prothrombinase, each recognizing and cleaving one of the factor Xa bonds on prothrombin. Each catalytic cycle would generate one of the intermediates, forming a prothrombinase poised to catalyze the succeeding reaction (50-51). An alternate component to either of these models is "channeling", where production of intermediate cleaved forms of prothrombin from prothrombinase is not obligatory and a percentage of the substrate is completely converted to thrombin without release of intermediates (52). Whether one of these models is more appropriate to explain the events necessary for prothrombin activation *in vivo* remains to be answered.

Efficiency of substrate recognition by prothrombinase has been linked with additional protein-protein interactions on the enzyme complex, not simply binding of the substrate to the active site of factor Xa (53-54). Not only does free factor Xa express exosites on its surface, analogous to several other coagulation factors, but new exosites are also induced by binding of factor Va, which influences binding to both factor Va and prothrombin (37). Examination of meizothrombin and prethrombin 2 in the presence or absence of an active site inhibitor indicated prothrombinase exosite interactions would likely dictate the sequence of bond cleavage, in support of the ordered cleavage model described previously (55-56). Further experimental evidence supported a role for one or both of the fragment domains of prothrombin in mediating binding to factor Va through effects on the anion-binding (pro)exosite I of prothrombin (57-59). The significance of these exosite-mediated interactions in regulating not only the production of thrombin, but

also its function and specificity though multiple ligand binding, is now at the forefront of coagulation and serine proteinase research.

Pathogenic Bacteria and Blood-borne Infection

The finely tuned balance afforded by the opposing arms of the coagulation, anticoagulation, and fibrinolytic systems can be altered by numerous pathological processes, from genetic abnormalities leading to production of dysfunctional coagulation factors to acquired conditions such as bacterial infection. Many species of pathogenic bacteria can prompt the breakdown of hemostatic regulation though expression and secretion of multiple proteins which function as virulence factors. Gram-negative and gram-positive organisms can modulate both the intrinsic (contact) and extrinsic pathways of coagulation, through inherent cell wall components, cell wall-bound receptors which bind adhesion proteins, or secreted factors which modify the function of host cells or coagulation factors. Bacteria also express surface and secreted proteins which serve as defense against elements of the innate and acquired immune systems, amplifying their ability to invade, proliferate, and disseminate in the human host. Changing the balance between coagulation, fibrinolysis, and inflammation can trigger severe infections such as systemic sepsis or septic shock, but almost any organ can serve as the focal point for blood-borne infection, especially in highly vascularized areas such as the lungs or heart.

Pathogens can initiate the intrinsic pathway of coagulation both directly and indirectly, through either serving as a surface for assembly of contact factors or by secreting proteinases which activate or degrade the factors. Assembly of factor XII, factor XI, prekallikrein, and HMWK has been shown on the surfaces of the gram-negative bacteria *Escherichia coli* and *Salmonella typhimurium*, mediated by fibrous surface proteins (60). Activation of factor XIIa and kallikrein results in cleavage of

HMWK and release of the potent proinflammatory and hypotensive peptide bradykinin, which ultimately increases vascular permeability. Cysteine proteinases have been identified from several bacterial species, including *Streptococcus pyogenes* (speB) and *Staphylococcus aureus* (staphopain), which directly cleave plasma kininogens to release bradykinin (61-62). Bacterial cell wall components, such as endotoxin (gram-negative) or peptidoglycan-polysaccharide polymers (gram-positive), have also been linked with stimulation of the intrinsic pathway (63). The end result of contact activation is enhanced permeability and leakage of plasma from the vasculature, which may improve bacteria survival and dissemination.

Activation of the extrinsic pathway and the fibrinolytic system by pathogens can be promoted by both endogenous proteins and secreted factors from bacteria, as well. Expression of tissue factor on monocytes and endothelial cells has been detected in response to a number of bacterial species, possibly through induction of pro-inflammatory cytokines by bacterial cell wall products. The consequence of this atypical pattern of tissue factor activity is a strong procoagulant stimulus, which may be a fundamental step in the development of coagulant disorders (64). In contrast to generation of fibrin clots through the procoagulant pathway, the abnormal breakdown of fibrinogen is employed by bacteria as well. The central fibrinolytic zymogen plasminogen can be recruited to the bacteria through cell surface-localized glycolytic enzymes and receptors such as the *Streptococcus pyogenes* M-like protein PAM, which function to localize the zymogen with the non-proteolytic plasminogen activator, streptokinase (65). Secreted by several species of streptococci, streptokinase forms a conformationally activated streptokinase·plasminogen complex which can cleave other molecules of plasminogen to plasmin; a similar, although proteolytic, mechanism is employed by staphylokinase from *Staphylococcus aureus*. Invasive bacteria can use recruited plasmin on their surface to degrade fibrin barriers formed in the initial

procoagulant response, extracellular matrix, and components of the immune system, contributing to expansion of the infection (66).

Investigations on the gram-positive bacterium *Staphylococcus aureus* have established its substantial role as a human pathogen, influenced in large part by its broad colonization of nasal passages in many human populations. *S. aureus* instigates not only skin and wound infections, but also serious or chronic conditions such as infectious endocarditis and septic arthritis. Certain subsets of the population are at higher risk for staphylococcal infection, including intravenous drug users and patients with compromised immune systems, with infections often originating from surgical procedures or injuries to the skin surface which allow entry into the bloodstream. Recent years have brought increased risk of both community- and hospital-acquired infection, compounded by the development of significant antibiotic resistance in some strains of *S. aureus* (67). Methicillin resistance was first detected in the 1960's, and methicillin-resistant *S. aureus* (MRSA) is now a major concern in environments where people live in close proximity, such as communal homes or resident hospitals. Resistance can derive from high bacterial production of β-lactamases, enzymes which break down β-lactam antimicrobial agents such as penicillin and methicillin, but it is also dictated by bacterial expression of membrane-bound penicillin-binding proteins (PBPs) which govern recognition by the antibiotics (68). While the emergence of methicilin resistance has precipitated the use of stronger antibiotics such as vancomycin, often thought of as a last-resort treatment, this course of action has also advanced the development of vancomycin resistance, first found in *S. haemolyticus* and *S. epidermidis*, but eventually detected in several strains of *S. aureus*. Vancomycin functions through a different mechanism than methicillin (by inhibiting protein synthesis), but it suffers from low therapeutic efficacy due to low bactericidal activity against staphylococci and difficulty in achieving suitable concentrations in tissues during therapy (69). As conventional

antimicrobials such as methicillin and vancomycin lose value as therapeutics, other approaches for preventing and treating staphylococcal disease must be found.

S. aureus produces a very wide repertoire of secreted and cell-surface proteins which provide survival advantages in the host, not the least of which is conferring protection from the host immune system during an infection. The most basic example is the presence of a polysaccharide microcapsule in most strains, which functions in both biofilm formation and avoidance of phagocytosis by immune cells (67). Some high virulence strains of staphylococci can also directly survive phagocytosis by neutrophils through upregulation of whole arrays of protein factors which provide resistance to oxidative stress, regulate capsule synthesis, or function as virulence factors (70). The components of the complement system function in both innate and acquired immunity, through recruitment of molecules that target foreign cells for destruction. These processes may be bypassed by production of proteins that either inhibit complement, such as Efb (extracellular fibrinogen-binding protein) or Ehb (Efb homologous protein) (71), or functionally deplete it, like Spi (72). Likewise, staphylococcal protein A is a surface-anchored protein which binds immunoglobulin (specifically IgG) to cover the bacteria with atypically oriented IgG, preventing neutrophil recognition (73).

A common characteristic among staphylococcal surface-associated and secreted proteins is the ability to bind host proteins involved in adhesion or matrix formation, such as fibrinogen, fibronectin, and collagen. Proteomic analysis of extracellular protein production from two highly virulent methicillin-resistant *S. aureus* strains has identified variation in expression of a number of known virulence factors, including adhesins (74). These pathogenic bacterial extracellular proteins are divided into two major groups defined by their localization (Fig. 5). Proteins remaining associated to the surface of the bacteria, either through covalent binding to cell wall peptidoglycan, ionic interactions, or transmembrane domains, have been termed MSCRAMMs (microbial surface

components recognizing adhesive matrix molecules). Secreted exoproteins that do not associate with the bacterial surface, but are released into the surrounding medium, are called SERAMs (secretable expanded repertoire adhesive molecules) (75). These "exoproteins" can alter infectivity and disease progression through both initiating bacterial adherence to host matrix and interfering with immune recognition.

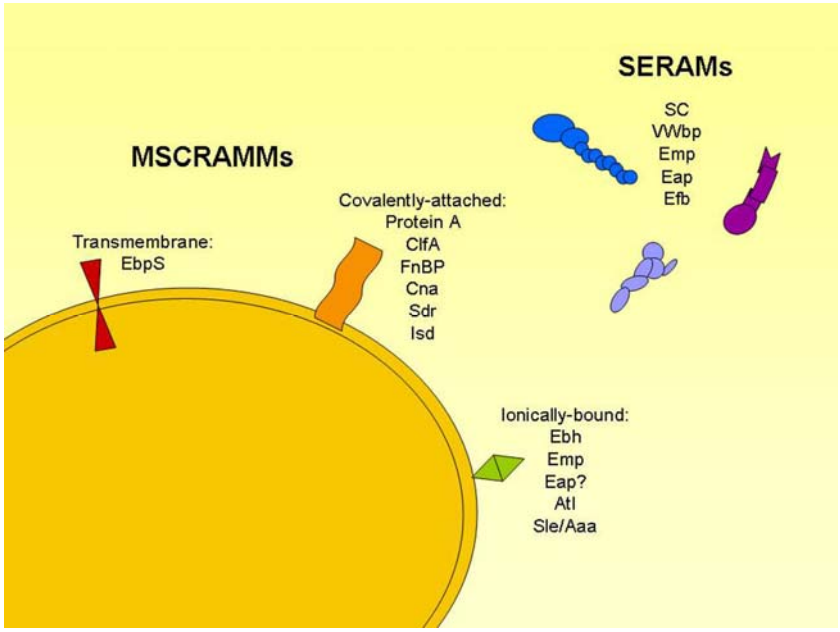

Figure 5. Different modes of localization and secretion of adhesive exoproteins by pathogenic bacteria. Cell surface-associated proteins (MSCRAMMs) can be transmembrane, covalently-attached through the action of sortases, or ionically-bound to other proteins or peptidoglycans on the cell itself. SERAMs have no cell-wall binding motif and are secreted into the surrounding medium, but some (such as Emp and Eap) can also bind back to the bacterial surface through secondary interactions.

Some of the most investigated exoproteins are those in the MSCRAMM family, in particular those that were initially identified as recognizing fibronectin. Most strains of *S. aureus* express two related products, FnBP-A and FnBP-B, which have been strongly linked with fibronectin-dependent host cell invasion. Binding of the adhesion molecule by FnBP on the bacterial surface assists in localizing the pathogen to host cells through

the cellular fibronectin integrin $\alpha_5\beta_1$, which instigates signaling pathways in the host cell that promote engulfment of the bacteria. This invasive phenotype can protect the pathogen from immune defenses and antibiotic treatments (76), and it can contribute to procoagulant responses by increasing tissue factor activity in the vasculature through recruitment of monocytes to the invaded endothelial cells (77). Additional regions in FnBP-A have also been found to bind to fibrinogen (78), illustrating the promiscuity that is often found in both the MSCRAMMs and SERAMs that may allow them to function in multiple environments and pathologies. In addition, not only can FnBP directly recognize both fibronectin and fibrinogen, but it has also been found to serve as a substrate for factor XIIIa, the transglutaminase responsible for cross-linking of fibrin. Factor XIIIa can form covalent bonds between FnBP and fibronectin/fibrin, potentially stabilizing attachment of bound bacteria to the matrix (79).

Other MSCRAMMs also have diverse prospective roles in the infectivity and eventual pathology of *S. aureus*. Clumping factor A (ClfA) is another cell-wall bound protein which shares a similar structural organization to FnBP. They both contain COOH-terminal LPXTG motifs for covalent attachment to the bacteria surface and an NH_2-terminal domain that mediates fibrinogen recognition (80). In contrast to FnBP, ClfA does not facilitate host cell invasion; it likely protects against neutrophil phagocytosis by coating the bacteria in fibrinogen, blocking antibody and complement attachment (81). ClfA is found in all clinical isolates of *S. aureus*, and it elicits physical clumping of the bacteria in plasma and may contribute to platelet aggregation through fibrinogen-bridging of the pathogen (and IgG) to the platelet integrin $\alpha_{IIb}\beta_3$ (82). Protein A, also covalently anchored to the bacterial surface, is generally associated with high-affinity binding of immunoglobulin that effectively reduces pathogen opsonization through blockage of the Fc region on IgG. It has additionally been shown to bind von Willebrand factor, which may also play a part in adhesion of staphylococci during infection (83).

The SERAM family of staphylococcal exoproteins has been less significantly characterized, which may be due to the uncertainty of assigning pathological functions to proteins which can act at sites remote from the centralized site of infection. The prevailing hypothesis is that the secreted proteins can, through interactions with extracellular matrix, establish colonization to certain tissues or organs. Unlike some of the MSCRAMMs, there is no pattern of structural homology among most of the SERAMs, although they all bind to adhesion proteins (84). One of the most ubiquitous secreted exoproteins is Efb (extracellular fibrinogen binding protein); it is found in all clinical isolates and shows constitutive expression, unlike other proteins which recognize fibrinogen (85). In an animal wound-infection model, inactivation of the Efb gene was found to decrease *S. aureus* virulence (86), supporting a potential role as a staphylococcal virulence factor. It was later found to interact with fibrinogen bound directly to platelets, as well as to an unidentified platelet surface receptor, causing inhibition of platelet aggregation through non-functional fibrinogen presentation (87). Furthermore, immune responses may be disturbed by the presence of Efb, due to the ability of the exoprotein to bind to complement component C3 and inhibit its activity (88). Another frequently-examined factor is Eap, or extracellular adherence protein, which displays uniquely widespread recognition of not only several adhesion proteins, including fibrinogen and fibronectin, but also prothrombin and the endothelial cell adhesion molecule ICAM-1 (84). Eap has been found to oligomerize and bind to bacterial surfaces, initiating cell aggregation (89), and like FnBP, its broad binding capacity could be a factor in internalization by host cells (90). Numerous *S. aureus* strains express slightly different variants of the Eap product, resulting from varied numbers of repeat sequences and early translation termination (91). This variability may be important in the overall function of Eap in infection and its potential ability to serve as a bridging molecule between cells and other secreted factors.

Staphylocoagulase and the Zymogen Activator and Adhesion Proteins (ZAAP's)

Secretion of the SERAM exoprotein staphylocoagulase (SC) is acknowledged as a defining clinical characteristic of *Staphylococcus aureus*, and has long been considered to have a function in the pathology of the bacteria. The potent instigation of blood coagulation by a substance secreted from staphylococci has been recognized for many decades, beginning with initial observations in the 1930's and 1940's. Identification and isolation of a coagulase from staphylococcal cultures that could interact with an "activator" present in plasma and produce fibrin formation was the first step in characterization of what would eventually become known as staphylocoagulase. Many studies aimed to establish the identity of the plasma component, the "coagulase-reacting factor" or CRF, putting forth hypotheses that included conversion of the coagulase itself to a thrombin-like agent (92). Differential precipitation procedures quickly eliminated both fibrinogen and albumin as direct agents (93), but another largely disputed target was the thrombin precursor, prothrombin, which became the focus of numerous investigations. Although kinetic similarities existed between physiological prothrombin activation and formation of the thrombin-like activator, comparison of the efficiency of several known inhibitors of thrombin activation, including heparin and calcium removal, seemed to indicate that prothrombin was not involved in the activity (94-95). Despite this finding, the isolation of prothrombin and CRF fractions from human plasma showed some functional overlap, suggesting that at least a portion (but not all) of the prothrombin molecule may be required for coagulase activity (96).

Improved purification of the free SC fraction from *S. aureus* provided better descriptions of the specificity of the procoagulant activity. Early tests had reported potent *in vivo* activity, which was confirmed by Duthie and Haughton in both human plasma and intravenous injection into rabbits (97). Along with a previous study by the same authors, this also gave one of the first indications of species specificity in SC, with

mice requiring ~30-fold higher doses to see similar effects (98). A rigorous comparison of human thrombin with “thrombin-coagulase” was carried out in 1967 to delineate the differences between the two species, including susceptibility to inhibition, clotting activity, and activity towards some physiological thrombin substrates. The coagulase species could not activate factor XIII, factor V, or factor VIII, nor could it aggregate platelets. The highly-efficient thrombin inhibitors antithrombin III, α_2-macroglobulin, and hirudin also had no effect on the coagulase activity, despite its similarities to thrombin in clotting of fibrinogen (99). The enhanced specificity of the coagulase complex even led to suggestions for its use as a hemostatic agent for bleeding conditions, due to a hypothetically lower risk of coagulation factor depletion (100).

Further advances in expression and purification started the first stringent biochemical characterization of the complex formed between SC and prothrombin. Several very important features were described, including optimal activity at an equimolar stoichiometry, a complex molecular weight corresponding to the sum of the individual protein molecular weights, and corresponding amino acid compositions and NH_2-terminal sequences. In addition, antibodies against the coagulase-prothrombin complex did not precipitate thrombin, just the assumed components, implying that proteolysis was not a factor in the activity (101). The first suggestion of a role for conformational changes in the catalytic domain of prothrombin came from kinetic studies in 1983, which showed high affinity binding of prothrombin and protection of human thrombin, but not factor Xa or bovine thrombin, from antithrombin inhibition (102). Competitive complex formation studies with different proteolytic fragments of prothrombin confirmed localization of SC binding to the thrombin domain, primarily to the COOH-terminal end of the thrombin B-chain. The specificity of this interaction was underscored by the inability of other structurally similar coagulation factors, including factor X, factor IX, and protein C, to inhibit complex formation (103). The concept of SC-

mediated structural changes specifically within the active site of prothrombin was furthered through the discovery of differences in the enzymatic activity of SC-thrombin and SC-prethrombin 1 with both fibrinogen and small tripeptide substrates compared to α-thrombin (104-105). The major structural requirements within SC itself that regulated prothrombin recognition and activation were also determined. Chymotryptic fragmentation of SC revealed the minimal functional portion necessary for prothrombin binding and procoagulant activity equivalent to the full-length protein, which corresponded to an NH_2-terminal fragment consisting of residues 1-324 of SC (106-107).

Correlation of the function of SC with its full primary structure was possible after nucleotide sequencing of three different strains of *S. aureus*, strains BB, 213, and 8325-4 (108-110). Surprisingly, the regions containing the NH_2-terminal prothrombin binding domain showed only ~50% conservation between the strains, with higher homology in the central region of SC (111). The strain-specific sequence differences in the NH_2-terminal section of SC may be the basis for antigenic diversity detected between SC proteins, in both early analyses and more recent surveys of staphylococcal genetics (112-114). The COOH-terminal halves also shared a very similar pattern of repeated units, composed of 27 residues each, with varying numbers of repeats between strains (108). These repeats were later described as specifically binding fibrinogen, with the overall degree of affinity governed by the number of repeats (115).

Concomitant with the *in vitro* behavior of SC becoming more defined, the *in vivo* role of coagulase in staphylococcal pathology was investigated in several different models of infection. Use of coagulase-negative strains or mutants in rat models of experimental endocarditis show no significant role for coagulase in affecting the course of the disease, despite a role hypothesized from its activity on fibrinogen (116-117). Moreover, no association has been seen between coagulase expression and development of *S. aureus*-induced septic arthritis (118). In contrast, coagulase-deficient

mutants of *S. aureus* demonstrated markedly reduced virulence in a mouse model of mastitis, especially when paired with loss of α-hemolysin, resulting in reduced necrosis in the mammary lesions (119). In addition, a clear connection has been observed in a murine model of hematogenous pulmonary infection, where the level of coagulase production correlated with increased proliferation of the bacteria and potential development of a protective fibrin membrane around the infecting bacteria colony (120). More recently, reduction of coagulase expression through targeting of the mRNA with short interfering RNA also reduced bacterial viability in the same pulmonary model of infection, suggesting a functional role for SC in this pathology (121). Like many of the secreted exoproteins, uncovering a clear role for SC in the infectivity of such a widely-pathogenic bacterium as *S. aureus* is problematic, and further investigation of SC as a virulence factor in other models of disease is warranted.

Previous biochemical observations on SC had indicated that prothrombin activation occurred in the absence of proteolysis (101), suggesting an uncommon pathway that had only been hypothesized in studies on activation of trypsin and one other secreted bacterial product, the streptococcal protein streptokinase (25). A peptide corresponding to the NH_2-terminal residues of trypsin was found to generate a zymogen-enzyme conformational transition in bovine trypsinogen, in the absence of actual proteolysis of the activation bond, leading to proposal of a mechanism called “molecular sexuality” (26). In this, activation could be mediated by insertion of the NH_2-terminus of a secondary protein into the Ile-16 binding pocket of the target serine proteinase zymogen. The result would be a conformationally, but reversibly, activated zymogen that could display at least some of the enzymatic specificity of the proteolytically activated enzyme. This process has been examined indirectly for streptokinase-induced activation of plasminogen, even though the overall mechanism includes proteolysis of a secondary “substrate” molecule of plasminogen which has made detection of the initial

conformational steps difficult (122). The first confirmation of a strict requirement for the first NH_2-terminal residues in the activity of streptokinase was found through deletion of the first isoleucine residue, which prevents functional expression of the active site on the plasminogen complex (123-124). Later kinetic studies have explored the contribution to affinity from the first 10 residues of streptokinase, concluding a role for both NH_2-terminal insertion and high affinity interactions with the remainder of the streptokinase molecule (125).

The most recent investigations have more fully described the mechanism of prothrombin activation by SC through a combination of biochemical and structural analyses, including X-ray crystallography, enzyme kinetics, and equilibrium binding. Crystal structures of α-thrombin·Met-SC(1-325) and prethrombin 2·SC(1-325), each with a thrombin-specific tripeptide chloromethyl ketone inhibitor in the active site, were solved to 2.2 Å resolution. Prethrombin 2, which contains only the inactive catalytic domain of the prothrombin molecule, showed rearrangement of the normally disordered activation domain into a conformation similar to thrombin, reflecting the conformational changes that occur in the presence of both SC and the active site inhibitor. Most significantly, the Ile^1 SC NH_2-terminus was fully defined in the structure, where it created the salt bridge with Asp^{194} characteristic of classical serine proteinase activation. Additional binding interactions were also identified in the complex structures, in particular the association of SC with both the 148-loop and the anion binding exosite I of (pre)thrombin. The structural results were verified with kinetic analysis, which showed loss of >98% of the SC activity upon deletion of the first two NH_2-terminal residues (Ile-Val) and a requirement for the 1-146 portion of SC to give full conformational activation of prothrombin. In contrast, SC(147-234) was associated with high affinity binding of prothrombin. Equilibrium binding experiments with an exosite I-specific fluorescence probe (fluorescein-labeled hirudin(54-65)) also confirmed the ability of SC to bind to

exosite I through competition with the hirudin probe. This report provided the first structural evidence of the molecular sexuality mechanism, strengthening the concept of non-proteolytic zymogen activation by an exogenous bacterial activator (126).

Subsequent investigations have delineated further aspects of SC-induced prothrombin activation, including the complementary roles of the different regions of the NH_2-terminal half of SC (the D1-D2 domains) in contributing to prothrombin binding and activation (127). In addition, the behavior of the prothrombin·SC complex with both small tripeptide chromogenic substrates and fibrinogen has been compared to thrombin. The prothrombin·SC complex exhibits increased affinity for fibrinogen, and the NH_2-terminal domains seem to form a unique fibrinogen-recognition exosite in the complex, all of which may be important factors in the *in vivo* specificity of the complex (128). Finally, a structural basis for the species specificity of SC has also been defined with bovine prothrombin, where SC derived from a human pathogenic strain of *S. aureus* is not able to completely insert its NH_2-terminal peptide, resulting in incomplete formation of the active site and poor enzymatic activity (129).

The crystal structures of SC in complex with thrombin and prethrombin 2 revealed a unique structural fold that has led to its classification with a number of structurally homologous bacterial proteins into a new functional family called the zymogen activator and adhesion proteins, or ZAAPs (Fig. 6). SC(1-325), the prothrombin-binding NH_2-terminal half of SC, contains two distinct rod-like domains (D1 and D2) angled in relation to each other, that each consist of three α-helices; D2 also contains three additional smaller α-helices clustered near the distal end of the domain. The SC helices make contact with portions of (pre)thrombin critical for substrate and cofactor recognition, including the majority of the 148 loop (which shifts

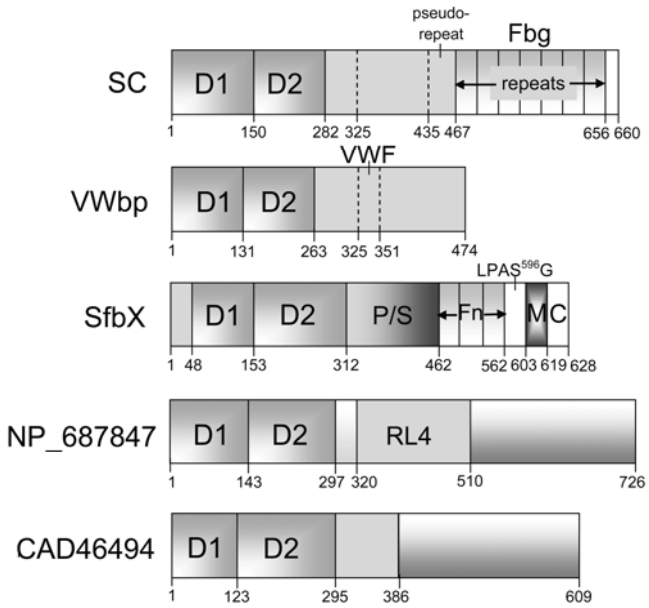

Figure 6. Schematic domain organization of ZAAP family members. All contain homologous D1-D2 domains in the NH_2-terminus, and putative adhesion binding regions in the COOH-terminal half.

between two SC helices) and Tyr^{76} in exosite I, which is surrounded by a hydrophobic cavity between helices (126). The predominantly helical nature of SC is completely different from that of streptokinase, which is a three-domain β-sheet structure. SC has a predicted domain organization composed of the two NH_2-terminal helical domains, a central region that is most likely structurally unorganized, and the COOH-terminal region containing seven 27-amino acid repeats (and one pseudorepeat sequence) that also governs fibrinogen binding. With this pattern as a guide, one secreted factor, von Willebrand factor-binding protein (which will be discussed in the following section), and three additional bacterial products from two species of streptococcus are predicted to exhibit similar NH_2-terminal zymogen-associated activity and COOH-terminal adhesion protein recognition. *Streptococcus pyogenes* expresses a cell-wall bound protein called SfbX, which is expected to have two D1-D2 domains in its NH_2-terminus and a distal fibronectin-binding region. Unpublished preliminary studies suggest that SfbX is also

able to interact with both prothrombin and thrombin. Two uncharacterized proteins from *Streptococcus agalactiae*, NP_687847 and CAD46494, are predicted to have D1-D2 structure, but the potential COOH-terminal binding partners have not yet been identified for either protein (130). The occurrence of this domain organization within exoproteins from several different species of pathogenic bacteria suggests a possible advantage for expression of these multi-functional proteins.

Von Willebrand Factor-Binding Protein – Early Discovery and Characterization

As the only other *S. aureus* ZAAP to be identified so far, von Willebrand factor-binding protein (VWbp) was originally isolated and characterized in 2002 through a putative COOH-terminal interaction with the multimeric adhesion protein von Willebrand factor (VWF) (131). The basis of this original study by a group from Sweden was to identify new exoproteins from *S. aureus* which could directly bind VWF, building on recent research that revealed staphylococcal protein A as a specific cell-surface receptor for this adhesion protein (83). Fragmented genomic DNA from *S. aureus* strain Newman was ligated into a phagemid vector and transformed into *E. coli* to produce a "shotgun" phage-display library of approximately 10^7 clones, each displaying a portion of *S. aureus* gene product on the surface of the cell (132). Selection of phagemids which expressed proteins that could recognize VWF was performed through incubation of the library in microtiter wells coated in VWF, removal of unbound material, and elution of positive phages. Enriched phage stocks were produced and used for subsequent panning sessions to isolate phages with high specificity for the adhesion protein. After sequencing, 26 clones were found to contain portions of the same gene (designated *vwb* for von Willebrand factor binding), which was subsequently cloned from the parental *S. aureus* strain DNA. Sequence alignments identified a specific 26-residue portion within the COOH-terminal half of the protein responsible for binding of VWF (131).

The resulting recombinant protein was named VWbp and expressed in two different forms, a full-length product encoding residues 1-482 and a truncation including only 124-392, for functional characterization. Polyclonal antibodies against the truncation were produced and used to detect native VWbp in western blots of *S. aureus* culture supernatant; the protein was also purified from the cultures on immobilized antibodies. A single band of ~66 kDa was detected, and the identity and specificity of the interaction with VWF was validated through treatment of the blots with VWF and VWF-specific antibodies. Binding of VWF was further examined in specific phagemid panning against a number of other adhesion proteins, including fibronectin, fibrinogen, and vitronectin, giving the highest number of phagemids against VWF. Lastly, the authors also demonstrated that VWF could be purified from human serum over a column containing immobilized recombinant VWbp (131).

Soon after publication of the initial report on VWbp, the predicted structural homology and low sequence identity of VWbp with SC (Fig. 7 and 8), and its potential as a prothrombin activator, was revealed in the SC crystallography study (126). With this as a starting point, the Swedish researchers subsequently described VWbp as a functional coagulase. Efficient clotting of human and porcine plasma was demonstrated, with varying degrees of efficiency with plasma from other species. This species-specific procoagulant activity was most evident with bovine plasma, which took 6 hours to clot, and mouse, rabbit, and rat plasmas which did not clot at all within 18 hours. Fibrinogen-plasma plate coagulation assays denoted species-specificity as well, with human plasma plates showing the most evident formation of fibrin. Use of truncated VWbp constructs in the basic coagulation assays isolated the coagulase function to the NH_2-terminal portion of the protein, in agreement with the proposed domain structure from the SC study. Furthermore, the importance of prothrombin in the procoagulant activity of VWbp

```
SC_1-283        IVTKDYSKESRVNENSKYGTLISDWYLKGRLTSLESQFINALGILETYHYGEKEYKDAKD
VWbp_1-263      VVSGEKNPYVSKALELKDKSNKSNSYEN-YRDSLES-LISSLSFADYEKYEEPEYEKAVK

SC_1-283        KLMTRILGEDQYLLERKKVQYEEYKKLYKKYKEENPTSKVKMKTFDQYTIEDLTMREYNE
VWbp_1-263      KYQQKFMAEDDALKN---------------FLNEEKKIKNADISRKSNNLLGLTHERYSY

SC_1-283        LTESLKSAVKDFEKDVEIIENQHHDLKPFTDEMEEKATARVDDLANKAYSVYFAFVRDTQ
VWbp_1-263      IFDTLKKNKQEFLKDIEEIQLKNSDLKDFNNTEQHNADVEINNLENKVLMVGYTFYN--T

SC_1-283        HKTEALELKAKVDLVLGDEDKP---HRISNERIEKEMIKDLESIIEDFFIETGLNKPDNI
VWbp_1-263      NKDEVEELYSELDLIVGEVQDKSDKKRAVNQRMLNRKKEDLEFIIDKFFKKIQQERPESI

SC_1-283        TSYDSSKHHYKNHSEGFEALVKETREAVTNANDSWKTKTVKKYGET
VWbp_1-263      PALTSE----KNHNQTMALKLKADTEAAKNDVSKRSKRSLNTQNNK
```

Figure 7. Sequence alignment of the amino acids of the D1-D2 domains of SC and VWbp. VWbp (*S. aureus* strain Mu50) shares 26% sequence identity (*green*) and an additional 25% sequence conservation (*yellow*) with SC (*S. aureus* strain Tager 104). The COOH-terminal sequences show almost no homology. (Alignment constructed with CLUSTALW.)

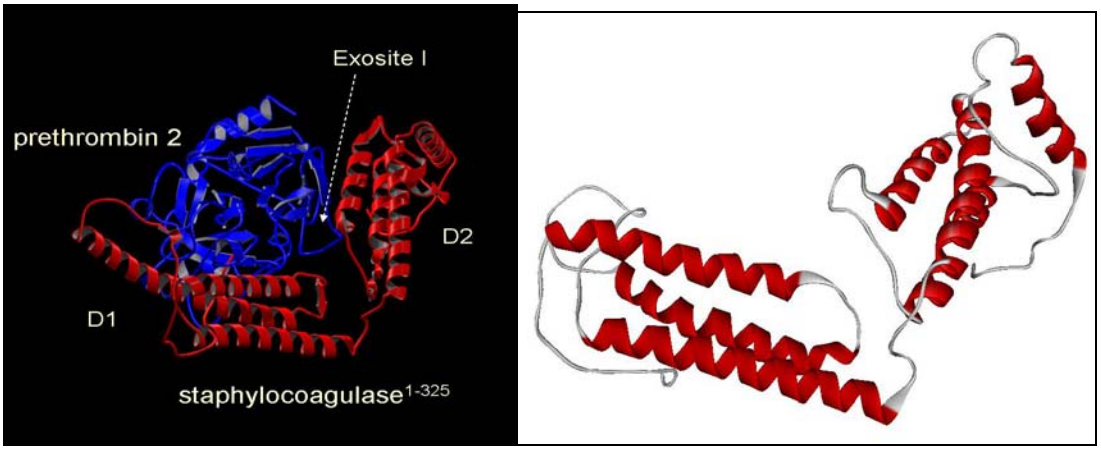

Figure 8. Comparison of SC(1-325) crystal structure to homologous VWbp(1-263) model. Domain organization and homology between SC and VWbp. Model provided by Drs. Pablo-Fuentes Prior and Wolfram Bode.

was indicated in clotting assays with plasma from other species supplemented with human prothrombin (133).

VWbp is the only *S. aureus* SERAM thus far which recognizes VWF, and few bacterial proteins specifically binding VWF have been identified from *S. aureus* or other pathogens. Two cell-surface proteins, staphylococcal protein A (83) and a protein

expressed by the coagulase-negative species *Staphylococcus lugdunensis* (134), have VWF-binding sections located in regions containing repetitive sequences, but there is no sequence homology or common motif between these sites or the VWF recognition sequence in VWbp. It is straightforward to propose a role for cell surface proteins in directly contributing to localization of bacterial cells through interactions with extracellular matrix or plasma proteins, but not so for secreted proteins which are not restricted in their distribution during an endovascular infection. The dual functionality of VWbp as a coagulase and an adhesin may present both illumination and difficulty in assigning a role for VWbp in the pathology of *S. aureus*.

Concluding Remarks and Goal of Thesis Research

Given that VWbp is a comparatively recent addition to the staphylococcal family of SERAMs, very little has been established about either the significance of its interaction with VWF or the consequences of its procoagulant activity. Definition of its disparate functions is necessary to first recognize any similarities or differences of VWbp to other known proteins, in particular SC, and to understand what physiological processes could be influenced by the presence of VWbp. The fact that the gene for VWbp has been found in all of the clinical and laboratory strains of *S. aureus* that have been examined so far, even though these strains also secrete SC (131), is indicative of distinct functions for each protein, despite a general similarity for initiating blood coagulation. Whether VWbp is capable of directly manipulating prothrombin to elicit clotting of fibrinogen, in a manner similar to that of SC, is significant to the field of serine proteinase biochemistry, as SC and streptokinase are the only proteins associated with allosteric zymogen activation. In addition, the predicted structural homology between the two proteins (and the other ZAAP members) presents opportunities to uncover additional targets for therapeutic intervention during infection and to expand the present

body of knowledge on the tactics employed by pathogenic bacteria within their arsenal of secreted exoproteins.

This work resulted in three first-author manuscripts (two published and one in preparation):

Heather K. Kroh, Peter Panizzi, Paul E. Bock. "Von Willebrand factor-binding protein is a hysteretic conformational activator of prothrombin." *Proceedings of the National Academy of Science, U.S.A.* (2009) May 12;106(19):7786-7791. (*Chapter 2*)

Heather K. Kroh, Paul E. Bock. "Effect of zymogen domains and active site occupation on conformational activation of prothrombin by von Willebrand factor-binding protein." *Journal of Biological Chemistry* (2010), in preparation. (*Chapter 3*)

Heather K. Kroh, Guido Tans, Gerry A. F. Nicolaes, Jan Rosing, Paul E. Bock. "Expression of allosteric linkage between the sodium ion binding site and exosite I of thrombin during prothrombin activation." *Journal of Biological Chemistry.* (2007) Jun1; 282(22):16095-104. (*Chapter 4*)

The focus of this thesis is the characterization of the molecular mechanism of prothrombin activation by VWbp--first and foremost the ability of VWbp to conformationally activate the zymogen form through insertion of its own NH_2-terminus into the NH_2-terminal binding cleft (the molecular sexuality mechanism). The descriptions of this and the unique, substrate-driven, hysteretic kinetic mechanism of prothrombin activation by VWbp are covered in Chapter 2, along with identification of fibrinogen as the specific substrate of the prothrombin-VWbp complex. Chapter 3 addresses the role of allostery in regulating binding and activation of prothrombin by VWbp, specifically illustrating the effect of the small zymogen domains of prothrombin on the function of VWbp, as well as the cofactor effect of substrate on complex formation. Finally, Chapter 4 presents a detailed mechanistic study of allosteric regulation of exosite expression in proteolytic intermediates of canonical prothrombin activation.

References

1. Ruggeri ZM (2003) Von Willebrand factor, platelets, and endothelial cell interactions. *J. Thromb. Haemost.* 1:1335-1342.

2. Seré KM & Hackeng TM (2003) Basic mechanisms of hemostasis. *Semin. Vasc. Med.* 3:3-12.

3. Davie EW & Ratnoff OD (1964) Waterfall sequence for intrinsic blood clotting. *Science* 145:1310-1312.

4. Macfarlane RG (1964) An enzyme cascade in the blood clotting mechanism, and its function as a biochemical amplifier. *Nature (London)* 202:498-499.

5. Gailani D & Renné T (2007) Intrinsic pathway of coagulation and arterial thrombosis. *Arterioscler. Thromb. Vasc. Biol.* 27:2507-2513.

6. Mann KG, Butenas S, & Brummel K (2003) The dynamics of thrombin formation. *Arterioscler. Thromb. Vasc. Biol.* 23:17-25.

7. Butenas S & Mann KG (1996) Kinetics of human factor VII activation. *Biochemistry* 35:1904-1910.

8. Morrissey JH, Macik BG, Neuenschwander PF, & Comp PC (1993) Quantitation of activated factor VII levels in plasma using a tissue factor mutant selectively deficient in promoting factor VII activation. *Blood* 81:734-744.

9. Olsen OH & Persson E (2008) Cofactor-induced and mutational activity enhancement of coagulation factor VIIa. *Cell. Mol. Life Sci.* 65:953-963.

10. Mackman N, Tilley RE, & Key NS (2007) Role of the extrinsic pathway of blood coagulation in hemostasis and thrombosis. *Arterioscler. Thromb. Vasc. Biol.* 27:1687-1693.

11. Mann KG (2003) Thrombin formation. *Chest* 124:4S-10S.

12. Butenas S, van't Veer C, & Mann KG (1997) Evaluation of the initiation phase of blood coagulation using ultrasensitive assays for serine proteases. *J. Biol. Chem.* 272:21527-21533.

13. Nicolaes GAF & Dahlbäck B (2002) Factor V and thrombotic disease: Description of a janus-faced protein. *Arterioscler. Thromb. Vasc. Biol.* 22:530-538.

14. Weisel JW (2005) Fibrinogen and fibrin. *Adv. Protein Chem.* 70:247-299.

15. Gomez K, McVey JH, & Tuddenham E (2005) Inhibition of coagulation by macromolecular complexes. *Haematologica* 90:1570-1576.

16. Pike RN, Buckle AM, Le Bonniec BF, & Church FC (2005) Control of the coagulation system by serpins: Getting by with a little help from glycosaminoglycans. *FEBS Lett.* 272:4842-4851.

17. Pratt CW & Church FC (1993) General features of the heparin-binding serpins antithrombin, heparin cofactor II and protein C inhibitor. *Blood Coagulation and Fibrinolysis* 4:479-490.

18. Tollefsen DM (2007) Heparin cofactor II modulates the response to vascular injury. *Arterioscler. Thromb. Vasc. Biol.* 27:454-460.

19. Jackson CJ & Xue M (2008) Activated protein C--An anticoagulant that does more than stop clots. *Int. J. Biochem. Cell Biol.* 40:2692-2697.

20. Griffin JH, Fernández JA, Gale AJ, & Mosnier LO (2007) Activated protein C. *J. Thromb. Haemost.* 5 (Suppl. 1):73-80.

21. Adams TE & Huntington JA (2006) Thrombin-cofactor interactions: Structural insights into regulatory mechanisms. *Arterioscler. Thromb. Vasc. Biol.* 26:1738-1745.

22. Rijken DC & Lijnen HR (2009) New insights into the molecular mechanisms of the fibrinolytic system. *J. Thromb. Haemost.* 7:4-13.

23. Perona JJ & Craik C, S. (1995) Structural basis of substrate specificity in the serine proteases. *Protein Sci.* 4:337-360.

24. Khan AR & James MNG (1998) Molecular mechanisms for the conversion of zymogens to active proteolytic enzymes. *Protein Sci.* 7:815-836.

25. Huber R & Bode W (1978) Structural basis of the activation and action of trypsin. *Acc. Chem. Res.* 11:114-122.

26. Bode W & Huber R (1976) Induction of the bovine trypsinogen-trypsin transition by peptides sequentially similar to the N-terminus of trypsin. *FEBS Lett.* 68(2):231-236.

27. Nolte HJ & Neumann E (1979) Kinetics and mechanism for the conformational transition in p-guanidinobenzoate bovine trypsinogen induced by the isoleucine-valine dipeptide. *Biophysical Chemistry* 10:253-260.

28. Bode W & Huber R (1978) Crystal structure analysis and refinement of two variants of trigonal trypsinogen: trigonal trypsin and PEG (polyethylene glycol) trypsinogen and their comparison with orthorhombic trypsin and trigonal trypsinogen. *FEBS Lett.* 90:265-269.

29. Gertler A, Walsh KA, & Neurath H (1974) Catalysis by chymotrypsinogen. Demonstration of an acyl-enzyme intermediate. *Biochemistry* 13(6):1302-1310.

30. Kerr MA, Walsh KA, & Neurath H (1975) Catalysis of serine proteases and their zymogens. A study of acyl intermediates by circular dichroism. *Biochemistry* 14:5088-5094.

31. Schechter I & Berger A (1967) On the size of the active site in proteases. I. Papain. *Biochem. Biophys. Res. Commun.* 27:157-162.

32. Perona JJ & Craik C, S. (1997) Evolutionary divergence of substrate specificity within the chymotrypsin-like serine protease fold. *J. Biol. Chem.* 272:29987-29990.

33. Krem MM, Rose T, & Di Cera E (1999) The C-terminal sequence encodes function in serine proteases. *J. Biol. Chem.* 274:28063-28066.

34. Mann KG, Elion J, Butkowski RJ, Downing MR, & Nesheim ME (1981) Prothrombin. *Methods Enzymol.* 80:286-302.

35. Bode W (2006) Structure and interaction modes of thrombin. *Blood Cells, Molecules, and Diseases* 36(2):122-130.

36. Krishnaswamy S (2005) Exosite-drive substrate specificity and function in coagulation. *J. Thromb. Haemost.* 3:54-67.

37. Bock PE, Panizzi P, & Verhamme IMA (2007) Exosites in the substrate specificity of blood coagulation reactions. *J. Thromb. Haemost.* 5 (Suppl. 1):81-94.

38. Di Cera E (2008) Thrombin. *Mol. Aspects Med.* 29:203-254.

39. Heldebrant CM & Mann KG (1973) The activation of prothrombin I. Isolation and preliminary characterization of intermediates *J. Biol. Chem.* 248:3642-3652.

40. Heldebrant CM, Butkowski RJ, Bajaj SP, & Mann KG (1973) The activation of prothrombin II. Partial reactions, physical and chemical characterization of the intermediates of activation. *J. Biol. Chem.* 248:7149-7163.

41. Esmon CT, Owen WG, & Jackson CM (1974) A plausible mechanism for prothrombin activation by factor Xa, factor Va, phospholipid, and calcium ions. *J. Biol. Chem.* 249:8045-8047.

42. Esmon CT, Owen WG, & Jackson CM (1974) The conversion of prothrombin to thrombin II. Differentiation between thrombin- and factor Xa-catalyzed proteolyses. *J. Biol. Chem.* 249(2):606-611.

43. Krishnaswamy S, Mann KG, & Nesheim ME (1986) The prothrombinase-catalyzed activation of prothrombin proceeds through the intermediate meizothrombin in an ordered, sequential reaction. *J. Biol. Chem.* 261(19):8977-8984.

44. Carlisle TL, Bock PE, & Jackson CM (1990) Kinetic intermediates in prothrombin activation: Bovine prethrombin 1 conversion to thrombin by factor X. *J. Biol. Chem.* 265(35):22044-22055.

45. Krishnaswamy S, Church WR, Nesheim ME, & Mann KG (1987) Activation of human prothrombin by human prothrombinase: Influence of factor Va on the reaction mechanism. *J. Biol. Chem.* 262:3291-3299.

46. Walker RK & Krishnaswamy S (1994) The activation of prothrombin by the prothrombinase complex: The contribution of the substrate-membrane interaction to catalysis. *J. Biol. Chem.* 269:27441-27450.

47. Orcutt SJ & Krishnaswamy S (2004) Binding of substrate in two conformations to human prothrombinase drives consecutive cleavage at two sites in prothrombin. *J. Biol. Chem.* 279:54927-54936.

48. Bianchini EP, Orcutt SJ, Panizzi P, Bock PE, & Krishnaswamy S (2005) Ratcheting of the substrate from the zymogen to proteinase conformations directs the sequential cleavage of prothrombin by prothrombinase. *Proc. Natl. Acad. Sci. U. S. A.* 102(29):10099-10104.

49. Hacisalihoglu A, Panizzi P, Bock PE, Camire RM, & Krishnaswamy S (2007) Restricted active site docking by enzyme-bound substrate enforces the ordered cleavage of prothrombin by prothrombinase. *J. Biol. Chem.* 282(45):32974-32982.

50. Brufatto N & Nesheim ME (2003) Analysis of the kinetics of prothrombin activation and evidence that two equilibrating forms of prothrombinase are involved in the process. *J. Biol. Chem.* 278(9):6755-6764.

51. Kim PY & Nesheim ME (2007) Further evidence for two functional forms of prothrombinase each specific for either of the two prothrombin activation cleavages. *J. Biol. Chem.* 282(45):32568-32581.

52. Boskovic DS, Bajzar LS, & Nesheim ME (2001) Channeling during prothrombin activation. *J. Biol. Chem.* 276(31):28686-28693.

53. Orcutt SJ, Pietropaolo C, & Krishnaswamy S (2002) Extended interactions with prothrombinase enforce affinity and specificity for its macromolecular substrate. *J. Biol. Chem.* 278(48):46191-46196.

54. Krishnaswamy S (2005) Exosite-driven substrate specificity and function in coagulation. *J. Thromb. Haemost.* 3:54-67.

55. Krishnaswamy S & Betz A (1997) Exosites determine macromolecular substrate recognition by prothrombinase. *Biochemistry* 36:12080-12086.

56. Boskovic DS & Krishnaswamy S (2000) Exosite binding tethers the macromolecular substrate to the prothrombinase complex and directs cleavage at two spatially distinct sites. *J. Biol. Chem.* 275(49):38561-38570.

57. Anderson PJ, Nesset A, Dharmawardana KR, & Bock PE (2000) Characterization of proexosite I on prothrombin. *J. Biol. Chem.* 275(22):16428-16434.

58. Anderson PJ, Nesset A, & Bock PE (2003) Effects of activation peptide bond cleavage and fragment 2 interactions on the pathway of exosite I expression during activation of human prethrombin 1 to thrombin. *J. Biol. Chem.* 278(45):44482-44488.

59. Anderson PJ & Bock PE (2003) Role of prothrombin fragment 1 in the pathway of regulatory exosite I formation during conversion of human prothrombin to thrombin. *J. Biol. Chem.* 278(45):44489-44495.

60. Herwald H*, et al.* (1998) Activation of the contact-phase system on bacterial surfaces--a clue to serious complications in infectious disease. *Nature Medicine* 4(3):298-302.

61. Imamura T*, et al.* (2005) Induction of vascular leakage through release of bradykinin and a novel kini by cysteine proteinases from *Staphylococcus aureus*. *J. Exp. Med.* 201(10):1669-1676.

62. Frick I-M, Björck L, & Herwald H (2007) The dual role of the contact system in bacterial infectious disease. *Thromb. Haemostasis* 98:497-502.

63. DeLa Cadena RA*, et al.* (1991) Role of kallikrein-kinin system in pathogenesis of bacterial cell wall-induced inflammation. *Am. J. Physiol.* 260:G213-G219.

64. Tapper H & Herwald H (2000) Modulation of hemostatic mechanisms in bacterial infectious disease. *Blood* 96:2329-2337.

65. Bergmann S & Hammerschmidt S (2007) Fibrinolysis and host response in bacterial infections. *Thromb. Haemostasis* 98:512-520.

66. Sun H (2006) The interaction between pathogens and the host coagulation system. *Physiology* 21:281-288.

67. Lowy FD (1998) *Staphylococcus aureus* infections. *N. Engl. J. Med.* 339:520-532.

68. Mulligan ME, Standiford HC, & Kauffman CA (1993) Methicillin-resistant *Staphylococcus aureus*: A consensus review of the microbiology, pathogenesis, and epidemiology with implications for prevention and management. *Am. J. Med.* 94:313-328.

69. Hiramatsu K (1998) Vancomycin resistance in Staphylococci. *Drug Resistance Updates* 1:135-150.

70. Voyich JM*, et al.* (2005) Insights into mechanisms used by *Staphylococcus aureus* to avoid destruction by human neutrophils. *J. Immunol.* 175:3907-3919.

71. Hammel M*, et al.* (2007) Characterization of Ehp, a secreted complement inhibitory protein from *Staphylococcus aureus*. *J. Biol. Chem.* 282(41):30051-30061.

72. Burman JD*, et al.* (2008) Interaction of human complement with Sbi, a staphylococcal immunoglobulin-binding protein: Indications of a novel mechanism of complement evasion by *Staphylococcus aureus*. *J. Biol. Chem.* 283(25):17579-17593.

73. Foster TJ (2005) Immune evasion by staphylococci. *Nature Reviews Microbiology* 3:948-958.

74. Burlak C*, et al.* (2007) Global analysis of community-associated methicillin-resistant *Staphylococcus aureus* exoproteins reveals molecules produced *in vitro* and during infection. *Cell. Micro.*:1-19.

75. Clarke SR & Foster SJ (2006) Surface adhesins of *Staphylococcus aureus*. *Advances in Microbial Physiology* 51:187-224.

76. Hauck CR & Ohlsen K (2006) Sticky connections: extracellular matrix protein recognition and integrin-mediated cellular invasion by *Staphylococcus aureus*. *Curr. Opin. Microbio.* 9:5-11.

77. Heyring R, van de Gevel J, Que Y-A, Moreillon P, & Beekhuizen H (2007) Fibronectin-binding proteins and clumping factor A in *Staphylococcus aureus* experimental endocarditis: FnBPA is sufficient to activate human endothelial cells. *Thromb. Haemostasis* 97:617-626.

78. Wann ER, Gurusiddappa S, & Höök M (2000) The fibronectin-binding MSCRAMM FnBPA of *Staphylococcus aureus* is a bifunctional protein that also binds to fibrinogen. *J. Biol. Chem.* 275(18):13863-13871.

79. Matsuka YV, Anderson ET, Milner-Fish T, Ooi P, & Baker S (2003) *Staphylococcus aureus* fibronectin-binding protein serves as a substrate for coagulation factor XIIIa: Evidence for factor XIIIa-catalyzed covalent cross-linking to fibronectin and fibrin. *Biochemistry* 42:14643-14652.

80. Rivera J, Vannakambadi G, Höök M, & Speziale P (2007) Fibrinogen-binding proteins of Gram-positive bacteria. *Thromb. Haemostasis* 98:503-511.

81. Higgins J, Loughman A, van Kessel KPM, van Strijp JAG, & Foster TJ (2006) Clumping factor A of *Staphylococcus aureus* inhibits phagocytosis by human polymorphonuclear leucocytes. *FEMS Microbiol. Lett.* 258:290-296.

82. Loughman A*, et al.* (2005) Roles for fibrinogen, immunoglobulin and complement in platelet activation promoted by *Staphylococcus aureus* clumping factor A. *Mol. Microbiol.* 57(3):804-818.

83. Hartleib J*, et al.* (2000) Protein A is the von Willebrand factor binding protein on *Staphylococcus aureus*. *Blood* 96:2149-2156.

84. Chavakis T, Wiechmann K, Preissner KT, & Herrmann M (2005) *Staphylococcus aureus* interactions with the endothelium: The role of bacterial "Secretable Expanded Repertoire Adhesive Molecules" (SERAM) in disturbing host defense systems. *Thromb. Haemostasis* 94:278-285.

85. Palma M, Wade D, Flock M, & Flock J-I (1998) Multiple binding sites in the interaction between an extracellular fibrinogen-binding protein from *Staphylococcus aureus* and fibrinogen. *J. Biol. Chem.* 273(21):13177-13181.

86. Palma M, Nozohoor S, Schennings T, Heimdahl A, & Flock J-I (1996) Lack of the extracellular 19-kilodalton fibrinogen-binding protein from Staphylococcus aureus decreases virulence in experimental wound infection. *Infect. Immun.* 64(12):5284-5289.

87. Shannon O & Flock J-I (2004) Extracellular fibrinogen binding protein, Efb, from *Staphylococcus aureus* binds to platelets and inhibits platelet aggregation. *Thromb. Haemostasis* 91:779-789.

88. Lee LYL, Liang X, Höök M, & Brown EL (2004) Identification and characterization of the C3 binding domain of the *Staphylococcus aureus* extracellular fibrinogen-binding protein (Efb). *J. Biol. Chem.* 279(49):50710-50716.

89. Palma M, Haggar A, & Flock J-I (1999) Adherence of *Staphylococcus aureus* is enhanced by an endogenous secreted protein with broad binding activity. *J. Bacteriol.* 181(9):2840-2845.

90. Haggar A*, et al.* (2003) Extracellular adherence protein from *Staphylococcus aureus* enhances internalization into eukaryotic cells. *Infect. Immun.* 71(5):2310-2317.

91. Hussain M, Becker K, von Eiff C, Peters G, & Herrmann M (2001) Analogs of Eap protein are conserved and prevalent in clinical *Staphylococcus aureus* isolates. *Clin. Diag. Lab. Immunol.* 8(6):1271-1276.

92. Smith W & Hale JH (1944) The nature and mode of action of staphylococcus coagulase. *Br. J. Exp. Path.* 25:101-110.

93. Tager M (1948) Studies on the coagulase-reacting factor: 1. The reaction of staphylocoagulase with the components of human plasma. *Yale J. Biol. Med.* 20(4):369-380.

94. Miale JB (1949) The role of staphylocoagulase in blood coagulation II. Coagulation in the absence of calcium and in the presence of fluorides, heparin, and azo dyes. *Blood* 4:1317-1322.

95. Tager M & Lodge AL (1951) Influence of the physiological blood clotting process on the coagulation of blood by staphylocoagulase. *J. Exp. Med.* 94(1):73-85.

96. Tager M (1956) Studies on the nature and the purification of the coagulase-reacting factor and its relation to prothrombin. *J. Exp. Med.* 104(5):675-686.

97. Duthie ES & Haughton G (1958) Purification of free staphylococcal coagulase. *Biochem. J.* 70(1):125-134.

98. Duthie ES (1954) Evidence for two forms of staphylococcal coagulase. *J. Gen. Microbiol.* 10:427-436.

99. Soulier JP & Prou-Wartelle O (1967) Study of thrombin-coagulase. *Thrombosis et Diathesis Haemorrhagica* 17:321-334.

100. Mojovic B, Mojovic N, Tager M, & Drummond MC (1969) Staphylocoagulase as a hemostatic agent. *Yale J. Biol. Med.* 42:11-20.

101. Hemker HC, Bas BM, & Muller AD (1975) Activation of a pro-enzyme by a stoichiometric reaction with another protein: The reaction between prothrombin and staphylocoagulase. *Biochim. Biophys. Acta* 379:180-188.

102. Hendrix H, Lindhout T, Mertens K, Engels W, & Hemker HC (1983) Activation of human prothrombin by stoichiometric levels of staphylocoagulase. *J. Biol. Chem.* 258(6):3637-3644.

103. Kawabata S-i, Morita T, Iwanaga S, & Igarashi H (1985) Staphylocoagulase-binding region in human prothrombin. *J. Biochem. (Tokyo)* 97:325-331.

104. Kawabata S-I, Morita T, Iwanaga S, & Igarashi H (1985) Enzymatic properties of staphylothrombin, an active molecular complex formed between staphylocoagulase and human prothrombin. *J. Biochem. (Tokyo)* 98(6):1603-1614.

105. Kawabata S-i, Morita T, Iwanaga S, & Igarashi H (1985) Difference in enzymatic properties between α-thrombin-staphylocoagulase complex and free α-thrombin. *J. Biochem. (Tokyo)* 97:1073-1078.

106. Kawabata S-i*, et al.* (1986) The amino acid sequence of the procoagulant- and prothrombin-binding domain isolated from staphylocoagulase. *J. Biol. Chem.* 261(2):527-531.

107. Kawabata S-i, Morita T, Miyata T, Iwanaga S, & Igarashi H (1986) Isolation and characterization of staphylocoagulase chymotryptic fragment: Localization of the procoagulant- and prothrombin-binding domain of this protein. *J. Biol. Chem.* 261(3):1427-1433.

108. Kaida S*, et al.* (1987) Nucleotide sequence of the staphylocoagulase gene: Its unique COOH-terminal 8 tandem repeats. *J. Biochem. (Tokyo)* 102:1177-1186.

109. Kaida S, Miyata T, Yoshizawa Y, Igarashi H, & Iwanaga S (1989) Nucleotide and deduced amino acid sequences of staphylocoagulase gene from *Staphylococcus aureus* strain 213. *Nucleic Acids Res.* 17(21):8871.

110. Phonimdaeng P, O'Reilly M, Nowlan P, Bramley AJ, & Foster TJ (1990) The coagulase of *Staphylococcus aureus* 8325-4. Sequence analysis and virulence of site-specific coagulase-deficient mutants. *Mol. Microbiol.* 4(3):393-404.

111. Kawabata S-I & Iwanaga S (1994) Structure and function of staphylothrombin. *Semin. Thromb. Hemostasis* 20(4):345-350.

112. Zen-Yoji H, Terayama T, & Benoki M (1961) Studies on staphylococcal coagulase I. Antigenic differences of coagulase and distribution of the anticoagulase in human sera. *Jpn. J. Microbiol.* 5(2):237-247.

113. Carter PE, Begbie K, & Thomson-Carter FM (2003) Coagulase gene variants associated with distinct populations of *Staphylococcus aureus*. *Epidemiol. Inf.* 130:207-219.

114. Watanabe S*, et al.* (2009) Genetic diversity of staphylocoagulse genes (coa): Insight into the evolution of variable chromosomal virulence factors in *Staphylococcus aureus*. *PLoS ONE* 4(5):e5714.

115. Heilmann C, Herrmann M, Kehrel BE, & Peters G (2002) Platelet-binding domains in 2 fibrinogen-binding proteins of *Staphylococcus aureus* identified by phage display. *J. Infect. Dis.* 186:32-39.

116. Baddour LM, Tayidi MM, Walker E, McDevitt D, & Foster TJ (1994) Virulence of coagulase-deficient mutants of *Staphylococcus aureus* in experimental endocarditis. *J. Med. Microbiol.* 41:259-263.

117. Moreillon P*, et al.* (1995) Role of *Staphylococcus aureus* coagulase and clumping factor in pathogenesis of experimental endocarditis. *Infect. Immun.* 63(12):4738-4743.

118. Gemmell CG, Goutcher SC, Reid R, & Sturrock RD (1997) Role of certain virulence factors in a murine model of *Staphylococcus aureus* arthritis. *J. Med. Microbiol.* 46:208-213.

119. Jonsson P, Lindberg M, Haraldsson I, & Wadstrom T (1985) Virulence of *Staphylococcus aureus* in a mouse mastitis model: Studies of alpha hemolysin, coagulase, and protein A as possible virulence determinants with protoplast fusion and gene cloning. *Infect. Immun.* 49(3):765-769.

120. Sawai T*, et al.* (1997) Role of coagulase in a murine model of hematogenous pulmonary infection induced by intravenous injection of *Staphylococcus aureus* enmeshed in agar beads *Infect. Immun.* 65(2):466-471.

121. Yanagihara K*, et al.* (2006) Effects of short interfering RNA against methicillin-resistant *Staphylococcus aureus* coagulase *in vitro* and *in vivo*. *J. Antimicrob. Chemother.* 57:122-126.

122. Bajaj SP & Castellino FJ (1977) Activation of human plasminogen by equimolar levels of streptokinase. *J. Biol. Chem.* 252(2):492-498.

123. Wang S, Reed GL, & Hedstrom L (1999) Deletion of Ile1 changes the mechanism of streptokinase: Evidence for the molecular sexuality hypothesis. *Biochemistry* 38:5232-5240.

124. Wang S, Reed GL, & Hedstrom L (2000) Zymogen activation in the streptokinase-plasminogen complex: Ile1 is required for the formation of a functional active site. *Eur. J. Biochem.* 267:3994-4001.

125. Boxrud PD, Verhamme IMA, Fay WP, & Bock PE (2001) Streptokinase triggers conformational activation of plasminogen through specific interactions of the amino-terminal sequence and stabilizes the active zymogen conformation. *J. Biol. Chem.* 276(28):26084-26089.

126. Friedrich R*, et al.* (2003) Staphylocoagulase is a prototype for the mechanism of cofactor-induced zymogen activation. *Nature* 425:535-539.

127. Panizzi P*, et al.* (2006) Novel fluorescent prothrombin analogs as probes of staphylocoagulase-prothrombin interactions. *J. Biol. Chem.* 281:1169-1178.

128. Panizzi P*, et al.* (2006) Fibrinogen substrate recognition by staphylocoagulase-(pro)thrombin complexes. *J. Biol. Chem.* 281(2):1179-1187.

129. Friedrich R*, et al.* (2006) Structural basis for reduced staphylocoagulase-mediated bovine prothrombin activation. *J. Biol. Chem.* 281(2):1188-1195.

130. Panizzi P, Friedrich R, Fuentes-Prior P, Bode W, & Bock PE (2004) The staphylocoagulase family of zymogen activator and adhesion proteins. *Cell. Mol. Life Sci.* 61:1-6.

131. Bjerketorp J*, et al.* (2002) A novel von Willebrand factor binding protein expressed by *Staphylococcus aureus*. *Microbiology* 148:2037-2044.

132. Rosander A, Bjerketorp J, Frykberg L, & Jacobsson K (2002) Phage display as a novel screening method to identify extracellular proteins. *J. Microbiol. Meth.* 51:43-55.

133. Bjerketorp J, Jacobsson K, & Frykberg L (2004) The von Willebrand factor-binding protein (vWbp) of *Staphylococcus aureus* is a coagulase. *FEMS Microbiol. Lett.* 234:309-314.

134. Nilsson M*, et al.* (2004) A von Willebrand factor-binding protein from *Staphylococcus lugdunensis*. *FEMS Microbiol. Lett.* 234:155-161.

CHAPTER II

VON WILLEBRAND FACTOR-BINDING PROTEIN IS A HYSTERETIC CONFORMATIONAL ACTIVATOR OF PROTHROMBIN

Heather K. Kroh*, Peter Panizzi†, and Paul E. Bock*

*Department of Pathology, Vanderbilt University School of Medicine, Nashville, TN 37232-2561

†Center for Molecular Imaging Research, Massachusetts General Hospital, Charlestown, MA 02129-2060

(This research was originally published in:
Proceedings of the National Academy of Sciences, U.S.A. 2009;106(19):7786-7791.

Abstract

Von Willebrand factor-binding protein (VWbp), secreted by *Staphylococcus aureus*, displays secondary structural homology to the three helix bundle, D1 and D2 domains of staphylocoagulase (SC), a potent conformational activator of the blood coagulation zymogen, prothrombin (ProT). In contrast to the classical proteolytic activation mechanism of trypsinogen-like serine proteinase zymogens, insertion of the first two residues of SC into the NH_2-terminal binding cleft on ProT (molecular sexuality) induces rapid conformational activation of the catalytic site. Based on plasma clotting assays, the target zymogen for VWbp may be ProT, but this has not been verified and the mechanism of ProT activation is unknown. We demonstrate that VWbp activates ProT conformationally in a mechanism requiring its Val^1-Val^2 residues. By contrast to SC, full time-course kinetic studies of ProT activation by VWbp demonstrate that it activates ProT by a substrate-dependent, hysteretic kinetic mechanism. VWbp binds weakly to ProT (K_D 2.5 μM) to form an inactive complex, which is activated through a slow conformational change by tripeptide chromogenic substrates and its specific physiological substrate, identified here as fibrinogen (Fbg). This mechanism increases the specificity of ProT activation by delaying it in a slow reversible process, with full activation requiring binding of Fbg through an exosite expressed on the activated ProT*·VWbp complex. The results suggest that this unique mechanism regulates pathological fibrin (Fbn) deposition to VWF-rich areas during *S. aureus* endocarditis.

Introduction

The tightly regulated balance between procoagulant, anticoagulant, and fibrinolytic pathways in blood is kinetically controlled by the rates of proteolytic activation of zymogens of the chymotrypsinogen family. The classical proteolytic activation mechanism is initiated by cleavage at Arg^{15}-Ile^{16} (chymotrypsinogen numbering), followed by insertion of the Ile^{16} NH_2-terminus into the NH_2-terminal binding cleft, and formation of a critical salt bridge with Asp^{194} (1-3). This triggers folding of segments of the catalytic domain, which forms the substrate binding site and oxyanion hole required for activity. The mechanism is fundamentally conformational in that zymogens are in unfavorable equilibrium between conformationally active forms which vary in equilibrium constants from 10^8 (trypsinogen) (4) to ~7 (single-chain tissue-type plasminogen activator) (5). Dipeptides that mimic the conserved NH_2-termini (Ile-Val or Val-Val) induce structural changes in trypsinogen toward the active proteinase conformation (1, 3), and tight-binding inhibitors like bovine pancreatic trypsin inhibitor convert trypsinogen fully to the conformation of trypsin (3).

By contrast, staphylocoagulase (SC) from *Staphylococcus aureus* activates the coagulation zymogen prothrombin (ProT) non-proteolytically, and formation of the tightly-bound ProT·SC complex initiates direct cleavage of Fbg into Fbn (6, 7). The ProT·SC(1-325) complex expresses a new exosite that mediates specific substrate recognition of Fbg, while full length SC(1-660) also interacts with Fbg as an adhesion protein through COOH-terminal repeat sequences (8, 9). This benefits the pathogen by facilitating escape from the host defense system through formation of protective Fbn-platelet-bacteria vegetations in acute bacterial endocarditis (10).

VWbp, also secreted by *S. aureus*, was first identified by phage-display of an *S. aureus* (Newman) DNA library screened against von Willebrand factor (VWF) (11), leading to its classification as an adhesion protein. Binding to both immobilized and

soluble VWF is mediated by a 26-amino acid region within VWbp (11), but the physiological significance of this interaction has not been established. VWbp was further recognized as a putative member of the bifunctional zymogen activator and adhesion protein (ZAAP) family for which SC is the prototype (12, 13). It was subsequently postulated to be an SC homolog from its 25% sequence identity with SC and clotting of human plasma (14).

The structure of the NH_2-terminal half of SC, SC(1-325), is unique, with a characteristic elbow-like fold between two domains (D1-D2) comprised of 3-helix bundles (13). Secondary structure modeling of the corresponding D1-D2 domains of VWbp(1-263) revealed a high degree of similarity (13). Structural and kinetic studies of SC demonstrated insertion of the first two NH_2-terminal residues of SC into the NH_2-terminal binding cleft in the ProT catalytic domain (13). The NH_2-terminus forms a salt bridge with Asp^{194} (13), triggering the conformational change that activates the catalytic site. This “molecular sexuality” mechanism (1) has only been demonstrated for SC and the plasminogen activator streptokinase (15), whereas essentially nothing is known about the mechanism of plasma clotting by VWbp.

The specific interactions responsible for the procoagulant activity of VWbp have not been defined, and the mechanism of its activation of ProT is unknown. In the present studies, we defined the molecular basis and unusual hysteretic kinetic mechanism of ProT activation by VWbp and identified Fbg as its specific substrate, which are postulated to play a role in the pathology of *S. aureus* infection.

Results

Conformational Activation of ProT by VWbp(1-263) and VWbp(1-474)

Whether VWbp(1-263) and full length VWbp(1-474) activate ProT through a conformational change was examined using three-step active site-specific labeling: (1) inactivation of active species in ProT-VWbp mixtures with N^{α}-[(acetylthio)acetyl]-*D*-Phe-Pro-Arg-CH_2Cl (ATA-FPR-CH_2Cl), (2) generation of a free thiol with NH_2OH, and (3) covalent attachment of 5-(iodoacetamido)fluorescein (5-IAF) (16). SDS-gel electrophoresis of samples from reactions including all three steps showed specific, covalent incorporation of fluorescein into ProT only (Fig. 1, lanes 4), with no proteolysis of the zymogen for either VWbp(1-263) or VWbp(1-474). Stringent controls omitting one of the steps of the labeling scheme confirmed that all of the labeling steps were necessary for probe incorporation (Fig. 1, lanes 3, 5-7).

Activation of Pre 1 by the NH_2-terminal insertion mechanism

To ascertain whether VWbp activates ProT through the molecular sexuality mechanism, VWbp(1-474) was compared in kinetic assays of prethrombin 1 (Pre 1; ProT lacking the fragment 1 domain) activation to the NH_2-terminal deletion mutants, VWbp(2-474) and VWbp(3-474). Initial rates of ProT activation could not be employed quantitatively in this analysis due to their inherent curvature, whereas initial rates of Pre 1 activation by VWbp(1-474) were nearly linear. Deletion of the first NH_2-terminal Val residue of VWbp reduced its activity at saturation ~78%, while deletion of both Val^1 and Val^2 completely inactivated VWbp (Fig. 2). Qualitatively similar results were obtained with ProT, with no detectable activity for VWbp(3-474).

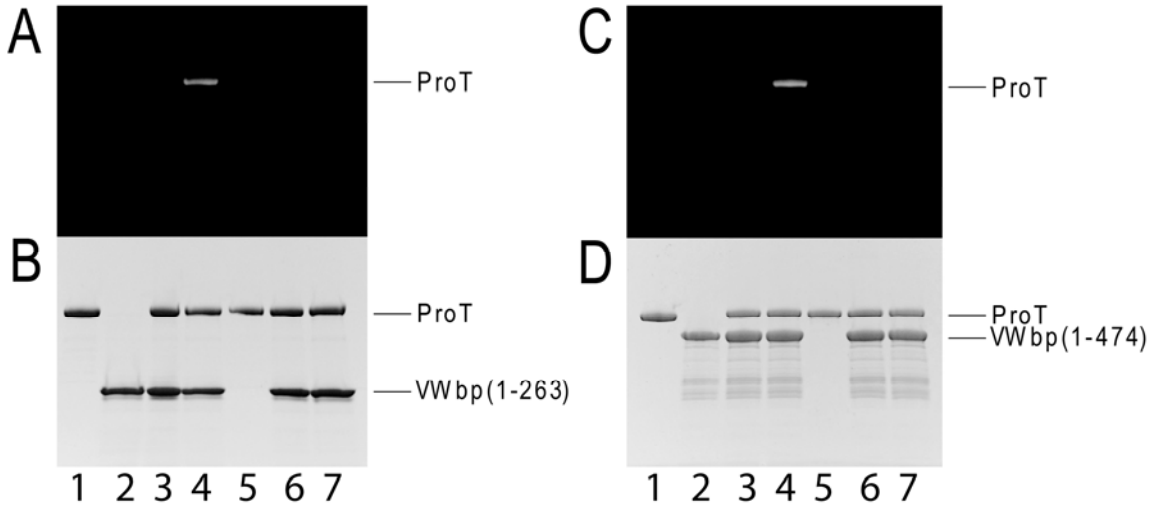

Figure 1. Active-site specific labeling of ProT·VWbp(1-263) and ProT·VWbp(1-474) complexes assessed by SDS-gel electrophoresis. Fluorescence (A and C) and protein-stained (B and D) SDS gels for reactions containing 15 μM ProT and 50 μM VWbp(1-263) (A and B) or VWbp(1-474) (C and D). Reduced samples of ProT (*lane 1*) and VWbp (*lane 2*), ProT-VWbp inactivated with ATA-FPR-CH_2Cl (*lane 3*), and inhibited complex incubated with NH_2OH and 5-IAF (*lane 4*). Control samples were ProT incubated without VWbp (*lane 5*), omission of the NH_2OH step (*lane 6*), or the complex blocked with excess FPR-CH_2Cl before sequential incubation with ATA-FPR-CH_2Cl and 5-IAF (*lane 7*).

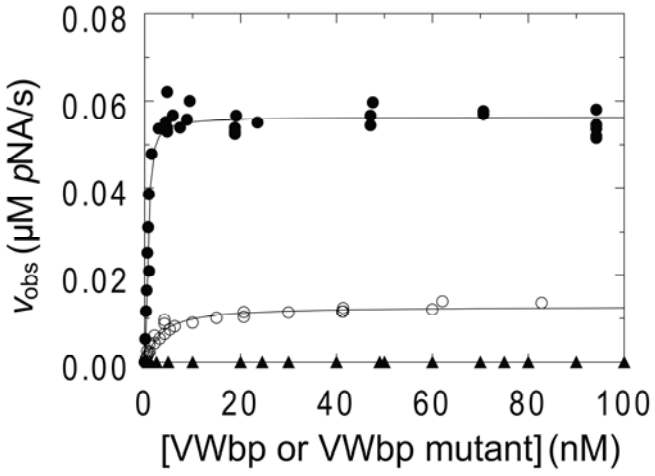

Figure 2. Pre 1 activation by NH_2-terminal truncation mutants of VWbp. Initial velocities (v_{obs}) of hydrolysis of 100 μM *D*-Phe-Pip-Arg-*p*NA are shown for mixtures of 1 nM Pre 1 as a function of VWbp(1-474) (●), VWbp(2-474) (○), or VWbp(3-474) (▲) concentration. The *lines* represent the least-squares fits of the quadratic binding equation.

Kinetic analysis of ProT activation

The rates of tripeptide-*p*-nitroanilide (*p*NA) chromogenic substrate hydrolysis by ProT activated by either VWbp(1-263) or VWbp(1-474) showed upward curvature over time. While this could be a result of a slow equilibration time for ProT·VWbp complex formation, varying the preincubation time of the reaction before substrate addition up to 1 h had very little effect on the curvature (see Supplemental Data). Due to the apparent effect that binding of substrate by ProT·VWbp(1-263) had on the activation kinetics, progress curves collected as a function of substrate and VWbp(1-263) concentration were truncated at ≤ 10% substrate depletion and analyzed individually with the classical hysteresis equation (Eqn. 1, Materials and Methods) (17, 18). The excellent nonlinear least-squares fits indicated that the curvature initiated by substrate was a single exponential process (not shown). The observed rate constants increased hyperbolically with increasing VWbp(1-263) concentration and decreased with increasing substrate concentration (not shown). This ruled out a mechanism involving an unfavorable pre-existing conformational equilibrium between active and inactive forms of ProT in which VWbp(1-263) bound only the active form that also bound substrate. This mechanism predicts a decrease in k_{obs} with increasing VWbp(1-263) concentration, rather than the observed increase. The decease in k_{obs} with increasing substrate concentration suggested that substrate binding followed the slow conformational change.

To evaluate the mechanism further, two chromogenic substrates (*D*-Phe-Pip-Arg-*p*NA and Tosyl-Gly-Pro-Arg-*p*NA) having a ~5-fold difference in K_m for thrombin were employed in full time-course activation progress curve analysis. Progress curves collected as a function of substrate and VWbp(1-263) concentration were analyzed simultaneously by numerical integration of the differential rate equations for candidate mechanisms combined with nonlinear least-squares fitting with DYNAFIT (19). The hysteretic mechanism shown in Scheme 1 produced a consistent fit to the data for both

substrates (Fig. 3), with the parameters listed in Table 1. To obtain the best fit, product inhibition was included in the mechanism as a single binding step (not shown in Scheme 1). Including a conformational equilibrium succeeding product binding did not improve

Scheme 1.

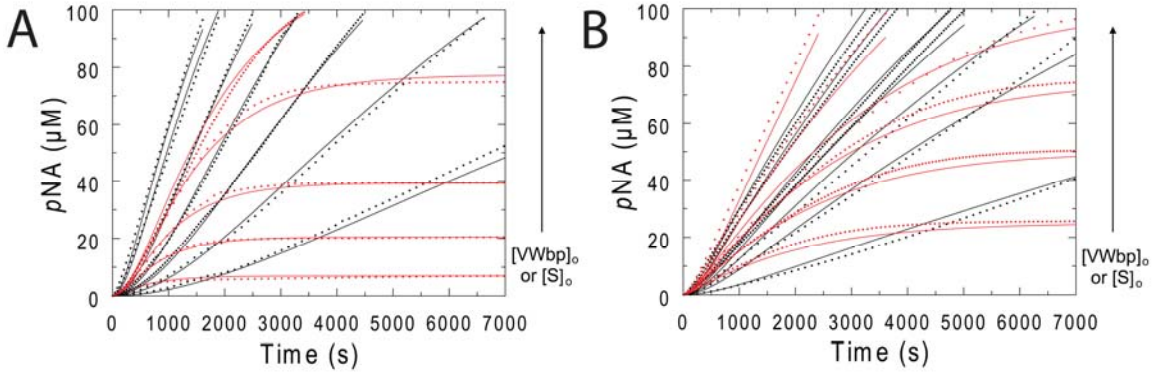

Figure 3. Full time-course analysis of the kinetics of ProT activation by VWbp(1-263). (A) Progress curves for hydrolysis of *D*-Phe-Pip-Arg-*p*NA by mixtures of VWbp(1-263) and ProT, at 200 μM substrate (*black points*), contained 1 nM ProT and 0.025, 0.075, 0.15, 0.3, 0.6, 3, or 10 μM VWbp. Substrate depletion assays (*red points*) contained 1 nM ProT, 1 μM VWbp, and concentrations of 7, 20, 40, 78, or 116 μM substrate. (B) Progress curves for hydrolysis of 200 μM Tosyl-Gly-Pro-Arg-*p*NA (*black points*) contained 1 nM ProT and 0.1, 0.3, 0.5, 0.75, 1, 3, or 10 μM VWbp. Substrate depletion assays (*red points*) contained 1 nM ProT, 5 μM VWbp, and 25, 50, 75, 100, 150, or 500 μM substrate. Representative examples of the whole data set are shown for each substrate, which contained 17-24 progress curves over 0.025-10 μM VWbp and 5-500 μM substrate. Data are shown as every tenth *point*, and the fit with the mechanism in Scheme 1 and parameters in Table 1 is represented by *solid lines*.

the fit. In Scheme 1, the initial inactive ProT·VWbp(1-263) complex is formed with low affinity (K_D 2.2-2.4 μM) in a rapid equilibrium step. ProT·VWbp(1-263) is in an unfavorable, slow equilibrium with active ProT*·VWbp(1-263), and tight binding of

substrate to the ProT*·VWbp(1-263) complex shifts the equilibrium towards the active form. The slow shift in equilibrium increases the rate of substrate hydrolysis, responsible for the upward curvature of the progress curves. The fitted parameters showed that both substrates exhibited 2- to 4-fold lower K_m for the ProT*·VWbp(1-263) complex compared to thrombin (Table 1). The analysis also revealed an unfavorable equilibrium constant (K_{con} 9 ± 1 and 9 ± 6) for the slow conformational change, and excellent agreement between the individual rate constants (k_{C1}, k_{C2}) to form ProT*·VWbp(1-263) for the two substrates (Table 1). In addition, the apparent affinity (K_D) of ProT for formation of the initial inactive ProT·VWbp(1-263) complex was nearly identical with either substrate (2.4 μM and 2.2 μM) (Table 1).

Table 1. Summary of kinetic parameters (± 2 S.D.) for ProT activation by VWbp(1-263) from the hysteretic mechanism shown in Scheme 1, where K_I is the dissociation constant for competitive product inhibition.

Parameters	*D*-Phe-Pip-Arg-*p*NA	Tosyl-Gly-Pro-Arg-*p*NA
K_m (thrombin)	2.5 ± 0.2 μM	11.3 ± 0.3 μM
k_{cat} (thrombin)	77 ± 1 s^{-1}	164 ± 1 s^{-1}
K_D	2.4 ± 0.1 μM	2.2 ± 0.2 μM
K_{con} (k_{C2}/k_{C1})	9 ± 1	9 ± 6
k_{C1}	0.0052 ± 0.0001 s^{-1}	0.0053 ± 0.0004 s^{-1}
k_{C2}	0.049 ± 0.005 s^{-1}	0.047 ± 0.028 s^{-1}
K_m	0.6 ± 0.2 μM	6 ± 4 μM
k_{cat}	95 ± 1 s^{-1}	50 ± 1 s^{-1}
K_I	2.2 ± 0.3 μM	30 ± 20 μM

Results obtained with other substrates with K_m in the 100-300 μM range were not fit well by the mechanism in Scheme 1 because of the importance of obtaining near-saturation within the experimentally accessible concentration range. A more complex mechanism involving significant activity for the inactive complex failed to produce consistent fits or reasonable parameters. The possibility that autocatalytic cleavage of ProT to Pre 1, previously reported for SC (6) and SC(1-325) (20), accounted for the hysteresis was evaluated by western blotting under conditions identical to those used for collecting the progress curves (see Supplemental Data). At the highest VWbp(1-263) concentration (10 μM) in the kinetic studies, 23 ± 9% (mean and range) of ProT was converted into Pre 1 over the whole time-course for both substrates. At 1 μM VWbp(1-263), Pre 1 formation was reduced to 1-10%. Analysis of individual progress curves at 10 μM VWbp showed little effect on their shape, demonstrating that Pre 1 formation did not account for the observed hysteresis.

Competitive binding of VWbp(1-263) and [5-F]Hir(54-65) to ProT

To investigate the binding interactions involved in ProT activation by VWbp, independent of substrate-mediated effects, competitive binding titrations of the proexosite I-specific probe [5-F]Hir(54-65) and VWbp(1-263) with ProT were performed (Fig. 4). The decrease in fluorescence of [5-F]Hir(54-65) titrated with ProT in the absence of VWbp(1-263) gave a K_D consistent with previous results (2.8 ± 0.3 μM) (21). Analysis of the fluorescence changes in the presence and absence of VWbp(1-263) as a function of native ProT concentration gave a K_D of VWbp(1-263) for proexosite I on ProT of 2.5 ± 0.3 μM, nearly identical to the values determined kinetically. Furthermore, the ability of VWbp(1-263) to compete with the labeled peptide for binding to ProT indicates that VWbp binds to proexosite I (13).

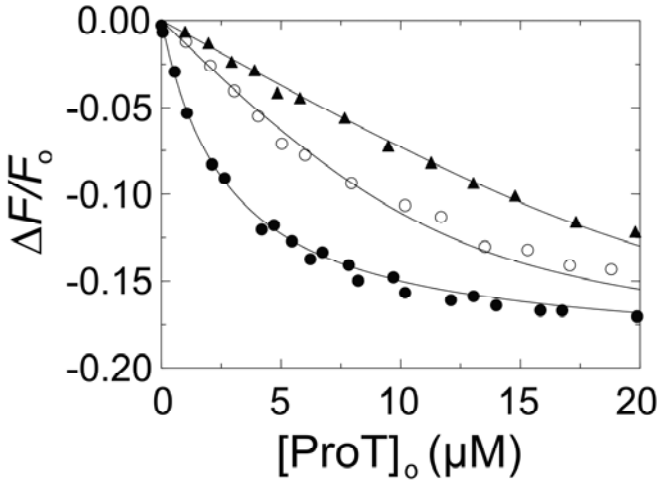

Figure 4. Competitive binding of native ProT to [5-F]Hir(54-65) and VWbp(1-263). Fractional change in fluorescence ($\Delta F/F_o$) of 48 nM [5-F]Hir(54-65) as a function of total native ProT concentration ($[ProT]_o$) at 0 (●), 10 (○), and 20 μM (▲) VWbp(1-263). The *lines* represent the simultaneous fit by the cubic equation with the parameters given in the text.

Clotting of Fbg by ProT·VWbp(1-263)

We examined human Fbg as a potential substrate by monitoring the clotting of Fbg by mixtures of ProT and VWbp(1-263), as detected by the increase in turbidity (Fig. 5). The capacity of VWbp(1-263) to trigger formation of a Fbn clot demonstrates that Fbg is the first substrate identified for the ProT·VWbp(1-263) complex. The complex displayed efficient clotting of Fbg at 10 nM ProT, and in contrast to immediate cleavage of Fbg by 10 nM thrombin or ProT·SC(1-325) complex, which showed a brief ~30 sec lag, all of the ProT·VWbp(1-263) assays showed a much longer, reproducible lag in the time-course (Fig. 5). No increase in turbidity was seen until ~220 sec after addition of ProT at 1 μM VWbp(1-263), implicating the hysteretic mechanism in recognition of the natural substrate. Although an exhaustive survey of other potential substrates was not done, kinetic assays revealed no activation of the thrombin substrates, protein C, factor V, or factor XI, or two other coagulation zymogens (factor IX and factor X) by ProT·VWbp(1-263). In addition, the thrombin-selective serpins antithrombin and heparin

cofactor II did not inhibit the activity of the ProT·VWbp(1-263) complex in the presence or absence of heparin (not shown).

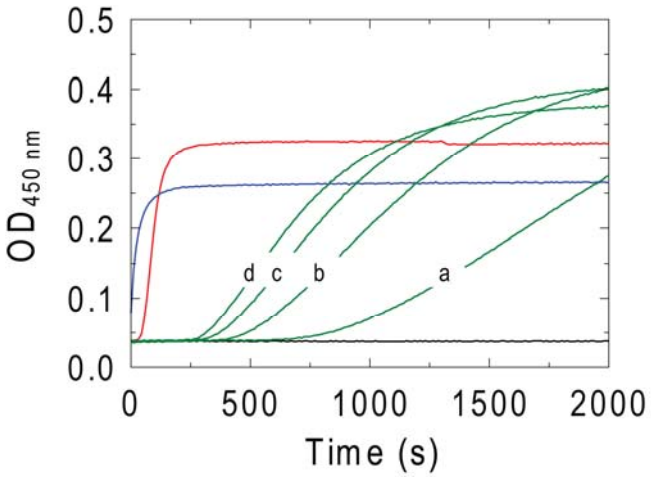

Figure 5. Clotting of Fbg by mixtures of ProT and VWbp(1-263). Increase in turbidity for mixtures of 0.5 mg/ml Fbg and 10 nM thrombin (*blue*), 10 nM ProT (*black*), 10 nM ProT·SC(1-325) (*red*), or 10 nM ProT and VWbp concentrations of 0.1 (*a*), 0.3 (*b*), 0.5 (*c*), or 1 μM (*d*) (*green*).

Discussion

Our results support the conclusion that VWbp is a new non-proteolytic ProT activator that utilizes molecular sexuality and employs a unique substrate-activated hysteretic kinetic mechanism. Active site-specific labeling of ProT with a fluorescent probe in mixtures with VWbp(1-263) or VWbp(1-474) provided a direct demonstration of non-proteolytic activation of the zymogen. These experiments also indicate that the SC(1-325)-homologous D1 and D2 domains of VWbp(1-263) are sufficient for ProT activation. Total loss of activity accompanying deletion of the first two NH_2-terminal residues of VWbp shows that it activates the ProT derivative, Pre 1, and ProT through the molecular sexuality mechanism.

Our studies and previous reports indicate that SC(1-325) has the same maximal chromogenic substrate activity as SC(1-660) (22) (P.P., H.K.K., and P.E.B, unpublished results). In contrast, ProT activation by full-length VWbp(1-474) displays higher activity than VWbp(1-263) (not shown), although VWbp(1-474) also shows hysteresis. The finding that Pre 1 activation by VWbp(1-474) shows less hysteresis than ProT implicates the fragment 1 domain in the mechanism. The COOH-terminal region of VWbp is associated with the higher activity of the ProT·VWbp complex, possibly through additional interactions that increase substrate affinity and/or hydrolysis. Kinetic analysis of ProT activation by VWbp demonstrates a hysteretic model of enzyme activation, where there is a slow response to an abrupt stimulus that controls the observed rate of catalysis (17). The hysteretic kinetic concept is applicable to a number of enzymes involved in metabolic regulation, and can result from isomerization, ligand displacement, or enzyme polymerization (17). While slow hysteretic transitions have been examined for several monomeric enzymes (18, 23), our results are the first to demonstrate hysteresis in serine proteinase zymogen activation.

As predicted from the kinetic model (Scheme 1), the K_D for formation of the inactive ProT·VWbp(1-263) complex and the rate constants for the slow conformational change were independent of the structures and kinetic parameters for two tripeptide-*p*NA substrates. The relatively low affinity of ProT·VWbp(1-263) complex formation revealed an additional disparity between the behavior of VWbp(1-263) and SC. Whereas SC(1-325) binds to native ProT with extremely high affinity (K_D 17-72 pM) (24), the initial affinity of ProT and VWbp(1-263) was 2.2-2.4 μM from the kinetic analysis and 2.5 μM from competitive binding experiments. The kinetic mechanism suggests that VWbp(1-263) binds the native ProT zymogen with a weaker affinity than the zymogen with a substrate occupying the active site. The weak affinity of VWbp(1-263) for ProT and the hysteretic generation of proteolytic activity represent a unique regulatory

mechanism in which the initially low affinity prevents premature activation of ProT, and the hysteresis delays the response to substrate, restricting Fbn formation. The hysteretic mechanism thus functions to increase the specificity of VWbp for Fbn formation compared to SC.

The NH_2-terminal insertion pocket, catalytic site, and certain regulatory exosites on coagulation proteinases are allosterically linked (25, 26). In the classical zymogen activation mechanism, these sites are rapidly expressed as part of the zymogen to proteinase conformational transition. Based on the linkage between these sites, the hysteretic conformational change between inactive and active forms of ProT·VWbp complex represents these events as a slow transition, unique among zymogen activation mechanisms. The need for substrate binding to complete the conformational change indicates that either NH_2-terminal insertion is an unfavorable intramolecular equilibrium or that the VWbp Val-Val NH_2-terminus inserts normally, but does not result in an optimal structure to effect full activation. Mutation of VWbp(1-474) Val^1 to Ile to mimic the SC NH_2-terminal dipeptide did not detectably affect the hysteretic behavior (not shown), indicating that the difference in the dipeptides is not responsible. For α-chymotrypsin, interconversion of an inactive conformation at high pH to the active form at neutral pH is controlled by protonation of the α-amino group of Ile^{16} (27). In pH-jump experiments, the rate constants for formation of the chymotrypsin active site correspond to k_{C1} and k_{C2} of 3 s^{-1} and 0.6 s^{-1}, respectively, and K_{con} of 0.2 (27). If the values for chymotrypsin are taken as representative of the rate of NH_2-terminal insertion and activation of the catalytic site for ProT, the values for ProT·VWbp(1-263) are 590-fold (k_{C1}) and 12-fold (k_{C2}) slower. This suggests that the activating conformational change for ProT·VWbp(1-263) is not limited by the rate constants for insertion and conformational activation, but by additional interactions of ProT with VWbp(1-263) that slow the activation process.

Screening of other coagulation zymogens for direct activation by VWbp indicates that it does not activate protein C, factor IX, factor X, or factor XII. The finding that VWbp binds to the low affinity precursor form of exosite I on ProT, and the established role of exosite I in thrombin interactions with protein substrates (including Fbg), inhibitors, and regulatory proteins (25) indicates that ProT·VWbp will exhibit highly restricted substrate and inhibitor specificity, preventing interactions with thrombomodulin, factor V, factor VIII, heparin cofactor II, and protease activated receptor-1 (25). Fbg substrate recognition by activation of proexosite I in the ProT·VWbp complex is not possible because this site is blocked by VWbp. Neither VWbp nor ProT alone bind Fbg, indicating that Fbg substrate recognition by the ProT·VWbp complex is mediated by expression of a new exosite. The occupation of exosite II in ProT by the fragment 2 domain restricts further the substrate specificity of VWbp by blocking heparin-accelerated inhibition by antithrombin, as well as exosite II-dependent binding of factors V, factor VIII, and the platelet receptor GPIbα (25). The studies show that Fbg is the only established substrate of the ProT·VWbp(1-263) complex that binds with sufficient affinity to shift the hysteretic conformational equilibrium to the active complex. The lag observed in the time-course of Fbg clotting assays initiated with ProT-VWbp(1-263) mixtures suggests that the dependence of the hysteretic kinetic mechanism on a protein substrate restricts activation of ProT by VWbp to areas rich in Fbg. Localized depletion of Fbg in an endocarditis vegetation may result in shutting off ProT·VWbp by the more rapid reversal of the conformational change. Additional results with VWbp(1-474) show no significant effect of the plasma concentration of VWF (150 nM) on the hysteretic mechanism of ProT activation, for either untreated VWF or the extended conformation induced by vortexing VWF under conditions that enhance VWF cleavage by ADAMTS13 (28).

The results of this study are the first to characterize the coagulation-specific molecular mechanisms behind a potential new virulence factor from *S. aureus*. As the first additional member of the ZAAP family of bifunctional conformational zymogen activators and adhesion proteins, elucidation of the role of VWbp in activation of coagulation during endocarditis may aid in the development of mechanism-based therapies. Further clarification of the interactions of VWbp with both ProT and plasma adhesion proteins will offer insight into how VWbp may serve to specifically localize ProT activation in the course of *S. aureus* infection. This raises the question of why are there two ProT activators, VWbp and SC, secreted by *S. aureus*. All *S. aureus* strains that contain the gene for VWbp also contain the gene for SC (11). The evolutionary advantage responsible for maintaining both activators is likely due to the differences in the adhesion protein targets and the kinetic mechanisms of ProT activation. In the context of endocarditis, the initial vascular injury of the endothelium on heart valves at high shear rates activates coagulation, with VWF mediating the early stages of platelet accumulation by tethering through exposed subendothelial collagen and the platelet GPIbα receptor, followed by conversion of Fbg to Fbn within the thrombus (29). Additional binding of platelets by VWF occurs after platelet activation by thrombin and is dependent upon the platelet integrin $\alpha_{IIb}\beta_3$ (30). *S. aureus* concurrently adheres to multiple extracellular matrix proteins, including fibronectin, collagen, and Fbn, through microbial surface components recognizing adhesive matrix molecules (MSCRAMMs) (31). Through initial association with VWF at transient sites of vascular injury, VWbp could restrict pathologic Fbn deposition to focal points in the vasculature, establishing new locations for bacterial dissemination. Thus, VWbp may catalyze the first assault in Fbn deposition, followed by rampant SC-mediated Fbn deposition and vegetation growth.

Materials and Methods

Protein and peptide purification

Human ProT, Pre 1, thrombin, Fbg, Y^{63}-sulfated fluorescein-labeled hirudin(54-65) ([5-F]Hir(54-65)), and ATA-FPR-CH_2Cl were prepared as described (16, 24, 32).

Cloning, expression, and purification of VWbp constructs

The VWbp(1-474) gene was amplified from *S. aureus* Mu50 strain (ATCC) genomic DNA and cloned into a modified pET30b(+) vector (Novagen) (24) using *Nco*I and *Xho*I restriction sites. VWbp was expressed with an NH_2-terminal His_6-tag and tobacco etch virus (TEV) proteinase cleavage site in Rosetta 2 (DE3) pLysS *E. coli* (Novagen) with isopropyl-D-thiogalactopyranoside induction. Recombinant VWbp protein was extracted from inclusion bodies by the use of 3 M NaSCN buffer, pH 7.4, and purified by Ni^{2+}-iminodiacetic acid chromatography. The His_6-tag was removed by overnight incubation with a 1:10 molar ratio of TEV proteinase to fusion protein similar to the procedure described for recombinant streptokinase (33). Mutants of VWbp(1-474) (VWbp(2-474), VWbp(3-474), and VWbp(1-263)) were generated by QuickChange site-directed mutagenesis (Stratagene). NH_2-terminal sequencing of all the VWbp constructs confirmed the correct Val-Val-Ser-Gly-Glu sequence. VWbp concentration was determined from the 280 nm-absorbance using the following calculated absorption coefficients ($(mg/ml)^{-1}cm^{-1}$) (34) and molecular weights: VWbp(1-263), 0.582, 30,700; VWbp(1-474), 0.488, 55,000.

Active-site specific labeling of ProT

VWbp(1-263) or VWbp(1-474) (50 μM) were incubated with ProT (15 μM) and ATA-FPR-CH_2Cl (125 μM) to covalently inactivate the ProT catalytic site formed in the active complex. The inhibited complex was incubated with 0.1 M NH_2OH in the presence of 33 μM 5-IAF to label the generated thiol. Probe incorporation (0.84-0.86 mol probe/mol ProT) was determined as described (16).

Pre 1 activation kinetic titrations

Titrations of Pre 1 activity as a function of VWbp(1-474), VWbp(2-474), or VWbp(3-474) concentration were measured by the increase in the initial rate of hydrolysis of 200 μM *D*-Phe-Pip-Arg-*p*NA at 405 nm and 25 ^{o}C. Pre 1 was incubated with VWbp for 20 min in 50 mM Hepes, 110 mM NaCl, 5 mM $CaCl_2$, 1 mg/ml polyethylene glycol (PEG) 8000, pH 7.4, before substrate addition. The maximum velocity was determined by nonlinear least-squares analysis of the hyperbolic titrations.

ProT activation kinetics

Progress curves for hydrolysis of two thrombin-specific chromogenic substrates (*D*-Phe-Pip-Arg-*p*NA and Tosyl-Gly-Pro-Arg-*p*NA) by mixtures of ProT and VWbp(1-263) were measured in the buffer described above. Full time-course assays were performed under both saturating and limiting substrate concentrations, with continuous data collection for 2 h, or until $A_{405\ nm}$ = 1.0. Proteins were incubated for 20 min at 25 ^{o}C before initiating the reactions by addition of substrate. Analysis of individual progress curves was performed on data truncated to ≤ 10% substrate depletion by fitting the integrated equation for the classical hysteresis mechanism,

$P_t = v_f t - \left(v_f - v_o\right)\left(1 - e^{-k_{obs}t}\right)/ k_{obs}$ (Eqn.1), where P_t is the product formed at time t, v_f and v_o are the final and initial velocities, and k_{obs} is the observed first-order rate constant (17). This equation is only applicable under conditions of minimal substrate depletion and product inhibition. Analysis of progress curves from full time-course assays under saturating and substrate depletion concentrations, and as a function of VWbp(1-263) concentration, were analyzed by simultaneous nonlinear least-squares fitting of the numerically-integrated differential rate equations for candidate mechanisms with DYNAFIT (19). The rate constants for initial binding of ProT and VWbp and binding of substrate were assumed to be diffusion controlled (10^8 $M^{-1}s^{-1}$) rapid equilibrium steps.

Fluorescence titrations

Competitive binding of [5-F]Hir(54-65) and VWbp(1-263) to ProT was measured in titrations of mixtures of 48 nM labeled peptide and VWbp as a function of ProT concentration in the same buffer used for the kinetics. Continuous time-course measurements were taken for each point in the titration that included a buffer blank, [5-F]Hir(54-65) alone, addition of VWbp(1-263), and addition of native ProT. This separated the fluorescence change measured in the first 2 min, representing the rapidly established competitive binding equilibria, from slower proteolysis of the ProT·VWbp complex. Fluorescence (8 nm slits) at 520 nm with excitation at 491 nm was measured with an SLM 8100 spectrofluorometer at 25 ^{o}C, in PEG 20,000-coated acrylic cuvettes. The fluorescence changes expressed as $(F_{obs} - F_o)/F_o = \Delta F/F_o$ in the absence and presence of two fixed concentrations of VWbp(1-263) (10 and 20 μM) were fit simultaneously by the cubic equation for tight competitive binding to obtain the K_D's for [5-F]Hir(54-65) binding to ProT (K_P) and VWbp(1-263) binding to ProT (K_C), with the stoichiometry fixed at 1 (32).

Fibrin turbidity assays

Cleavage of Fbg by either thrombin, ProT·SC(1-325), or ProT·VWbp(1-263) complexes was monitored from the increase in turbidity at 450 nm at 25 ^{o}C in the above-described buffer using a microtiter plate reader. Fbg was added (0.5 mg/ml) to various concentrations of VWbp(1-263), 10 nM SC(1-325), or buffer and reactions were started immediately by addition of 10 nM ProT or thrombin.

Acknowledgements

The project described was supported by NIH Grant R37 HL071544 from the National Heart, Lung, and Blood Institute (P.E.B.) and H.K.K. was supported by Training Grant 2-T32 HL07751.

Supplemental Data (Published)

Introduction

Previous studies of conformational activation of ProT by staphylocoagulase (SC) (35) and its fully active fragment SC(1-325) (20) showed that activation was associated with slow autocatalytic cleavage of ProT. Early studies demonstrated that at micromolar concentrations of ProT and SC, cleavage at the thrombin-sensitive Arg^{155}-Ser^{156} bond in ProT to form prethrombin 1 (Pre 1) and fragment 1 (F1) was accompanied by a large increase in fluorogenic substrate (Boc-Val-Pro-Arg-4-methylcoumaryl-7-amide) hydrolysis that was concluded to represent higher activity of the Pre 1·SC complex compared to the ProT·SC complex (35). These studies, performed at 0 °C, reported that bovine fibrinogen clotting activity was generated in less than 5 min, whereas maximum fluorogenic substrate activity was observed at 60 min. This slow time-dependence was not observed with Pre 1, for which clotting and fluorogenic substrate activity were both rapidly formed on addition of SC. Studies of SC(1-325) at micromolar concentrations and at 25 °C in the same buffer used in the VWbp experiments, showed that formation of Pre 1 was followed by much slower generation of prethrombin 2' (Pre 2') and fragment 2 (F2) resulting from cleavage of the second thrombin-sensitive bond in ProT at Arg^{284}-Thr^{285} (20). The kinetics of ProT activation by SC(1-325) at nanomolar concentrations, after preincubation in the absence of substrate for 20 min, were inconsistent with the Pre 1·SC(1-325) complex having significantly increased activity with a chromogenic substrate (*D*-Phe-Pip-Arg-*p*NA) compared to ProT·SC(1-325) (20). On the basis of these previous studies, the possibility that autoproteolytic cleavage of ProT to Pre 1 in mixtures with VWbp accounted for the observed hysteretic kinetics of ProT activation by

VWbp was investigated by SDS-gel electrophoresis, western blotting with a polyclonal anti-ProT antibody, and analysis of activation progress curves.

Results and Discussion

Proteolysis in mixtures of 10 μM VWbp(1-263) and 5 μM ProT was assessed by SDS-gel electrophoresis (Fig. 1S). ProT was initially cleaved to Pre 1 and fragment 1 slowly over 180 min, with much smaller accumulation of Pre 2'. Incubation for 24 h resulted in full conversion of ProT and Pre 1 to Pre 2', fragment 1, and fragment 2.

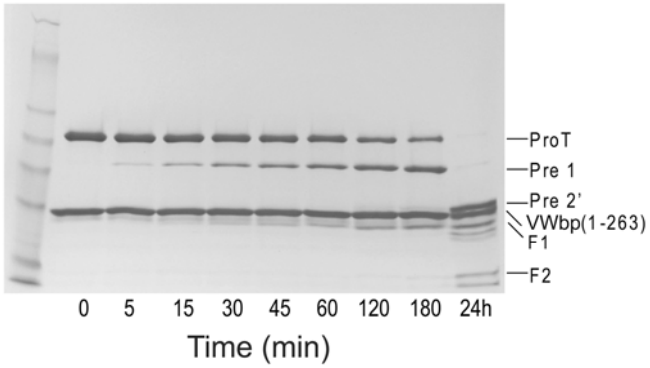

Figure 1S. Proteolytic products generated in ProT-VWbp(1-263) mixtures assessed by SDS-gel electrophoresis. Nonreduced samples (7.2 μg ProT) of mixtures of 5 μM ProT and 10 μM VWbp incubated at 25 °C in 50 mM Hepes, 110 mM NaCl, 5 mM $CaCl_2$, 1 mg/ml PEG 8000, pH 7.4 were taken at the indicated times after mixing, subjected to electrophoresis on a SDS 4-15%-gradient gel, and stained with GelCode Blue protein stain (Thermo Scientific). Bands representing ProT, Pre 1, Pre 2', F1, and F2 are indicated.

Western blotting was used to quantitate the autocatalytic cleavage of ProT in the presence of VWbp under conditions identical to those used for the full time-course progress curve experiments (Fig. 3 of the chapter). Samples were removed from mixtures of 1 nM ProT and 10 μM VWbp(1-263) that were preincubated for 20 min before continued incubation in the absence or presence of 200 μM *D*-Phe-Pip-Arg-*p*NA or Tosyl-Gly-Pro-Arg-*p*NA (Fig. 2S). At the highest VWbp concentration used in the

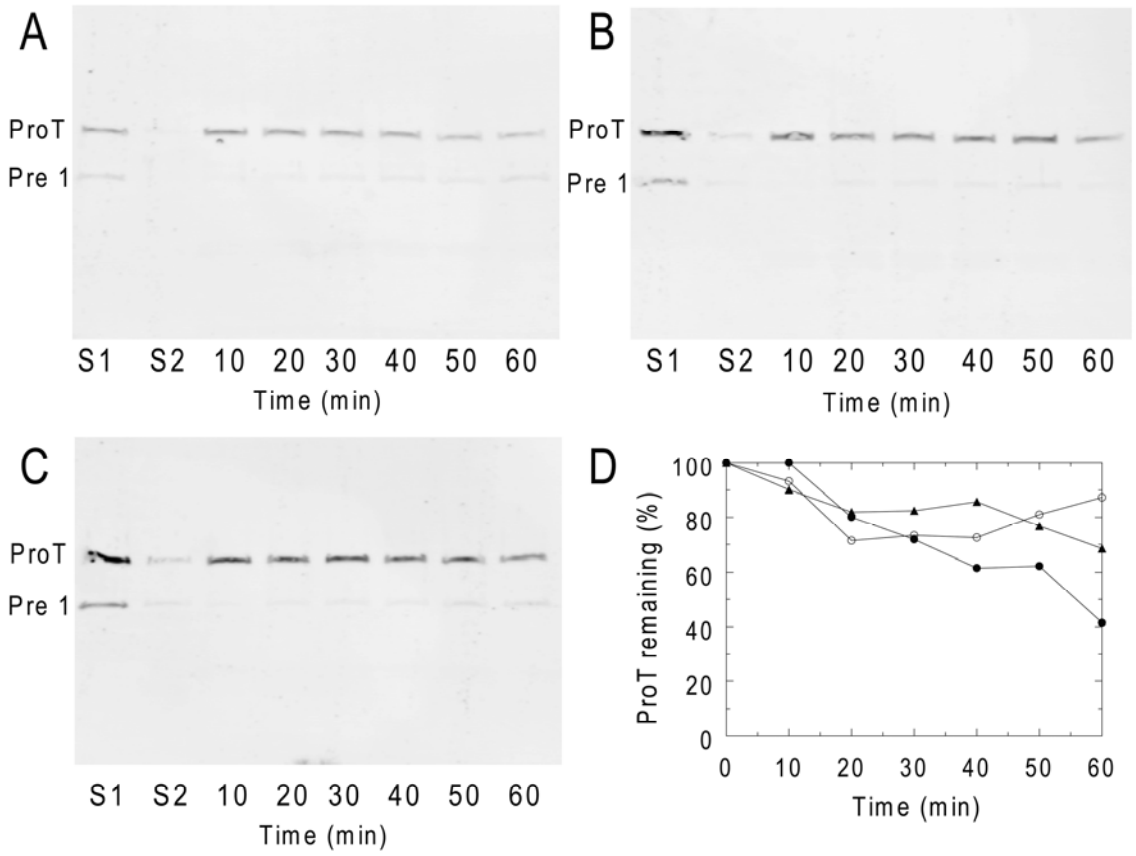

Figure 2S. Pre 1 generation in mixtures of 1 nM ProT and 10 μM VWbp(1-263) evaluated by western blotting. ProT and VWbp were incubated under the same conditions used in the progress curve studies at final concentrations of 1 nM and 10 μM, respectively. Samples taken at the indicated times were denatured under reducing conditions, separated by SDS 4-15% gradient gel electrophoresis, transferred onto polyvinyldiene difluoride membranes, and developed with a polyclonal anti-ProT antibody as described in Materials and Methods. *Lanes S1 and S2* on each gel are the equimolar standard mixtures of 1.5 ng ProT and1.0 ng Pre 1 (*S1*); and 0.3 ng ProT and 0.2 ng Pre 1 (*S2*) used for quantitation. (A) ProT and VWbp incubated in the absence of substrate. (B) ProT and VWbp preincubated for 20 min in the absence of substrate, followed by incubation in the presence of 200 μM *D*-Phe-Pip-Arg-*p*NA. (C) As in B except that the substrate was Tosyl-Gly-Pro-Arg-*p*NA. (D) Relative concentrations of ProT remaining (*%*) as a function of incubation time as in A (●), B, (○), and C (▲).

progress curve experiments (10 μM), 20% of ProT was converted into Pre 1 during the 20 min preincubation, which increased in the absence of substrate to 59% after 60 min (Fig 2S *A and D*). The experiment in which *D*-Phe-Pip-Arg-*p*NA was added after 20 min preincubation showed a similar, 29% conversion to Pre 1, which remained essentially

constant between 13-28% after addition of substrate for the subsequent 30 min of incubation, the time during which the progress curve was collected (Fig. 2S *B and D*). Similar results were obtained with Tosyl-Gly-Pro-Arg-*p*NA, with 18% conversion to Pre 1 during the preincubation, which remained nearly constant at 14-32% over the total 60 min incubation time (Fig. 2S *C and D*). The possibility that Pre 1 generation was due to trace levels of thrombin in the ProT preparation was ruled out by the absence of ProT cleavage in the standards containing equimolar ProT and Pre 1 that were incubated under the same conditions (Fig. 2S, *lane*s *S1 and S2*). Additional experiments

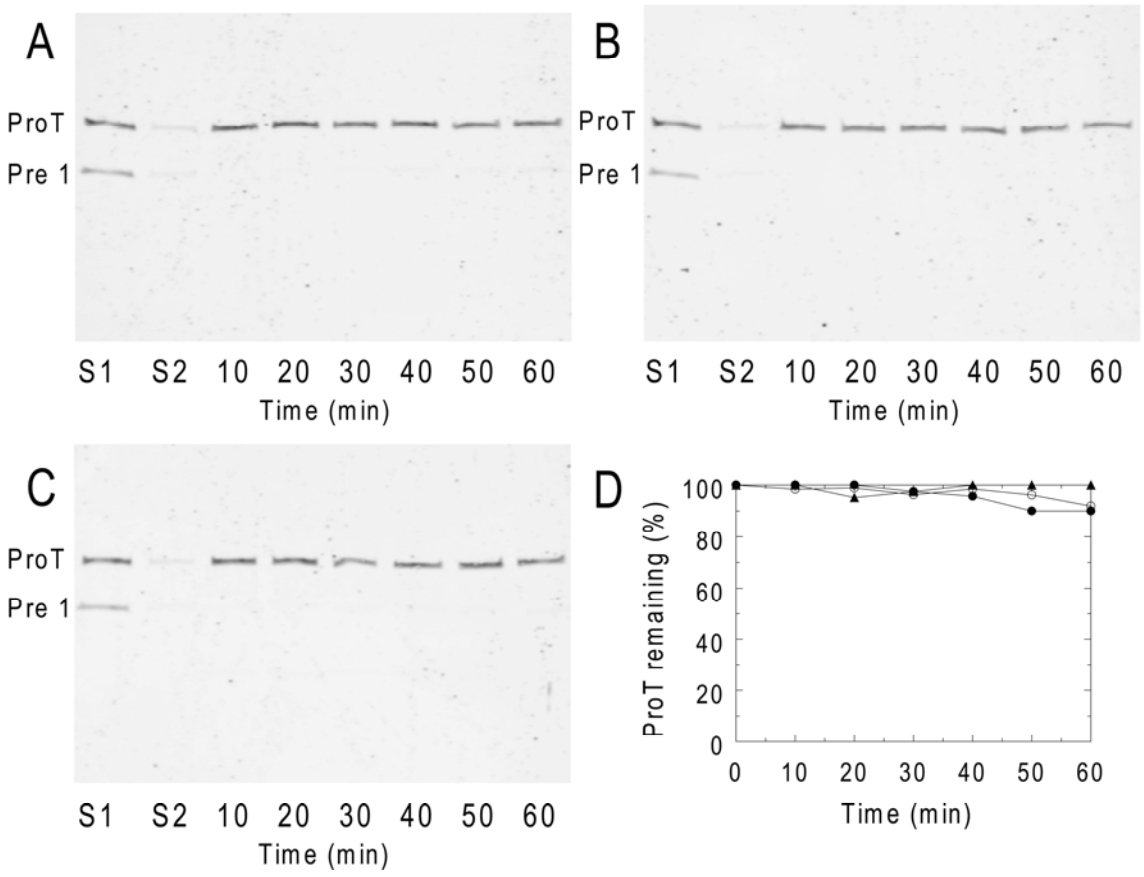

Figure 3S. Pre 1 generation in mixtures of 1 nM ProT and 1 μM VWbp evaluated by western blotting. (A), (B), (C), and (D), as described in the legend to Fig. 2S except that the concentration of VWbp was 1 μM.

performed at 1 nM ProT and 1 μM VWbp, a concentration of VWbp more representative of the progress curve experiments, showed less than 5% conversion of ProT to Pre 1 in the 20 min preincubation period (Fig. 3S *A and D*), which was similarly inhibited after addition of either of the two chromogenic substrates, reaching 1-10% after 60 min (Fig. 3S *B, C, and D*).

The results indicated that only a low level of 23 ± 9% (mean and range) of ProT was converted to Pre 1 at the highest VWbp concentration used in the progress curve experiments. Much lower levels of 1-10% Pre 1 were generated at 1 μM VWbp, conditions under which the progress curves were clearly hysteretic. The results support the conclusion that Pre 1 formation does not account for the concluded hysteretic mechanism.

To evaluate the effect of such low levels of Pre 1 on the progress curves, individual curves were collected after addition of substrate as a function of preincubation time of 1 nM ProT and 10 μM VWbp in the absence of substrate (Fig. 4S *A*). All of the progress curves, truncated at ≤ 5% substrate depletion for this analysis, were fit well by the hysteresis equation without significant deviations (not shown). Analysis of the progress curves gave v_o, the initial velocity, v_f, the final velocity, and k_{obs}, the apparent first-order rate constant. The dependence of these parameters on preincubation time, *i.e.* Pre 1 generation, showed no significant changes in v_f, and slight increases in v_o and k_{obs} (Fig. 4S *B*). During the 20 min preincubation period, v_o relative to v_f increased by ≤ 6% and k_{obs} increased 1.3-fold. These values were compared to those obtained for 1 nM Pre 1 activation by 10 μM VWbp as a function of preincubation time. Pre 1 activation by VWbp(1-263) also displays hysteresis, with k_{obs} values 1.5-3-fold faster than ProT. Pre 1 showed essentially no changes in v_o, v_f, or k_{obs} over 60 min (Fig. 4S *C*). The final velocity (v_f) for Pre 1 activation was only ~4% larger than that for ProT, indicating indistinguishable rates of hydrolysis of the chromogenic substrate by the Pre 1·VWbp

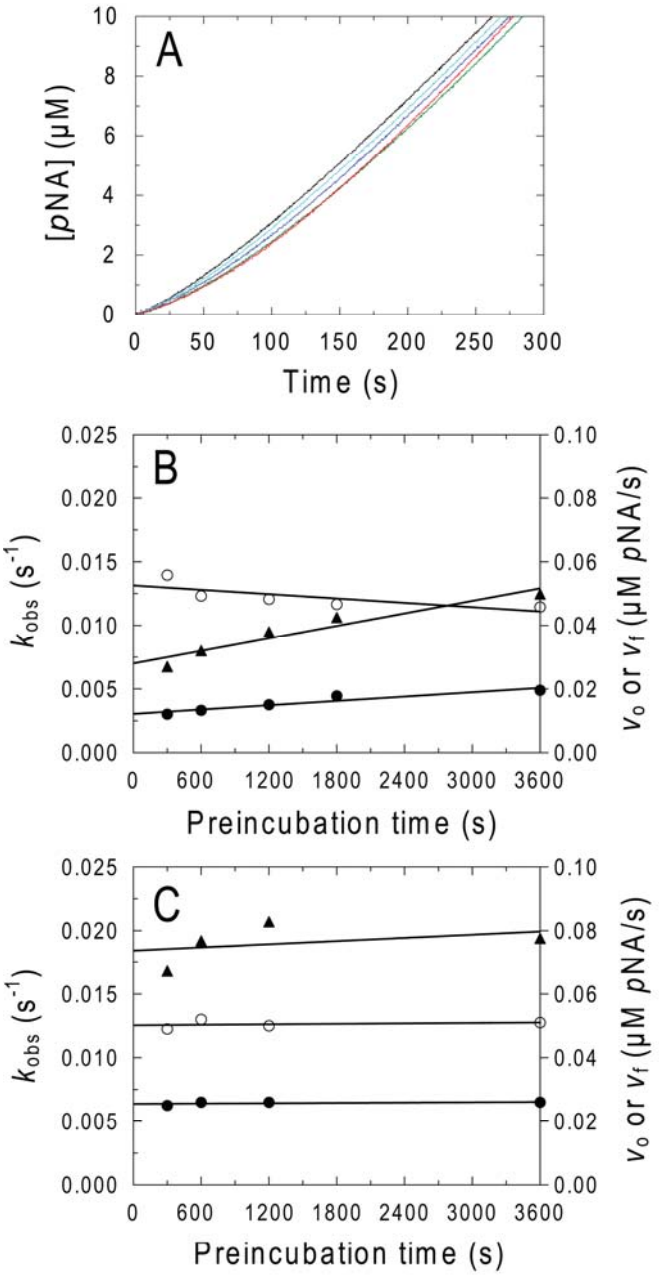

Figure 4S. Analysis of activation progress curves as a function of preincubation time of ProT or Pre 1 with VWbp(1-263) in the absence of substrate. (A) Progress curves of hydrolysis of 200 μM *D*-Phe-Pip-Arg-*p*NA (*pNA*) initiated by addition of substrate to mixtures of 1 nM ProT and 10 μM VWbp preincubated for 5 (*red*), 10 (*green*), 20 (*dark blue*), 30 (*light blue*), and 60 min (*black*). (B and C) Parameters for ProT or Pre 1 (1 nM) preincubated for the indicated time with 10 μM VWbp before addition of 200 μM *D*-Phe-Pip-Arg-*p*NA. (B) v_o (●) , v_f (○), and k_{obs} (▲) as a function of preincubation time for ProT reactions, and (C) Pre 1 reactions as in B. The *lines* represent linear least-squares fits.

and ProT·VWbp complexes. This contrasts the observations of Kawabata and coworkers for SC and a fluorogenic substrate (35). As can be seen by the raw data (Fig. 4S *A*), where the ordinate maximum represents 0.1 $A_{405\ nm}$, the indistinguishable chromogenic substrate activity of the Pre 1·VWbp and ProT·VWbp complexes, and the small effects of low levels of Pre 1 generation on the hysteresis parameters resulted in only modest changes in the shapes of the curves, which were within experimental error.

We conclude that the hysteretic kinetic behavior of ProT activation by VWbp cannot be accounted for by autocatalytic generation of Pre 1. The close correspondence between the best fit parameters of the mechanism in Scheme 1 in the paper that are independent of both chromogenic substrates, K_D, k_{C1}, and k_{C2}, strengthens the conclusion that relatively low levels of Pre 1 generation did not substantively affect the validity of the concluded hysteretic mechanism of ProT activation by VWbp.

Materials and Methods

SDS-gel Electrophoresis and Western Blotting

Time-course reactions were performed in 50 mM Hepes, 110 mM NaCl, 5 mM $CaCl_2$, 1 mg/ml PEG 8000, pH 7.4 at 25 ^oC. Samples were quenched directly into hot SDS treatment buffer containing 2-mercaptoethanol, boiled for 2 min, and separated on 4-15% gradient gels (Biorad). The protein bands were transferred onto polyvinyldiene difluoride membranes in Tris-glycine buffer containing 10% (v/v) methanol, and the membranes were blocked for 2 h in 50 mM Tris, 150 mM NaCl, pH 7.5, 0.1% (v/v) Tween-20 (TBS-T) containing 5% (w/v) nonfat dry milk. The membranes were incubated with a 1:500 dilution of anti-ProT polyclonal antibody (Abcam, ab48627) overnight, washed with TBS-T, and incubated with goat anti-rabbit IRDye 680 (Li-Cor) for 2 h. After

thorough washing of the membranes in TBS-T, the bands were visualized using a Li-Cor Odyssey Infrared Imaging System in the 700 nm detection channel.

Image Analysis and Quantitation

The integrated intensity for each detected band was determined with the Odyssey Imager software (v3.0). The signal ratio for the equimolar mixtures of ProT and Pre 1 (*S1*, *S2*) was used to correct the intensity of the Pre 1 bands for each lane to that of ProT, and the percentage of each band relative to the total intensity of each lane was calculated.

Progress Curve Analysis

Individual progress curves were collected in 50 mM Hepes, 110 mM NaCl, 5 mM $CaCl_2$, 1 mg/ml PEG 8000, pH 7.4 at 25 °C, truncated to ≤ 5 % substrate depletion, and fit by the hysteresis equation (Eqn. 1) as described in the Materials and Methods section of the chapter. Progress curves were collected as a function of preincubation time for mixtures of 10 μM VWbp(1-263) and 1 nM ProT or Pre 1, initiated by addition of 200 μM *D*-Phe-Pip-Arg-*p*NA.

Supplementary Data (Unpublished)

Effect of VWbp and SC on platelet aggregation and secretion

Rapid clotting of human plasma has been demonstrated for SC and VWbp, which is elicited by the formation of active ProT complexes with the bacterial proteins that directly bind and cleave fibrinogen into fibrin. The ProT-activator complexes can display this thrombin-like activity, despite restricted specificity for several typical thrombin substrates. Thrombin is known to activate platelets through their surface-bound protease-activated receptors (PARs) (36), and some early studies on SC explored its effect on basic platelet aggregation, but no conclusive association was found (37). Whether SC and VWbp have the capacity to trigger platelet aggregation and/or activation has not been fully investigated. Consequently, both proteins were assessed for platelet-specific activity in human platelet-rich plasma (PRP) and isolated washed platelets.

Platelet aggregation and activation were measured in an optical lumi-aggregometer (Chrono-Log) with the assistance of Dr. David Gailani in the Clinical Coagulation Laboratory at Vanderbilt University. Aggregation was monitored by optical density, and activation was simultaneously detected through the increase in fluorescence of a luciferase/luciferin reagent (Chrono-Lume®), an effect generated by the release of ATP from the dense granules of the activated platelets. PRP was produced from citrated whole blood, which was centrifuged at 900 rpm for 15 min and adjusted to ~300,000 cells/mL with platelet-poor plasma for use. Washed gel-filtered platelets were also isolated from PRP from citrated whole blood, which was subjected to additional centrifugation steps to gently pellet the cells. The cells were washed with Tyrode's buffer (126 mM NaCl, 2.7 mM KCl, 0.98 mM $MgCl_2$, 0.376 mM NaH_2PO_4, 15 mM HEPES, 5.6 mM dextrose, 0.35% BSA, pH 6.5), and citric acid and inhibitors were

added to prevent activation during purification. The platelet solution was applied to a Sepharose CL-4B gel-filtration column equilibrated in Tyrode's buffer (pH 7.4), and the filtered platelets were collected and counted. All platelet solutions were used within 3 h of preparation. VWbp(1-474) and SC(1-325) were diluted into 50 mM HEPES, 125 mM NaCl, pH 7.4 buffer, and varying concentrations of either protein were added to 450 µL of PRP or washed platelets with 50 µL of luciferase reagent. All data were collected at 37 ^{o}C with constant stirring in the aggregometer cuvette.

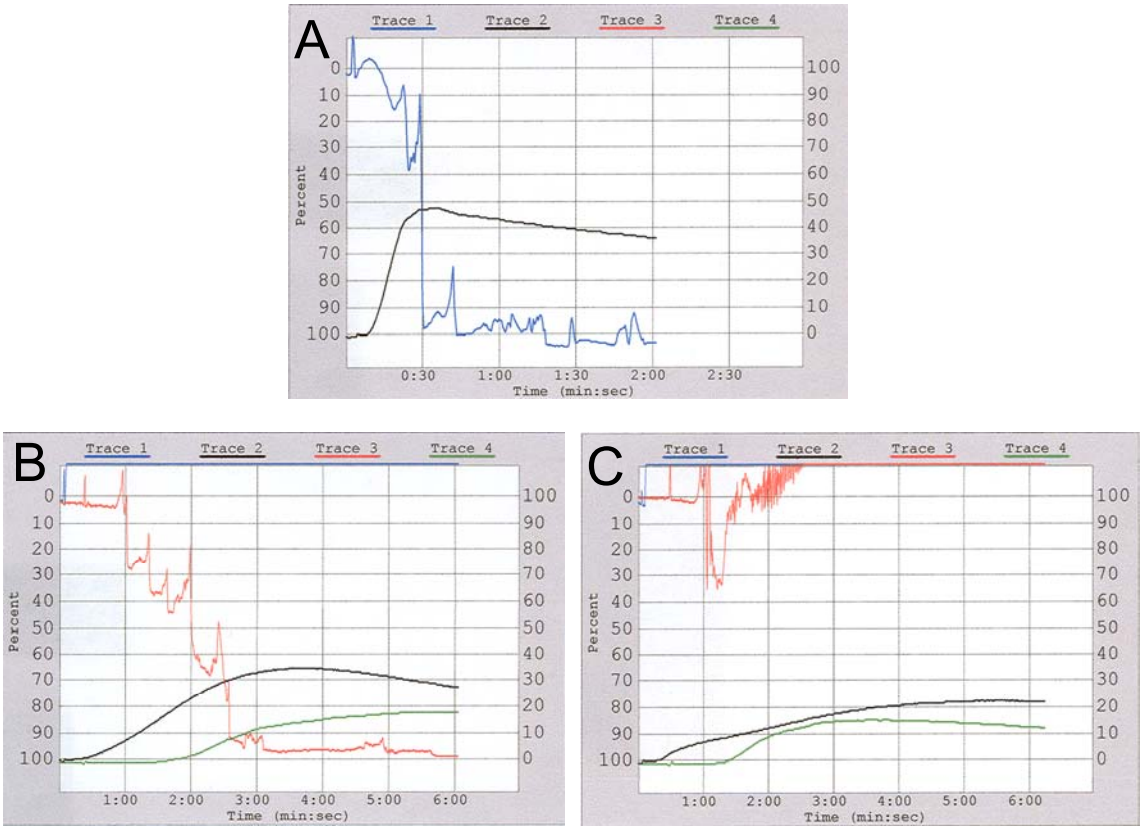

Figure 5S. Platelet aggregation and activation in PRP. (A) Thrombin standard showing characteristic rapid aggregation (*blue*) and dense granule ATP release (*black*). (B) Assays with SC(1-325), representative of rapid clotting of the plasma (*blue*, *red*) with slow ATP release at both 1 µM (*black*) and 10 µM SC (*green*). (C) VWbp(1-474) also rapidly forms a plasma clot (*blue*, *red*), but with even more delayed granule release at 2 µM (*black*) and 20 µM VWbp (*green)*.

Initial assays with PRP indicated that SC and VWbp quickly generated fibrin clots, detected by the change in optical density of the plasma. Addition of either bacterial protein also prompted a very slow activation response, illustrated by the relatively delayed release of the dense granule ATP (Fig. 5S *B and C*) compared to the thrombin control (Fig. 5S *A*). A second set of assays was performed with washed gel-filtered platelets to isolate the interactions of SC/VWbp with the platelets themselves. Upon addition of low concentrations of equimolar mixtures of ProT and SC or VWbp, no activation was detected. When a relatively high concentration of ProT·SC was used (1 μM), extremely slow granule release (after 8-10 min, data not shown) was measured, but this could not be replicated by higher (2 μM) concentrations of ProT·VWbp. A final set of assays was carried out with PRP in the presence of the therapeutic thrombin inhibitor lepirudin (hirudin) or the factor XIa blocking antibody O1A6 to rule out thrombin or factor XIa involvement. Slow granule release by SC and VWbp was again detected, which could not be blocked by lepirudin or O1A6. Comparison of these traces to those generated by reptilase, a snake venom enzyme which directly cleaves fibrinopeptide A from fibrinogen to cause clotting (38, 39), revealed a comparable slow release of granule ATP (not shown).

The pattern of slow platelet activation in the presence of SC and VWbp suggested that addition of the proteins to PRP triggered a process which resulted in granule release, but the absence of activation with the filtered platelet preparation ruled out a specific interaction of the active ProT·VWbp complex with receptors on the platelets. Release could be mediated by other enzymatic species in the plasma, but any contribution from trace amounts of thrombin or factor XIa was eliminated by the use of inhibitors and blocking antibodies. The ability of reptilase to generate similar slow platelet granule release, even though this enzyme interacts directly with fibrinogen to form a clot, indicates that such low level activity SC and VWbp is likely the result of an

interaction of the fibrin clot itself with the platelets. The fibrinogen receptor on platelets, integrin $\alpha_{IIb}\beta_3$, undergoes both local conformational changes and relocalization on the platelet surface during cell activation, which allows a high affinity interaction with the adhesion protein that affects cellular signaling (40). But rapid formation of a dense clot, such as that seen with SC and VWbp, could trap quiescent platelets within the fibrin mesh. Through processes that may be related to the activation of platelets on adsorbed fibrinogen and plasma proteins (41, 42), this could result in integrin activation that would produce minor levels of platelet activation, but be independent of specific PAR or integrin interactions with the ProT·SC or ProT·VWbp complex.

Autocatalytic proteolysis in mixtures of ProT and VWbp

Time-dependent conversion of ProT to the proteolytic derivatives Pre 1 and prethrombin 2' (Pre 2') has been shown to occur in mixtures of fluorescently-labeled (active site-blocked) ProT, native ProT, and SC(1-325) (24). The same pattern of proteolysis has been identified in mixtures of native ProT and VWbp(1-263) (43), suggesting a similar autocatalytic activity is generated within the conformationally activated ProT complexes. To explore whether cleavage of the thrombin-sensitive bonds between ProT fragment 1 and fragment 2 is occurring through intra- or intermolecular proteolysis, reactions containing both native and active site-blocked ProT analogs were examined to see whether species incapable of proteolysis were also converted to the smaller derivatives. Reactions containing Oregon Green-488-FPR-ProT (4 μM) and native ProT (4 μM) were initiated by addition of either VWbp(1-263) (16 μM) or VWbp(1-474) (8 μM) in 50 mM HEPES, 110 mM NaCl, 5 mM $CaCl_2$, 1 mg/mL PEG 8000, pH 7.4, and incubated at 25 ^{o}C. Samples were taken periodically up to 3 h and immediately quenched with Phe-Pro-Arg-CH_2Cl and hot SDS-PAGE loading buffer. The reactions were incubated overnight before a final sample was collected, then

samples for all time-points were examined by SDS-PAGE. The gels were visualized for fluorescence, followed by staining with Gel-Code Blue (Pierce) protein stain.

Both the fluorescence and protein-stained gels show fairly rapid generation of Pre 1 in both reactions, with much slower appearance of Pre 2', consistent with what had been previously observed with SC(1-325) (Fig. 6S). In mixtures with VWbp(1-263), all of the ProT is converted to Pre 2' after overnight incubation (Fig. 6S *B*), but a slightly different time-course is seen with VWbp(1-474). In this reaction, Pre 1 is formed rapidly, but the second cleavage event at Arg^{284} appears to occur at a much slower rate, with

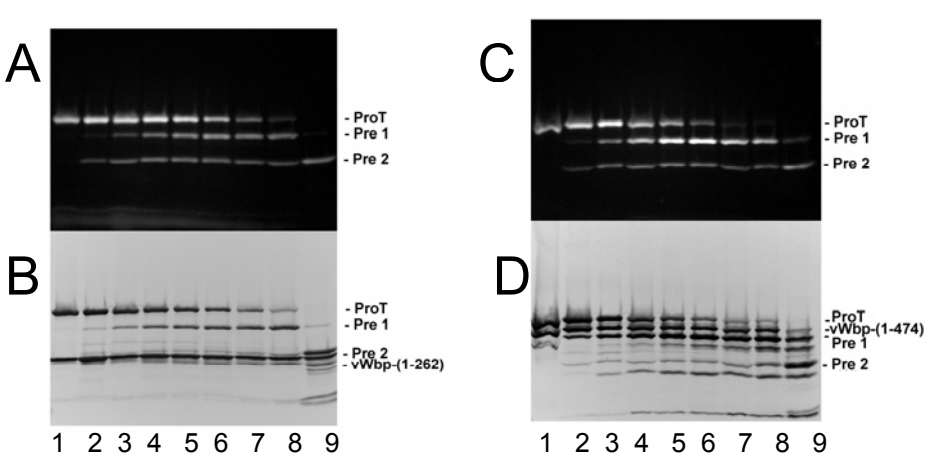

Figure 6S. Autocatalytic cleavage of ProT in the presence of VWbp(1-263) or VWbp(1-474). Time-course reactions of mixtures of Oregon Green 488-FPR-ProT (4 μM), native ProT (4 μM), and 16 μM VWbp(1-263) (A, B) or 8 μM VWbp(1-474) (C, D). Figure shows the fluorescent (A, C) and stained protein bands (B, D) for both reactions. Samples were removed at 0, 5, 20, 40, 60, 90, 120, and 180 min (*lanes 1-8*) and after 18 h (*lane 9*), and analyzed by SDS-PAGE.

some Pre 1 remaining after 18 h (Fig. 6S *D*). This may be the result of the COOH-terminal half of VWbp altering accessibility of this cleavage site through interactions with the fragment domains of ProT, something which would not occur with VWbp(1-263). The fact that all of both the native and active site-blocked ProT is proteolytically

converted indicates that intermolecular events play a significant role in the autocatalysis of ProT·VWbp.

References

1. Bode W & Huber R (1976) Induction of the bovine trypsinogen-trypsin transition by peptides sequentially similar to the N-terminus of trypsin. *FEBS Lett.* 68(2):231-236.

2. Huber R & Bode W (1978) Structural basis of the activation and action of trypsin. *Acc. Chem. Res.* 11:114-122.

3. Bode W (1979) The transition of bovine trypsinogen to a trypsin-like state upon strong ligand binding: II. The binding of the pancreatic trypsin inhibitor and of isoleucine-valine and of sequentially related peptides to trypsinogen and to *p*-guanidinobenzoate-trypsinogen. *J. Mol. Biol.* 127:357-374.

4. Pasternak A, Liu X, Lin T-Y, & Hedstrom L (1998) Activating a zymogen without proteolytic processing: Mutation of Lys 15 and Asn194 activates trypsinogen. *Biochemistry* 37:16201-16210.

5. Madison EL, Kobe A, Gething M-J, Sambrook JF, & Goldsmith EJ (1993) Converting tissue plasminogen activator to a zymogen: A regulatory triad of Asp-His-Ser. *Science* 262:419-421.

6. Kawabata S-I, Morita T, Iwanaga S, & Igarashi H (1985) Enzymatic properties of staphylothrombin, an active molecular complex formed between staphylocoagulase and human prothrombin. *J. Biochem. (Tokyo)* 98(6):1603-1614.

7. Kawabata S-I & Iwanaga S (1994) Structure and function of staphylothrombin. *Seminars in Thrombosis and Hemostasis* 20(4):345-350.

8. Kaida S*, et al.* (1987) Nucleotide sequence of the staphylocoagulase gene: Its unique COOH-terminal 8 tandem repeats. *J. Biochem. (Tokyo)* 102:1177-1186.

9. Heilmann C, Herrmann M, Kehrel BE, & Peters G (2002) Platelet-binding domains in 2 fibrinogen-binding proteins of *Staphylococcus aureus* identified by phage display. *J. Infect. Dis.* 186:32-39.

10. Mylonakis E & Calderwood SB (2001) Infective endocarditis in adults. *N. Engl. J. Med.* 345(18):1318-1330.

11. Bjerketorp J*, et al.* (2002) A novel von Willebrand factor binding protein expressed by *Staphylococcus aureus*. *Microbiology* 148:2037-2044.

12. Panizzi P, Friedrich R, Fuentes-Prior P, Bode W, & Bock PE (2004) The staphylocoagulase family of zymogen activator and adhesion proteins. *Cell. Mol. Life Sci.* 61:1-6.

13. Friedrich R*, et al.* (2003) Staphylocoagulase is a prototype for the mechanism of cofactor-induced zymogen activation. *Nature* 425:535-539.

14. Bjerketorp J, Jacobsson K, & Frykberg L (2004) The von Willebrand factor-binding protein (vWbp) of *Staphylococcus aureus* is a coagulase. *FEMS Microbiol. Lett.* 234:309-314.

15. Wang S, Reed GL, & Hedstrom L (1999) Deletion of Ile1 changes the mechanism of streptokinase: Evidence for the molecular sexuality hypothesis. *Biochemistry* 38:5232-5240.

16. Bock PE (1993) Thioester peptide chloromethyl ketones: reagents for active site-selective labeling of serine proteinases with spectroscopic probes. *Methods Enzymol.* 222:478-503.

17. Frieden C (1970) Kinetic aspects of regulation of metabolic processes: The hysteretic enzyme concept. *J. Biol. Chem.* 245(21):5788-5799.

18. Frieden C (1979) Slow transitions and hysteretic behavior in enzymes. *Annu. Rev. Biochem.* 48:471-489.

19. Kuzmic P (1996) Program DYNAFIT for the analysis of enzyme kinetic data: Application to HIV proteinase. *Anal. Biochem.* 237:260-273.

20. Panizzi P*, et al.* (2006) Novel fluorescent prothrombin analogs as probes of staphylocoagulase-prothrombin interactions. *J. Biol. Chem.* 281(2):1169-1178.

21. Anderson PJ, Nesset A, Dharmawardana KR, & Bock PE (2000) Characterization of proexosite I on prothrombin. *J. Biol. Chem.* 275(22):16428-16434.

22. Kawabata S-I*, et al.* (1987) Structure and function relationship of staphylocoagulase. *J. Protein Chem.* 6(1):17-32.

23. Neet KE & Ainslie GR (1980) Hysteretic Enzymes. *Methods Enzymol.* 64:192-227.

24. Panizzi P*, et al.* (2006) Fibrinogen substrate recognition by staphylocoagulase-(pro)thrombin complexes. *Journal of Biological Chemistry* 281(2):1179-1187.

25. Bock PE, Panizzi P, & Verhamme IMA (2007) Exosites in the substrate specificity of blood coagulation reactions. *J. Thromb. Haemost.* 5 (Suppl. 1):81-94.

26. Page MJ, MacGillivray RTA, & Di Cera E (2005) Determinants of specificity in coagulation proteases. *J. Thromb. Haemost.* 3:1-8.

27. Fersht AR (1972) Conformational equilibria in α- and δ-chymotrypsin. The energetics and importance of the salt bridge. *J. Mol. Biol.* 64:497-509.

28. Zhang P, Pan W, Rux AH, Sachais BS, & Zheng XL (2007) The cooperative activity between the carboxyl-terminal TSP1 repeats and the CUB domains of ADAMTS13 is crucial for recognition of von Willebrand factor under flow. *Blood* 110(6):1887-1894.

29. Ruggeri ZM (2003) Von Willebrand factor, platelets, and endothelial cell interactions. *J. Thromb. Haemost.* 1:1335-1342.

30. Ruggeri ZM, De Marco L, Gatti L, Bader R, & Montgomery RR (1983) Platelets have more than one binding site for von Willebrand factor. *J. Clin. Invest.* 72:1-12.

31. Hauck CR & Ohlsen K (2006) Sticky connections: extracellular matrix protein recognition and integrin-mediated cellular invasion by *Staphylococcus aureus*. *Curr. Opin. Microbio.* 9:5-11.

32. Bock PE, Olson ST, & Bjork I (1997) Inactivation of thrombin by antithrombin is accompanied by inactivation of regulatory exosite I. *J. Biol. Chem.* 272(32):19837-19845.

33. Panizzi P, Boxrud PD, Verhamme IMA, & Bock PE (2006) Binding of the COOH-terminal lysine residue of streptokinase to plasmin(ogen) kringles enhances formation of the streptokinase.plasmin(ogen) catalytic complexes. *J. Biol. Chem.* 281(37):26774-26778.

34. Pace CN, Vajdos F, Fee L, Grimsley G, & Gray T (1995) How to measure and predict the molar absorption coefficient of a protein. *Protein Science* 4:2411-2423.

35. Kawabata S, Morita T, Iwanaga S, & Igarashi H (1985) Enzymatic properties of staphylothrombin, an active molecular complex formed between staphylocoagulase and human prothrombin. *J. Biochem. (Tokyo)* 98(6):1603-1614.

36. Coughlin SR (1999) Protease-activated receptors and platelet function. *Thromb. Haemostasis* 82(2):353-356.

37. Semeraro N, Fumarola D, Pasquetto N, & Vermylen J (1974) Platelet aggregation and clot retraction by two preparations of staphylocoagulase. *Thromb. Res.* 4:819-827.

38. Stocker K & Barlow GH (1976) The coagulant enzyme from *Bothrops atrox* venom (batroxobin). *Methods Enzymol.* 45:214-223.

39. Meh DA, Siebenlist KR, Bergtrom G, & Mosesson MW (1993) Comparison of the sequence of fibrinopeptide A cleavage from fibrinogen fragment E by thrombin, atroxin, or batroxobin. *Thromb. Res.* 70:437-449.

40. Jackson SP (2007) The growing complexity of platelet aggregation. *Blood* 109:5087-5095.

41. Skarja GA, Brash JL, Bishop P, & Woodhouse KA (1998) Protein and platelet interactions with thermally denatured fibrinogen and cross-linked fibrin coated surfaces. *Biomaterials* 19:2129-2138.

42. Grunkemeier JM, Tsai WB, McFarland CD, & Horbett TA (2000) The effect of adsorbed fibrinogen, fibronectin, von Willebrand factor and vitronectin on the procoagulant state of adherent platelets. *Biomaterials* 21:2243-2252.

43. Kroh HK, Panizzi P, & Bock PE (2009) Von Willebrand factor binding-protein is a hysteretic conformational activator of prothrombin. *Proc. Natl. Acad. Sci. U. S. A.* 106(19):7786-7791.

CHAPTER III

EFFECT OF ZYMOGEN DOMAINS AND ACTIVE SITE OCCUPATION ON ACTIVATION OF PROTHROMBIN BY VON WILLEBRAND FACTOR-BINDING PROTEIN

Heather K. Kroh and Paul E. Bock

Department of Pathology, Vanderbilt University School of Medicine, Nashville, TN 37232-2561

Abstract

Prothrombin (ProT) is conformationally activated by von Willebrand factor-binding protein (VWbp) from *Staphylococcus aureus* through insertion of the NH_2-terminal residues of VWbp into the ProT catalytic domain. The rate of ProT activation by VWbp(1-263) has been shown to be controlled by a hysteretic kinetic mechanism initiated by substrate binding, and the present study evaluates activation of ProT by full-length VWbp(1-474) through activity progress curve analysis. Additional interactions from the COOH-terminal half of VWbp(1-474) strengthened the initial binding of VWbp to ProT, resulting in higher activity and an ~100-fold enhancement in affinity. The affinities of VWbp(1-263) or VWbp(1-474) were compared by equilibrium binding to the ProT derivatives prethrombin 1 (Pre 1), prethrombin 2, thrombin, meizothrombin, and meizothrombin desF1, and their corresponding active site-blocked analogs. In particular, loss of fragment 1 in Pre 1 enhanced affinity for both VWbp(1-263) and VWbp(1-474), resulting in a 12-26% increase in Gibbs free energy, implicating a regulatory role for fragment 1 in the activation mechanism. Active site labeling of all ProT derivatives with D-Phe-Pro-Arg-chloromethyl ketone, analogous to binding of a substrate, decreased their K_D's for VWbp into the subnanomolar range, reflecting the dependence of the activating conformational change on substrate binding. Further, generation of ProT proteolysis products in the presence of VWbp in human plasma was characterized by western blotting and demonstrated slow autocatalytic generation of Pre 1. The results suggest a role for ProT domains in the potential pathophysiological activation of ProT by VWbp, and may reveal a function for autocatalysis of the ProT•VWbp complexes during initiation of blood coagulation.

Introduction

As the inactive precursor of the serine proteinase thrombin, the zymogen prothrombin (ProT) occupies a central role in the regulation of blood coagulation. Sequential activation of upstream coagulation factors provides a web of feedback reactions which function in the temporal and spatial control of thrombin production, but additional mechanisms exist which modify the function of thrombin itself in response to specific physiological environments. Allostery, the regulation of protein function through binding of a ligand or another protein to a site distal from the active site (1), is a principal modulator of proteinase activity, and a large number of allosteric ligands have been identified for thrombin (2). A high degree of allosteric linkage has been found between the catalytic site of thrombin and the two electropositive exosites I and II that mediate substrate, inhibitor, and regulatory cofactor interactions with thrombin. The function of exosite I in particular is linked with proper formation of the active site following proteolysis of ProT at Arg^{320}-Thr^{321} (3-4), from a lower affinity conformation of this exosite (proexosite I) in the zymogen (5-6).

Comparable to what is observed with many proteinases, ProT exhibits a continuum of conformational changes in response to direct proteolytic events that can alter the specificity of exosite I for its ligands, such as the lower activity and affinity for fibrinogen seen with MzT (7). Loss of the two smaller domains of ProT (fragments 1 and 2) during activation exposes exosite II and may produce conformational shifts that affect association of other ligands, although this long distance effect has been debated (8-9). Conversely, the action of ligand binding to the exosites can change the recognition of substrates by the active site, as illustrated by the capacity of thrombomodulin to switch thrombin from procoagulant to anticoagulant by targeting cleavage of protein C (10). Thrombin ligands can interact with only one of the exosites to affect thrombin activity, or with both exosites through different regions of the ligand itself. The platelet receptor

GP1b binds to both exosite I and II through distinct regions on the receptor (11-12), yielding a two-pronged but linked association with the exosites that may generate responses unique from those seen with binding of a single exosite. Furthermore, allostery not only influences the interactions of thrombin with substrates, inhibitors, and regulatory macromolecules, but it also impacts binding of exogenous ligands such as the leech-derived inhibitor hirudin and some effectors from snake venoms (2).

The human pathogen *Staphylococcus aureus* is known to secrete two proteins which can each interact with (pro)exosite I on ProT, staphylocoagulase (SC) and von Willebrand factor-binding protein (VWbp) (13-15). Both are potent procoagulant factors capable of triggering rapid clotting of human plasma through direct cleavage of fibrinogen into fibrin by the ProT-activator complex, but this activity is not reliant on proteolysis of the activation loop of ProT. Instead, conformational activation of the zymogen occurs through direct binding interactions with the activator and, ultimately, insertion of the NH_2-terminus of either SC or VWbp into the NH_2-terminal binding cleft in the catalytic domain of ProT (15-16), forming the salt bridge with Asp^{194} (chymotrypsinogen numbering) that is characteristic of proteolytic activation (3). In contrast to the usually minor effects seen with other ligands, binding of SC or VWbp to ProT generates what could be described as a definitive allosteric transition, where an inactive zymogen precursor is completely converted to an active species though a non-proteolytic alternative to its common activation pathway.

In a previous study, we described the molecular mechanism of VWbp procoagulant activity, and in addition, identified the role for a distinctive substrate-induced hysteretic kinetic mechanism for activation of ProT by VWbp (15). Hysteresis has been classically defined for a number of regulatory metabolic enzymes as a slow transition or conformational change initiated by various processes, including polymerization and ligand displacement (17-18). The key initiator of hysteretic behavior

in VWbp-mediated ProT activation is a tight-binding substrate that alters a conformational equilibrium between inactive and active forms of the ProT·VWbp complex (15), which represents the first example of such hysteretic control in serine proteinase activation.

In addition to the recognized effect of substrate, preliminary kinetic and binding data indicated that the presence of the fragment domains of ProT, in particular fragment 1, imparts either a steric or allosteric impediment to fully productive binding of VWbp. The present study defines the contribution to protein-protein affinity of fragment 1 and 2 and the catalytic domain of ProT, and the predominantly unstructured COOH-terminal half of VWbp, as well as the magnitude of influence that active site occupation by a structural substrate mimic has on the binding behavior of VWbp. The preferential binding of certain ProT proteolysis products to VWbp likely has a significant influence on the pathophysiolgical behavior of VWbp, and may be essential to understanding its potential role as a staphylococcal virulence factor.

Experimental Procedures

Materials

HEPES was purchased from Research Organics (Cleveland, OH), and *D*-Phe-Pro-Arg-CH_2Cl (FPR-CH_2Cl) and Gly-Pro-Arg-Pro peptide (GPRP) were purchased from Bachem (Torrance, CA). H-*D*-Phe-Pip-Arg-*p*NA was obtained from Diapharma (West Chesterfield, OH). Purified ecarin, the ProT activator from the venom of *Echis carinatus*, was purchased from Pentapharm (Basal, Switzerland). Dansylarginine N-(3-ethyl-1,5-pentanediyl)amide (DAPA) was from Haematologic Technologies, Inc. (Essex Junction, VT). Tetramethylrhodamine-5-iodoacetamide dihydroiodide (5-TMRIA) was from Invitrogen (Carlsbad, CA). The rabbit polyclonal antibody directed against full length native human ProT (ab48627) was purchased from Abcam (Cambridge, MA), and

fluorescent secondary goat anti-rabbit IR 680 antibodies were from LI-COR Biosciences (Lincoln, NE). Immobilon-FL polyvinyldiene difluoride (PVDF) membranes were purchased from Millipore Corp. (Billerica, MA). Human factor I-deficient plasma was purchased from George King Biomedical, Inc. (Overland Park, KS).

Proteins

VWbp(1-263) and VWbp(1-474) were expressed and purified as described previously (15). Y^{63}-sulfated, fluorescein-labeled hirudin (54-65) ([5F]Hir(54-65)) was prepared as described (19). Native human ProT, Pre 1, and T were purified according to established procedures (4, 20). Native human Pre 2 was prepared by a modification of published methods (4, 21), adding a final chromatography step on a HiPrep 16/10 SP XL cation-exchange column (GE Healthcare) in 50 mM MES, 50 mM NaCl, pH 6.0 buffer. Pre 2 was separated from residual inhibited thrombin with a 0-700 mM NaCl gradient, concentrated, and dialyzed into 50 mM HEPES, 125 mM NaCl, pH 7.4 buffer for storage. The active site-blocked (FPR-) analogs and [TMR]FPR-ProT was produced by established methods (13, 20). Absorption coefficients ($E_{0.1\%}$ 280 nm) and molecular weights of the ProT derivatives used were as follows: ProT, 1.47 and 71,600; Pre 1, 1.78 and 49,900; Pre 2, 1.73 and 37,000; T, 1.74 and 36,600; MzT, 1.47 and 71,600; MzT(-F1), 1.78 and 49,900.

Preparation of recombinant MzT and FPR-MzT

A HEK-293 cell line stably transfected with a pCDNA 3.1 expression vector containing the recombinant human ProT(R155Q/R271Q/R284Q) mutant ($rProT_{QQQ}$) construct (22) was kindly provided by Dr. Sriram Krishnaswamy (Children's Hospital of Philadelphia, PA). The rProT mutant was expressed and purified as previously described (23), and stored in 5 mM MES, 150 mM NaCl, pH 6.0. To generate stable active MzT_{QQQ}, $rProT_{QQQ}$ (20 μM) was incubated with purified ecarin (6 EU/mL) and 200 μM DAPA in 0.1 M HEPES, 0.1 M NaCl, 1 mg/mL PEG 8000, pH 7.4, supplemented with

1/10 volume of 1 M HEPES, pH 7.6, for 2 h at 25 °C. The reaction was quenched by addition of 50 mM EDTA and immediately diluted 5-fold with 20 mM MES, 20 mM NaCl, pH 6.0 buffer. The MzT_{QQQ} was separated from residual unreacted $rProT_{QQQ}$ and ecarin by chromatography on a 1-ml Resource Q column (GE Healthcare) in 20 mM MES, pH 6.0 buffer, eluted with a 0-0.5 M NaCl gradient (24). To produce FPR-MzT_{QQQ}, a portion of the active enzyme was incubated with a 10-fold molar excess of FPR-CH_2Cl for 1 h at 22 °C. Active MzT_{QQQ} and FPR-MzT_{QQQ} were dialyzed against 5 mM MES, 150 mM NaCl, pH 6.0 buffer, and stored at -80 °C.

Preparation of FPR-MzT(-F1)

Native Pre 1 (20 μM) was activated by ecarin (6 EU/mL) in the presence of FPR-CH_2Cl (200 μM) for 2 h at 25 °C, and activation was quenched by addition of 50 mM EDTA. The quenched reaction was dialyzed overnight against 25 mM NaH_2PO_4, pH 6.5, and loaded onto an SP-Sephedex C-50 column equilibrated with the same buffer. Unreacted Pre 1 was eluted with 50 mM NaH_2PO_4, pH 6.5, followed by elution of FPR-MzT(-F1) with a 50 mM-300 mM NaH_2PO_4 gradient (24). The peak was pooled, concentrated, and dialyzed against 5 mM MES, 150 mM NaCl, pH 6.0, for storage.

Kinetic titrations of ProT activation

Full time-course progress curves for activation of ProT by VWbp(1-474) were collected, monitoring the rate of hydrolysis of H-*D*-Phe-Pip-Arg-*p*NA (S-2238) at 405 nm and 25 °C. Reactions contained either 1 nM ProT, varying concentrations of VWbp(1-474), and 200 μM H-*D*-Phe-Pip-Arg-*p*NA, or 1 nM ProT, 10 nM VWbp(1-474), and varying concentrations of H-*D*-Phe-Pip-Arg-*p*NA. Data were collected for 1 h, or until $A_{405\ nm}$ = 1.0. The progress curves of *p*-nitroaniline formation were analyzed by simultaneous nonlinear least-squares fitting in KinTek Global Kinetic Explorer using the hysteretic kinetic model described previously (15), assuming diffusion-controlled rapid equilibrium binding steps.

Fluorescence titrations with active ProT derivatives

Continuous fluorescence measurements were taken in 50 mM HEPES, 110 mM NaCl, 5 mM $CaCl_2$, 1 mg/mL PEG 8000, pH 7.4 at 25 ^oC. Fluorescence was monitored for a buffer blank, [5F]Hir(54-65) alone, after addition of VWbp(1-263) or VWbp(1-474), and immediately after addition of Pre 1, Pre 2, T, or MzT_{QQQ}. Data were collected with either a SLM 8100 or PTI QuantaMaster spectrofluorometer at λ_{ex} = 491 nm and λ_{em} = 520 nm. The fractional change in fluorescence was calculated as $(F_{obs} - F_o)/F_o = \Delta F/F_o$, and the data for each experiment were fit globally with the cubic equation for tight competitive binding to obtain the dissocation constants for each competitor and the stoichiometric factor. The Gibbs free energy of binding ($\Delta G_{binding}$) was calculated, using the equation $\Delta G_{binding} = RT\ln(K_D)$, where R = 1.98 $cal \cdot mol^{-1} \cdot degree^{-1}$ and T = 298.15 K (25 ^oC).

In situ production of MzT(-F1)

Because autocatalysis of thrombin-sensitive cleavage sites within ProT or Pre 1 occurs rapidly during conversion to MzT or MzT(-F1), active MzT(-F1) was produced *in situ* during the fluorescence experiments through activation of native Pre 1 by ecarin. Control time-course gel experiments mimicking the conditions used for the binding assays showed complete conversion of Pre 1 to MzT(-F1) within 20 min, with no detectable degradation of the proteins over this time period. Fluorescence measurements were collected in the same manner as for the active ProT derivatives above, but with inclusion of ecarin (2 EU/mL) in the cuvette before addition of Pre 1 and measurement of the final fluorescence values at 20 min after initiation of activation.

Fluorescence titrations with active-site blocked ProT derivatives

Titrations were performed in 50 mM HEPES, 110 mM NaCl, 5 mM $CaCl_2$, 1 mg/mL PEG 8000, pH 7.4, 1 mg/mL BSA, 10 μM FPR-CH_2Cl at 25 ^oC. Increasing concentrations of either VWbp(1-263) or VWbp(1-474) were titrated in the presence of

fixed concentrations of [TMR]FPR-ProT and either FPR-ProT, FPR-Pre 1, FPR-Pre 2, FPR-T, FPR-MzT_{QQQ}, or FPR-MzT(-F1). Data were collected at λ_{ex} = 558 nm and λ_{em} = 580 nm, with the fractional change in fluorescence, binding parameters, and free energy calculated as for the active ProT derivatives.

Western Blots with Factor I-deficient Human Plasma

Reactions contained 50% citrated human factor I-deficient plasma, 24 mM $CaCl_2$, 5 mM GPRP, and either 10 μM VWbp(1-263) or 1 μM VWbp(1-474) in 50 mM HEPES, 110 mM NaCl, 5 mM $CaCl_2$, 1 mg/mL PEG, pH 7.4. Incubations were performed at 25 ^oC for 1 h. Samples were removed from the reactions every 10 min, immediately quenched into hot SDS-PAGE loading buffer, and boiled for 2 min. Quenched reactions and standards were electrophoresed on 4-15% Tris-glycine gradient gels, and transferred to Immobilon-FL polyvinyldiene difluoride (PVDF) membranes in Tris/glycine western transfer buffer containing 10% methanol. Membranes were blocked for 1 h in 20 mM Tris, 150 mM NaCl, pH 7.5, 0.1% Tween-20 (TBS-T) containing 5% dry milk, washed with TBS-T, and incubated overnight with a primary rabbit anti-human ProT antibody (ab48627). The membranes were washed with TBS-T and incubated for 1 h with a goat anti-rabbit secondary LI-COR IR 680 antibody. Bands were visualized using a LI-COR Odyssey Infrared Imaging System in the 700-nm detection channel.

Results

Kinetic analysis of ProT activation by VWbp(1-474)

To confirm the role of hysteresis in the functional activity of full-length VWbp, VWbp(1-474) was employed in ProT activation assays. Although the degree of curvature in the rate of substrate cleavage seen with VWbp(1-474) is less than that of VWbp(1-263), the data were fit very well by the established hysteretic kinetic mechanism (Scheme 1) (Fig. 1). The calculated K_D for the initial formation of the mature ProT·VWbp

complex was 25.3 ± 0.1 nM, approximately 100-fold tighter binding than VWbp(1-263) (15), verifying that the COOH-terminal half of VWbp contributes greatly to the affinity of

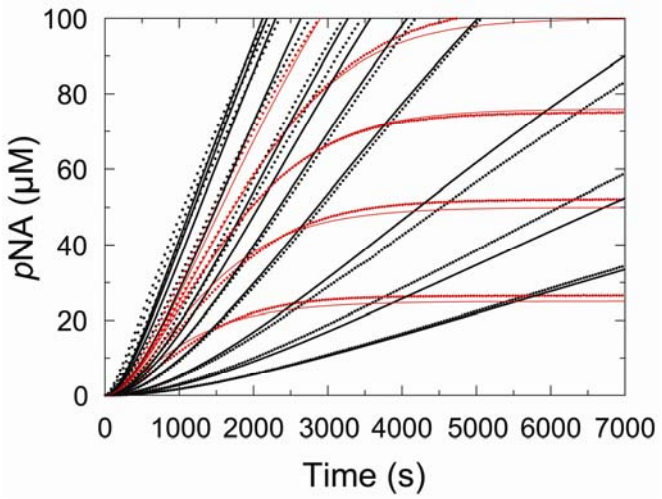

Figure 1. Full time-course kinetic analysis of ProT activation by VWbp(1-474). Progress curves for hydrolysis of D-Phe-Pip-Arg-*p*NA (S-2238), represented as the concentration of *p*NA, by mixtures of ProT and VWbp(1-474) include both saturating and limiting substrate assays. Mixtures of 1 nM ProT, 200 μM substrate, and 0.3, 0.5, 1, 2, 3, 4, 5, 10, 20, 30, or 40 nM VWbp are shown in *black*, with the data represented as every 10^{th} point and the fit as a *solid line*. Mixtures of 1 nM ProT, 10 nM VWbp, and 25, 50, 75, 100, or 150 μM substrate are shown in *red*. Data were collected and analyzed as described in "Experimental Procedures".

VWbp for ProT. The overall equilibrium constant for the conformational change between active ProT*·VWbp and inactive forms of the ProT·VWbp complex was also over 3-fold more favorable for the active form (K_{con} 3.1 ± 1.8), primarily due to an almost 3-fold slower reverse rate constant (k_{C2} 0.0185 ± 0.0005 s^{-1}) with a similar forward rate constant (k_{C1} 0.00592 ± 0.0004 s^{-1}) for the slow conformational change (15). The remaining parameters for chromogenic substrate hydrolysis (K_m 3.61 ± 0.01 μM; k_{cat} 63 ± 1 s^{-1}) showed a ~6-fold increase in K_m and a 34% decrease in k_{cat} compared to those determined for VWbp(1-263), giving only a slightly lower (6-fold) specificity constant (k_{cat}/K_m) (15).

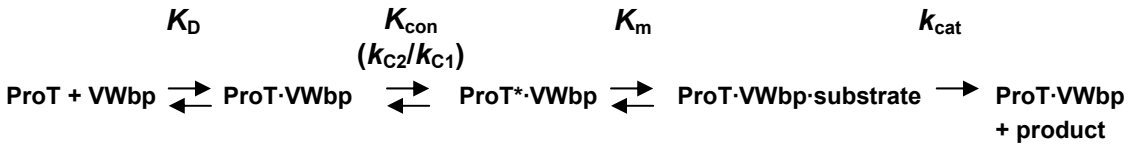

Scheme 1.

Binding of VWbp(1-263) or VWbp(1-474) to active ProT derivatives

The affinity of VWbp(1-263) for native ProT was previously determined with [5F]Hir(54-65) as a competitive ligand for proexosite I, supporting the relatively weak affinity determined from kinetic analysis with the same chromogenic substrate (K_D 2.5 ± 0.3 μM) (15). This experiment revealed that VWbp(1-263) binds directly to proexosite I on ProT, allowing an identical experimental design to be used to examine binding to all of the active ProT derivatives. Both VWbp(1-263) and VWbp(1-474) successfully competed with the labeled hirudin peptide for binding to all the derivatives (Figs. 2 and 3), with the results of the analyses summarized in Table 1. The stoichiometric factor was consistent throughout the experiments (0.8-1.2), representative of a 1:1 molar complex formed between VWbp and all of the ProT derivatives. The free energy changes (ΔG) (Fig. 6) for VWbp(1-263) decreased approximately 1.6-fold from -7.6 kcal/mole for native ProT to -12.0 kcal/mole for the active enzyme forms (T, MzT, MzT(-F1)). VWbp(1-474) revealed a similar relationship, with values ranging from -9.4 kcal/mole (ProT) to -12.9 kcal/mole (T) (Table 1).

Binding of VWbp(1-263) or VWbp(1-474) to active site-blocked ProT derivatives

To isolate the effect of active site occupation on the affinity of ProT and its derivatives for VWbp, both the zymogen and active enzyme forms were labeled with the covalent active site inhibitor FPR-CH_2Cl. The conformational changes associated with labeling with the inhibitor mimic the catalytic transition state representative of the

presence of a bound substrate (25), a process expected to substantially increase the affinity of VWbp for ProT due to the influence of substrates on the kinetic mechanism of activation. The resulting higher affinities for the active site-blocked analogs precluded use of the same experimental approach used for the active ProT derivatives. The fluorescent hirudin peptide could not effectively compete with either VWbp construct for binding, because of the massively higher affinity of the FPR-derivatives. To address this problem, [TMR]FPR-ProT was employed as a competitive ligand with the FPR-analogs, due to its similar high affinity for VWbp. Both VWbp(1-263) and VWbp(1-474) bound to all active site-blocked ProT derivatives (Fig. 4 and 5) with extremely tight, subnanomolar K_D's (Table 1), with VWbp(1-474) binding with lower picomolar affinities. As with the active ProT derivative experiments, the calculated parameters support formation of a 1:1 molar complex between the proteins. Free energy values were nearly identical for all active site-inhibited forms, for both VWbp(1-263) (-12.9 to -13.3 kcal/mole) and VWbp(1-474) (-13.2 to -15.9 kcal/mole) (Table 1, Fig. 6).

Autocatalysis of the ProT-VWbp complex in human plasma

As a potent procoagulant factor, VWbp triggers rapid clotting of human plasma. To examine the ability of VWbp to elicit autocatalytic activity within a complex with endogenous ProT, without interference from the physiological thrombin substrate fibrinogen, plasma congenitally deficient in fibrinogen (factor I) was used as a source of human ProT. Figure 7 shows that the ProT ·VWbp(1-474) complex produced detectable levels of Pre 1 in plasma mixtures, with a visible reduction in the amount of full-length ProT. A similar pattern was produced with VWbp(1-263), but to a lesser extent, with slower appearance of a Pre 1 band and less obvious disappearance of ProT.

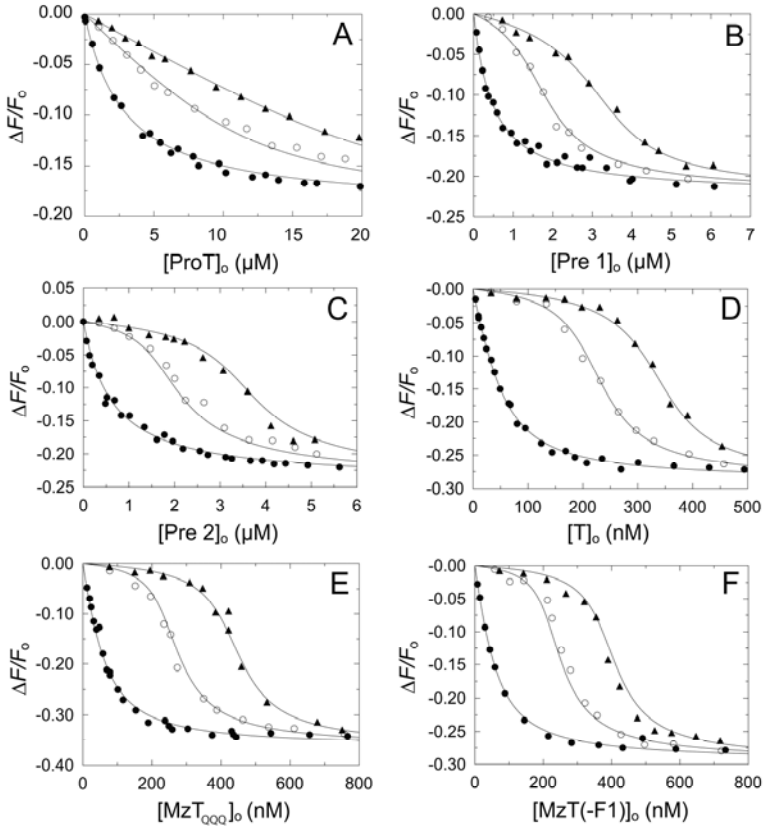

Figure 2. Competitive binding of VWbp(1-263) and [5F]Hir(54-65) to native ProT derivatives. Titrations of the change in fluorescence ($\Delta F/F_o$) of 48 nM [5F]Hir(54-65) as a function of total concentration of ProT derivative. *A*, ProT with 0 (●), 10 (○), and 20 μM (▲) VWbp, as previously published in Ref. (15), reproduced with permission. *B*, Pre 1 with 0 (●), 2.2 (○), and 4.3 μM (▲) VWbp. *C*, Pre 2 with 0 (●), 2.2 (○), and 4.3 μM (▲) VWbp. *D*, T with 0 (●), 273 (○), and 431 nM (▲) VWbp. *E*, MzT_{QQQ} with 0 (●), 273 (○), and 486 nM (▲) VWbp. *F*, MzT(-F1) with 0 (●), 273 (○), and 486 nM (▲) VWbp. The *solid lines* represent fits by the cubic binding equation with the parameters listed in Table 1. Binding experiments were performed and analyzed as described in "Experimental Procedures".

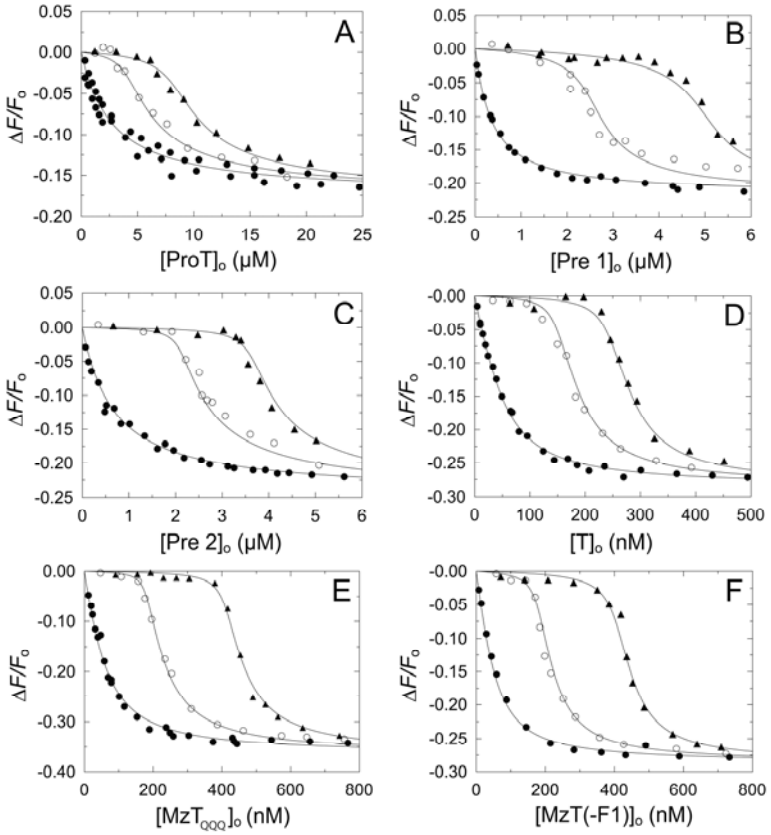

Figure 3. Competitive binding of VWbp(1-474) and [5F]Hir(54-65) to native ProT derivatives. Titrations of the change in fluorescence ($\Delta F/F_o$) of 48 nM [5F]Hir(54-65) as a function of total concentration of ProT derivative. *A*, ProT with 0 (●), 4 (○), and 8 μM (▲) VWbp. *B*, Pre 1 with 0 (●), 2 (○), and 4 μM (▲) VWbp. *C,* Pre 2 with 0 (●), 2 (○), and 3.5 μM (▲) VWbp. *D*, T with 0 (●), 154 (○), and 255 nM (▲) VWbp. *E*, MzT_{QQQ} with 0 (●), 154 (○), and 353 nM (▲) VWbp. *F*, MzT(-F1) with 0 (●), 154 (○), and 353 nM (▲) VWbp. The *solid lines* represent fits by the cubic binding equation with the parameters listed in Table 1. Binding experiments were performed and analyzed as described in "Experimental Procedures".

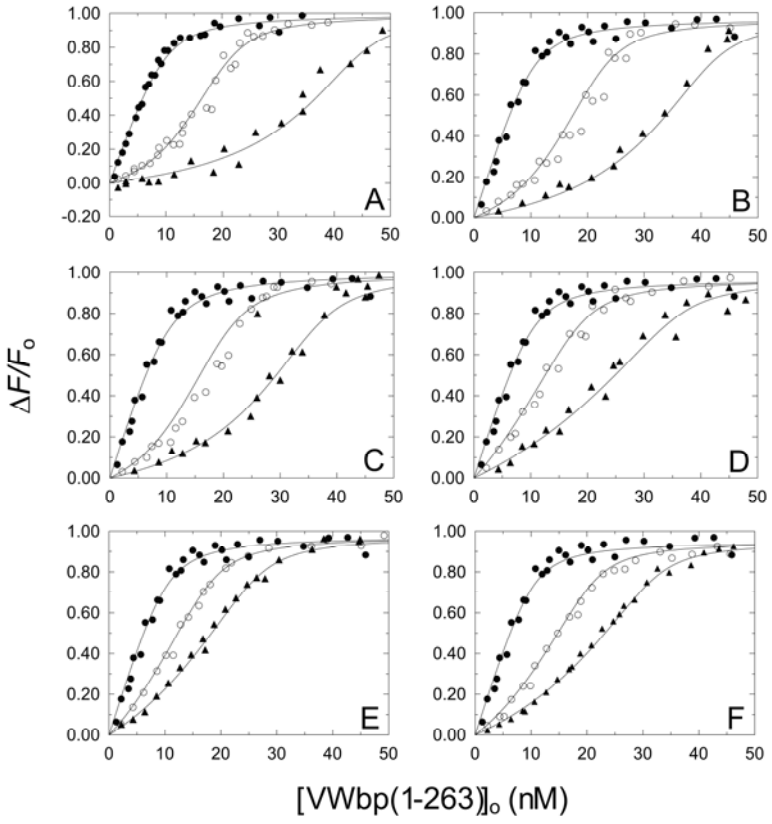

Figure 4. Binding of VWbp(1-263) to [TMR]FPR-ProT and active site-blocked ProT derivatives. Titrations of the change in fluorescence ($\Delta F/F_o$) of 10 nM [TMR]FPR-ProT as a function of total concentration of VWbp(1-263). *A*, FPR-ProT at 0 (●), 10 (○), and 30 nM (▲). *B*, FPR-Pre 1 at 0 (●), 11 (○), and 26 nM (▲). *C,* FPR-Pre 2 at 0 (●), 11 (○), and 26 nM (▲). *D*, FPR-T at 0 (●), 10 (○), and 31 nM (▲). *E*, FPR-MzT_{QQQ} at 0 (●), 10 (○), and 21 nM (▲). *F*, FPR-MzT(-F1) at 0 (●), 11 (○), and 21 nM (▲). The *solid lines* represent fits by the cubic binding equation with the parameters listed in Table 1. Binding experiments were performed and analyzed as described in "Experimental Procedures".

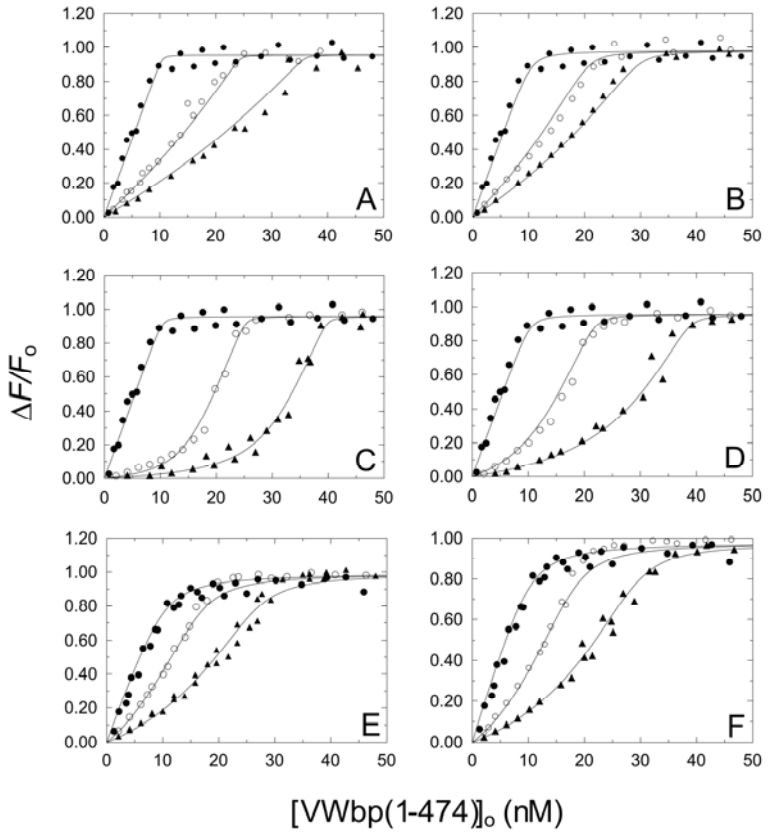

Figure 5. Binding of VWbp(1-474) to [TMR]FPR-ProT and active site-blocked ProT derivatives. Titrations of the change in fluorescence ($\Delta F/F_o$) of 10 nM [TMR]FPR-ProT as a function of total concentration of VWbp(1-263). *A*, FPR-ProT at 0 (●), 11 (○), and 21 nM (▲). *B*, FPR-Pre 1 at 0 (●), 11 (○), and 20 nM (▲). *C,* FPR-Pre 2 at 0 (●), 15 (○), and 30 nM (▲). *D*, FPR-T at 0 (●), 10 (○), and 26 nM (▲). *E*, FPR-MzT_{QQQ} at 0 (●), 10 (○), and 25 nM (▲). *F*, FPR-MzT(-F1) at 0 (●), 11 (○), and 24 nM (▲). The *solid lines* represent fits by the cubic binding equation with the parameters listed in Table 1. Binding experiments were performed and analyzed as described in "Experimental Procedures".

Table 1.
Summary of binding parameters
Dissociation constants (K_D) and other binding parameters are listed for competitive equilibrium binding of [5F]Hir(54-65) and VWbp(1-263) or VWbp(1-474) to unmodified ProT derivatives. Also listed are parameters obtained using [TMR]FPR-ProT as the probe with active site-blocked ProT analogs. Errors represent ± 2 SD. *Parameters from previous analysis found in (15).

Protein	Probe	K_D	*n*	$\Delta F_{max}/F_o$	ΔG	$\Delta\Delta G$ (ΔG_{der} - ΔG_{ProT})
VWbp(1-263)		*nM*	*mol VWbp/mol ProT*		*kcal/mol*	*kcal/mol (% change)*
ProT*	[5F]Hir(54-65)	2501 ± 336	1 (fixed)	-0.19 ± 0.01	-7.6	0.0
Pre 1	[5F]Hir(54-65)	84 ± 23	0.78 ± 0.05	-0.22 ± 0.01	-9.6	-2.0 (26%)
Pre 2	[5F]Hir(54-65)	55 ± 21	0.81 ± 0.05	-0.24 ± 0.01	-9.9	-2.3 (30 %)
T	[5F]Hir(54-65)	1.5 ± 0.3	0.74 ± 0.02	-0.29 ± 0.01	-12.0	-4.4 (58%)
MzT	[5F]Hir(54-65)	1.6 ± 0.6	0.85 ± 0.03	-0.37 ± 0.01	-11.9	-4.3 (57%)
MzT(-F1)	[5F]Hir(54-65)	1.3 ± 0.7	0.76 ± 0.04	-0.30 ± 0.01	-12.1	-5.3 (70%)
FPR-ProT	[TMR]FPR-ProT	0.153 ± 0.078	1.18 ± 0.07	1.00 ± 0.05	-13.3	-5.7 (75%)
FPR-Pre 1	[TMR]FPR-ProT	0.161 ± 0.088	1.24 ± 0.09	0.98 ± 0.05	-13.3	-5.7 (75%)
FPR-Pre 2	[TMR]FPR-ProT	0.210 ± 0.160	1.06 ± 0.12	1.00 ± 0.07	-13.1	-5.5 (72%)
FPR-T	[TMR]FPR-ProT	0.376 ± 0.184	0.84 ± 0.09	0.97 ± 0.04	-12.8	-5.2 (68%)
FPR-MzT	[TMR]FPR-ProT	0.318 ± 0.118	0.79 ± 0.07	0.98 ± 0.02	-12.9	-5.3 (70%)
FPR-MzT(-F1)	[TMR]FPR-ProT	0.252 ± 0.091	1.04 ± 0.07	0.95 ± 0.03	-13.0	-5.4 (71%)
VWbp(1-474)						
ProT	[5F]Hir(54-65)	112 ± 85	1.05 ± 0.10	-0.17 ± 0.01	-9.4	0.0
Pre 1	[5F]Hir(54-65)	19 ± 7	1.24 ± 0.05	-0.22 ± 0.01	-10.5	-1.1 (12%)
Pre 2	[5F]Hir(54-65)	7 ± 5	1.03 ± 0.04	-0.25 ± 0.01	-11.1	-1.7 (18%)
T	[5F]Hir(54-65)	0.30 ± 0.17	0.94 ± 0.02	-0.29 ± 0.01	-12.9	-3.5 (37%)
MzT	[5F]Hir(54-65)	0.30 ± 0.17	1.15 ± 0.02	-0.37 ± 0.01	-12.9	-3.5 (37%)
MzT(-F1)	[5F]Hir(54-65)	0.44 ± 0.23	1.14 ± 0.03	-0.29 ± 0.01	-12.7	-3.3 (35%)
FPR-ProT	[TMR]FPR-ProT	0.008 ± 0.048	1.23 ± 0.10	0.95 ± 0.02	-15.1	-5.7 (61%)
FPR-Pre 1	[TMR]FPR-ProT	0.073 ± 0.085	1.00 ± 0.10	0.98 ± 0.03	-13.8	-4.4 (47%)
FPR-Pre 2	[TMR]FPR-ProT	0.002 ± 0.004	0.99 ± 0.03	0.96 ± 0.02	-15.9	-6.5 (69%)
FPR-T	[TMR]FPR-ProT	0.015 ± 0.022	1.11 ± 0.06	0.96 ± 0.03	-14.7	-5.3 (56%)
FPR-MzT	[TMR]FPR-ProT	0.188 ± 0.091	0.68 ± 0.06	1.00 ± 0.03	-13.2	-3.8 (41%)
FPR-MzT(-F1)	[TMR]FPR-ProT	0.157 ± 0.080	0.81 ± 0.07	0.98 ± 0.03	-13.3	-3.9 (41%)

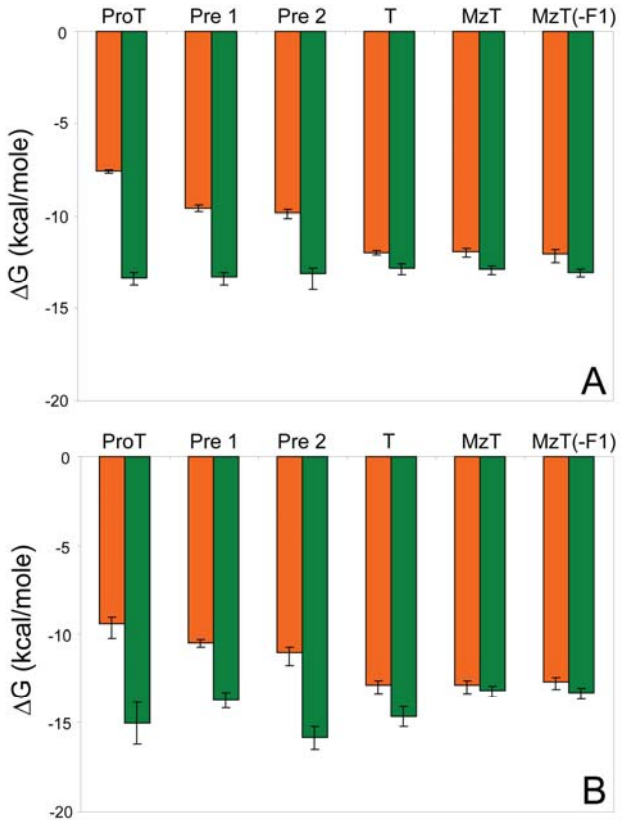

Figure 6. Changes in Gibbs free energy (∆G) from competitive equilibrium binding. Calculated free energy (*kcal/mole*) for experiments with VWbp(1-263) (*A*) and VWbp(1-474) (*B*). Native ProT proteolytic derivatives are in *orange*, FPR-derivatives are in *green*. Error bars represent ∆G determined from K_D ± 2 S.D (listed in Table 1), using the equation given in "Experimental Procedures."

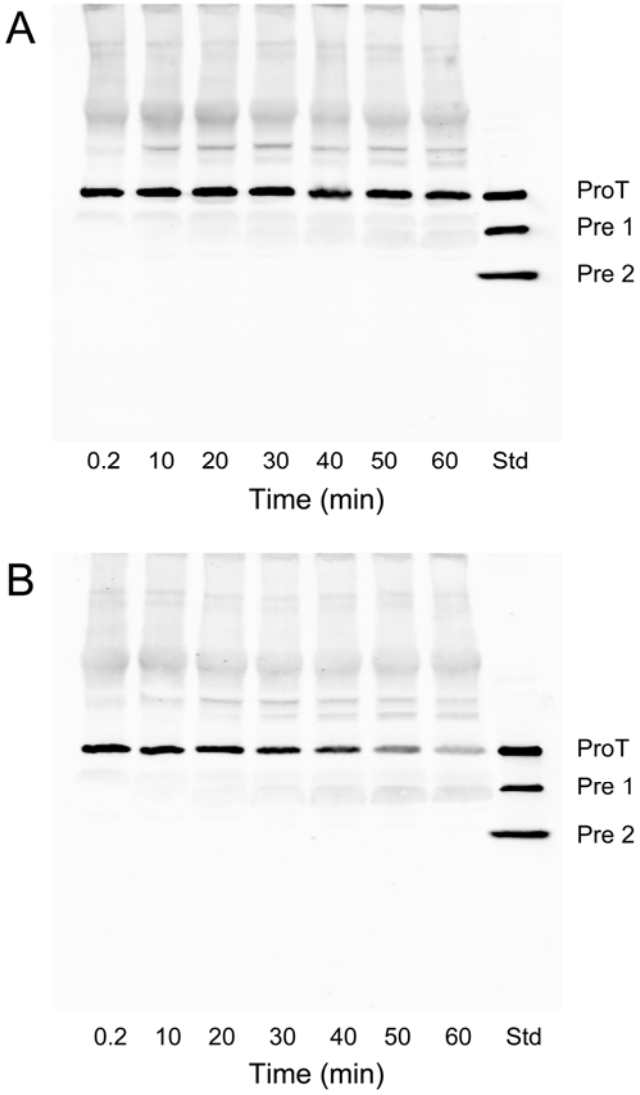

Figure 7. Autoproteolytic cleavage of endogenous plasma ProT by VWbp. Plasma ProT detected by western blotting in reactions containing 50% recalcified human factor I-deficient plasma and (*A*) 10 μM VWbp(1-263) or (*B*) 1 μM VWbp(1-474). Standards (*Std*) are equimolar amounts of native purified ProT, Pre 1, and Pre 2, equivalent to the expected initial molarity of plasma ProT. Electrophoresis and blotting were performed as described in “Experimental Procedures”.

Discussion

The current study reveals a substantial role for both the fragment 1 domain and activation-associated conformational changes in the mechanism of binding and activation of ProT by VWbp. A previous study characterized VWbp as interacting with proexosite I on ProT, due to its ability to compete for binding with the COOH-terminal peptide of hirudin, Hir(54-65) (15). Consistent with the pattern of behavior shown by many exosite I-specific ligands, including Hir(54-65), the increased affinity of VWbp for ProT derivatives with a more proteinase-like conformation suggests that VWbp can exploit the same steric and allosteric processes that govern thrombin recognition of other physiological ligands.

While VWbp is capable of binding (pro)exosite I and potentially altering the specificity of ProT through this interaction alone, a thorough analysis of the kinetics of ProT activation by VWbp(1-474) (Fig. 1) indicates that other regions of the zymogen are directly affected by the COOH-terminal half of VWbp. Whereas the NH_2-terminal half of VWbp is predicted to have a staphylocoagulase-homologous secondary structure composed of two alpha-helical bundles (26), multiple prediction analyses on the rest of VWbp assign almost no regular structure, apart from a 1-2 helix segment (~50 residues) at the distal end. The higher activity and ~100-fold higher affinity of VWbp(1-474) in forming the initial ProT·VWbp complex revealed in the kinetic analysis (Scheme 1) likely results from additional binding interactions which may affect the conformation of exosite I or facilitate insertion of the NH_2-terminus of VWbp into the activation pocket on ProT. The unstructured region of VWbp may sterically compete with or rearrage the small fragment domains to increase the overall affinity of VWbp for the zymogen. Whether this process is mediated by the largely disordered region or the relatively small COOH-terminal helical portion of VWbp remains unknown.

The small fragment domains of ProT themselves present a potential steric hindrance to binding by a macromolecular ligand such as VWbp, but release of these domains is normally strictly regulated during ProT activation. When it is not bound to a membrane surface through Ca^{2+}-mediated interactions between γ-carboxyglutamic acid residues and phosphatidylserine (27), the orientation of fragment 1 relative to the rest of the zymogen is largely undefined, although crystal structures of fragment 1, fragment 2, and MzT(-F1) have been solved (27-29). Release of the fragment 1 domain alone through cleavage at Arg^{155} is greatly inhibited in the presence of Ca^{2+} (30-31), and fragment 1 typically remains associated with fragment 2 in a proteolytic species termed fragment 1.2 (32). In canonical ProT activation, fragment 1.2 blocks exosite II until it is removed through cleavage by factor Xa at Arg^{271}, releasing thrombin from the prothrombinase complex. If cleavage at Arg^{271} occurs prior to proteolysis of the activation bond at Arg^{320}, fragment 1.2 retains a ~20-fold higher affinity (200 nM) (22) for the inactive catalytic domain compared to thrombin, which decreases the rate of its release from the activation complex. This proteolytic regulation is the key to temporal control of thrombin production as well as to limiting ligand interaction with an improperly activated thrombin molecule. Loss of one or both fragment domains not only relieves potential blocking interactions for binding of VWbp, but also produces minor allosteric effects within the activation domain of ProT itself (33) that could favor ligand-exosite association.

A potential role for these allosteric changes is indicated by the results of the competitive binding studies using ProT analogs with unmodified active sites, which revealed substantial increases in the affinity of VWbp as the fragment domains are removed (Table 1). The greatest enhancement results from loss of fragment 1, with ~30-fold higher affinity for VWbp(1-263) and a 6-fold change with VWbp(1-474). It is worth noting that even though VWbp(1-474) is capable of binding to all of the ProT

derivatives with higher affinities than VWbp(1-263), there is still an effect of the loss of fragment 1 despite the significant contribution of the COOH-terminus of VWbp to activity and affinity. A direct comparison of the Gibbs free energy values (ΔG) shows that there is a 12-26% increase in binding free energy upon loss of fragment 1 alone (Pre 1) for both VWbp constructs, but only a 4-6% increase upon subsequent loss of fragment 2 (Pre 2) (Table 1). The same pattern is not seen upon examination of the three active enzyme forms, T, MzT, and MzT(-F1), which all contain catalytic domains that have undergone conformational changes associated with proteolytic activation. VWbp(1-263) binds indistinguishably to all three species (K_D 1.3-1.6 nM), suggesting that the existence of a proteinase-like activation domain promotes an equally favorable structure for ligand binding. An identical relationship can be seen with VWbp(1-474), where even though it is capable of binding the active enzymes with ~5-fold tighter K_D's than VWbp(1-263), the presence of the fragment domains has no obvious detrimental effect. These results are consistent with previous studies of the influence of the fragment domains on the expression of exosite I, where loss of fragment 1 in Pre 1 increases the affinity of the exosite 7-fold for a fluorescently-labeled hirudin peptide, but any modulating effect of fragment 1 is canceled out by proteolytic activation of the zymogen (33).

What does this binding behavior indicate within the context of the hysteretic mechanism of activation by VWbp? A model of an optimal ProT conformation that supports initial high affinity association of VWbp would be implied from the binding studies alone, but VWbp likely both initiates allosteric changes in ProT and exploits structural alterations elicited by other ligands or proteolytic events. Several changes are needed to form a properly folded thrombin activation domain for substrate-binding, including shifts in the segment containing the Arg^{15}-Ile^{16} cleavage site and the flexible loops 142-152, 186-194, and 216-226 (3-4). Typically, formation of the salt bridge between Ile^{16} and Asp^{194} would conformationally link the new thrombin NH_2-terminus with

the substrate specificity pocket (3, 34), not requiring any other effectors to trigger the structural transition. In contrast, the key step in the model of activation by VWbp occurs upon binding of a substrate into what is presumed to be an imperfectly formed, inactive active site within a relatively low affinity ProT·VWbp complex, and this contact serves to generate a more catalytically competent, high affinity complex. The additional binding requirements for this slow transition to an active proteinase conformation share characteristics with substrate- and cofactor-mediated induced fit mechanisms of activation, such as those seen with the complement protease factor D or the factor VIIa/tissue factor complex (35-36). The activity of factor D is regulated by distortions within the catalytic triad and a unusually narrow substrate-binding (S1) cleft that are only relieved upon binding of its substrate, C3b-complexed factor B (37), analogous to the substrate-enhanced activity that is observed with VWbp in complex with ProT. Similarly, an altered active site is found in factor VIIa, and the enzyme exists in a state of incomplete activation with a conformation resembling an intermediate stage between zymogen and protease (38-39). Contact with its cofactor, tissue factor, favorably shifts the architecture of the factor VIIa active site, allowing the enzyme to cleave its natural substrates factor X and factor IX (40). This pathway shows parallels to the unfavorable equilibrium that exists between inactive and active forms of the ProT·VWbp complex in the absence of substrate (Scheme 1). The requirement for additional protein-protein interactions in mediating the activity of serine proteinases directs the specificity of the proteinase complex towards a more limited assemblage of substrates than would be seen with the canonical configuration of the enzyme alone.

The concept of substrate binding as a fundamental amplifier of ProT activation by VWbp is further strengthened by the equilibrium binding experiments with FPR-blocked ProT derivatives. Hydrolysis of substrate amide bonds by members of the trypsin family of enzymes, including thrombin, follows a well-defined chemical pathway initiated by

formation of a Michaelis complex and subsequent attack of the substrate carbonyl atom by Ser^{195} in the oxyanion hole, assisted by His^{57}, to give a hemiketal tetrahedral intermediate. The ensuing acyl-enzyme complex releases the first product, followed by hydrolysis of the acyl-enzyme through a second tetrahedral intermediate to restore the enzyme and release the second product (41). The tetrahedral intermediates resemble the transition state for the reactions, and this structure can be mimicked by several classes of covalent inhibitors, including tripeptide chloromethyl ketone inhibitors highly specific for serine proteinases (25, 42). Structural studies have shown that inhibition of thrombin by D-Phe-Pro-Arg-chloromethyl ketone (PPACK/FPR) gives a similar orientation of residues in the substrate-binding cleft of the enzyme as is seen with binding of substrates, but distinctly different from changes seen with binding of hirugen to exosite I alone (43). Thus, corresponding FPR-analogs of all the enzyme and zymogen derivatives of ProT were produced through either direct inhibition with FPR-CH_2Cl or through formation of a reversible, conformationally activated complex of the zymogen with staphylocoagulase (26), allowing incorporation of the inhibitor into the induced active site on the zymogen-activator complexes. The active site itself serves as the focus for the significant conformational changes which occur upon conversion of the inactive catalytic domain into thrombin, and the substrate-bound structural mimicry of the FPR-analogs allowed VWbp(1-263) and VWbp(1-474) to bind with 4-6-fold higher affinity than to the active enzymes, even with the zymogens containing fragments 1 or 2. Therefore, the ProT·VWbp complex does not simply require an “enzyme-like” orientation of the activation domain between the catalytic residues, oxyanion hole, and substrate-specificity site, but it also calls for occupation of the S1 site by an appropriate substrate, consistent with the hysteretic mechanism of activation.

The equilibrium binding studies confirm the ability of VWbp to bind to ProT with dramatically increased affinity in the presence of a substrate mimic, but the question

remains of whether the presence of fragment 1 or 2 has any detectable effect on the binding of VWbp with derivatives containing an active catalytic domain. The design of the binding assays with the active ProT derivatives allowed observation of changes in fluorescence immediately upon addition of the ProT analog to the [5F]Hir(54-65) and VWbp ligand mixture, and most of the assays showed very rapid equilibrium between the competing proteins. The only discrepancies were witnessed upon either addition of active MzT_{QQQ} or *in situ* activation of Pre 1 to MzT(-F1), where a noticeably longer time period was required to reach equilibrium and a stable fluorescence change. Panel A in Figure 8 shows two representative fluorescence traces for MzT_{QQQ} binding, with the assay containing VWbp(1-474) requiring an additional 40-50 sec to reach equilibrium. The fact that VWbp(1-263) does not show a lag indicates that the C-terminal half of VWbp has steric opposition from the fragment domains still found on MzT, and that the kinetics of binding are affected but not the fundamental equilibrium dissociation constant. A slightly different mechanism may be at work during conversion of Pre 1 to MzT(-F1) (Fig. 7B), where VWbp(1-263) and VWbp(1-474) both alter the kinetics of activation by ecarin to different degrees, compared to Pre 1 in the presence of [5F]Hir(54-65) alone. Whether this is a consequence of partial blockage of areas on the zymogen required for interaction with ecarin is unknown, but it could also be influenced by conformational changes in Pre 1 induced by VWbp which may alter accessibility of the activation bond or orientation of the fragment 2 domain. These findings suggest that the fragment domains introduce some degree of hindrance to VWbp, even with an optimal catalytic domain and exosite I conformation that ultimately favors high affinity binding.

Although VWbp can form an active complex with ProT exclusively through NH_2-terminal insertion and substrate-dependent changes in conformation, previous studies on both VWbp (15) and staphylocoagulase (13) have identified a pattern of autocatalysis consistent with cleavage at two thrombin-sensitive sites. In the presence of VWbp,

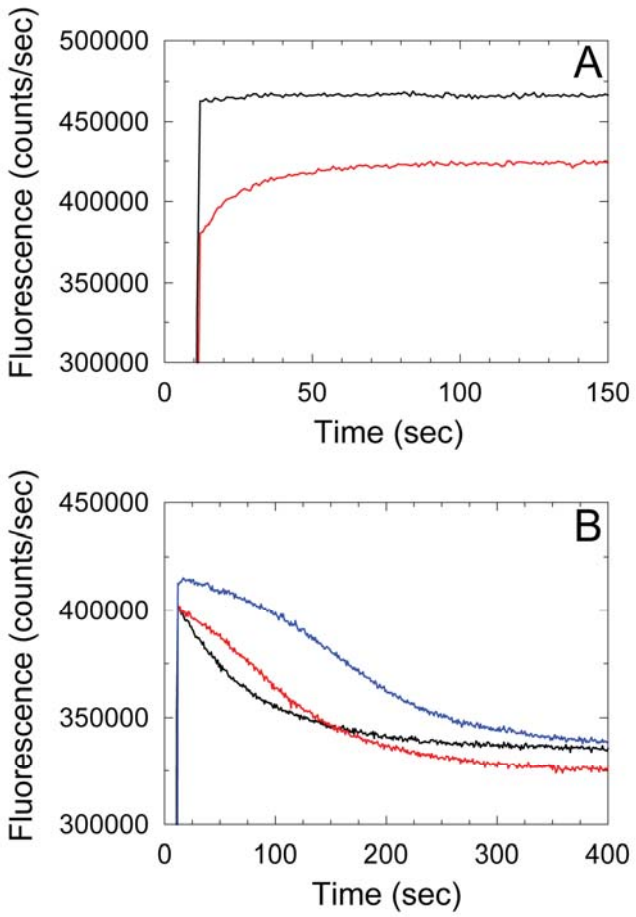

Figure 8. Comparison of fluorescence traces for binding of MzT_{QQQ} or MzT(-F1) by VWbp. *A*, Fluorescence of [5F]Hir(54-65) in the presence of 273 nM VWbp(1-263, immediately after addition of 152 nM MzT_{QQQ} (*black line*), or 353 nM VWbp(1-474) after addition of 417 nM MzT_{QQQ} (*red line*). *B*, Change in fluorescence of [5F]Hir(54-65) with 433 nM Pre 1 activated *in situ* to MzT(-F1) (*black line*), 143 nM Pre 1 activated in the presence of 273 nM VWbp(1-263)) (*blue line*), or 639 nM Pre 1 activated in the presence of 353 nM of VWbp(1-474) (*red line*).

production of Pre 1 from ProT has been detected in reaction mixtures at both high and low concentrations of ProT, with detection of a species called Pre 2' after extended incubations at high ProT concentrations (15). Both of these species have been produced *in vitro* through autocatalytic release of one or both of the fragment domains of ProT through proteolysis by thrombin, but in physiological ProT activation, the rapid formation of active MzT(-F1) from MzT by loss of fragment 1 through cleavage at Arg^{155}

is the more common pathway of domain release (44-45). A second site at Arg^{284} can also be targeted, producing the Pre 2' variant that lacks the first 13 NH_2-terminal residues normally found in Pre 2 and thrombin (46-47). The sequential and temporal characteristics of cleavage in ProT-VWbp mixtures accurately correspond with what is known about the mechanisms of feedback proteolysis in MzT and MzT(-F1), where both intramolecular and intermolecular events contribute to formation of proteolysis products (44), indicating that the proteolytic activity is consistent with ProT·VWbp exhibiting thrombin-like behavior. Loss of fragment 1 characteristically takes place though direct cleavage by the resident active site on each MzT molecule, most likely due to the inherent flexibility in the targeted region between the domains, allowing this intramolecular process to occur quickly after MzT production. The much slower time-course for appearance of Pre 2' stems from a greater dependence on intermolecular proteolysis, originating from a more constrained orientation of the cleavage site that limits the possibility for self-cleavage.

Due to the potential ramifications of autocatalysis of ProT while bound to VWbp, generation of the proteolytic intermediates was assessed in human plasma to establish whether they can actually be produced in a milieu of physiological ligands. Because the potent procoagulant activity of VWbp leads to fast clotting of plasma, which could interfere with complex and ligand accessibility, the reactions were examined in the near-absence of fibrinogen by using plasma from a congenitally deficient donor and the fibrin polymerization inhibitor peptide Gly-Pro-Arg-Pro. Over a time-course of 1 h, a control plasma sample without VWbp did produce a detectable amount of thrombin (not shown), which is not unexpected after recalcification of citrated plasma. Production of thrombin was not seen in reactions where a saturating level of VWbp was present, suggesting that binding of the activator to the zymogen prevents production of thrombin itself. Disappearance of ProT was observed with VWbp(1-474) over time, with corresponding

low-level detection of a band the same size as the Pre 1 standard (Fig. 8B). While the results of incubation of plasma with VWbp(1-263) were less dramatic, with a less distinguishable Pre 1 band (Fig. 8A), the pattern of cleavage with VWbp is consistent with that observed with purified proteins *in vitro*. Recognition of the Pre 1 band on the blots by the ProT antibody is likely less than expected from the rate of disappearance of ProT due to the presence of human serum albumin which migrates at nearly the same molecular weight as Pre 1. This issue will be resolved in future experiments utilizing immunoprecipitation of the ProT·VWbp complexes before separation on the gels, and the effect of fibrinogen on VWbp-initiated autocatalysis will also be examined in normal human plasma.

If VWbp is capable of eliciting formation of a procoagulant complex with ProT that is not only capable of cleaving fibrinogen into fibrin, but also contains the potential to rid itself of its regulatory zymogen fragment domains, what implications would this have for the pathological capacity of VWbp in a blood-borne staphylococcal infection? The most vital function of fragment 1 for ProT is to mediate binding of the zymogen to the platelet membrane, permitting association with factor Xa and factor Va in the prothrombinase complex for thrombin production. If VWbp can bind to membrane-bound ProT, as well as free ProT in the blood, premature release of high affinity procoagulant Pre 1*·VWbp complexes from platelet membranes could occur in a pathological dissemination mechanism (32). This would have the amplified effect of liberating serpin-insensitive protein complexes to downstream locations where they could freely associate with both von Willebrand factor and fibrinogen, setting up new foci for fibrin deposition and bacterial colonization. In addition to the role of VWbp on the activity of the complexes, indirect effects related to other regulatory ligands would also occur, including blockage of all exosite I-specific ligands by the presence of VWbp and a reduction in exosite II interactions from the presence of either fragment 1.2 or fragment 2. The end result

would be ProT·VWbp or Pre1·VWbp complexes with thrombin-like activity that are nearly impervious to inhibition or downregulation, but exhibit high specificity for the single substrate fibrinogen, due to the driving force of the substrate-mediated mechanism of VWbp zymogen activation.

Acknowledgements

We thank Dr. Sriram Krishnaswamy for the generous gift of the recombinant ProT construct, and Anthony Tharp and Ashok Maddur for excellent technical assistance. The project was supported by NIH Grant R37 HL071544 from the National Heart, Lung, and Blood Institute (P.E.B.) and H.K.K. was supported by Training Grant 2-T32 HL07751.

Supplemental Data (Unpublished)

Determination of molecular weights of VWbp and ProT·VWbp

Molecular weights (MW) of VWbp(1-263), VWbp(1-474), and Oregon Green-488-FPR-prothrombin ([OG]FPR-ProT) were determined separately and for a 1:1 ProT·VWbp complex by sedimentation velocity in a Beckman-Coulter XL-1 Analytical Ultracentrifuge (Dr. Cynthia Peterson, University of Tennessee-Knoxville). Continuous interference scans were collected for ~4 h at 50,000 rpm, 25-26 ^{o}C, and the refractive index data was used to calculate the approximate MW in SEDFIT v10.3 (Peter Schuck, NIH). Parameters used in analysis included: buffer viscosity, density = 0.01014, 1.00326; calculated partial specific volumes = 0.7241 (ProT), 0.7322 (VWbp(1-263)), 0.7278 (VWbp(1-474)). VWbp(1-263), VWbp(1-474), and [OG]FPR-ProT were prepared for analysis by simultaneous dialysis against two changes (4 L each) of 50 mM HEPES, 110 mM NaCl, 5 mM $CaCl_2$, pH 7.4, for at least 6 h before each change to ensure complete equilibration of the same buffer for all three proteins. Concentrations were measured by absorbance at 280 nm, and proteins were stored at -80 ^{o}C until use.

Empirical molecular masses of the two VWbp constructs were in good agreement with the theoretical values calculated from the amino acid compositions, giving values of 33 kDa for VWbp(1-263) and 56 kDa for VWbp(1-474) (calculated values = 31 kDa and 55 kDa). Native ProT has an empirical molecular mass of 72 kDa, and the value for [OG]FPR-ProT was nearly identical (74 kDa, Fig. 1S *A*). An equimolar mixture of VWbp(1-263) and [OG]FPR-ProT gave a molecular mass of 108 kDa for the complex (Fig. 1S *B*, theoretical = 103 kDa), with no indication of any unassociated protein, indicating that the NH_2-terminal half of VWbp is able to form a 1:1 complex with ProT. Identical stoichiometry was found for an equimolar reaction of VWbp(1-474) and [OG]FPR-ProT, resulting in a complex of 125 kDa (theoretical = 130 kDa). These

stoichiometries support the values calculated through equilibrium binding and confirm that ProT·VWbp complexes do not dimerize in solution.

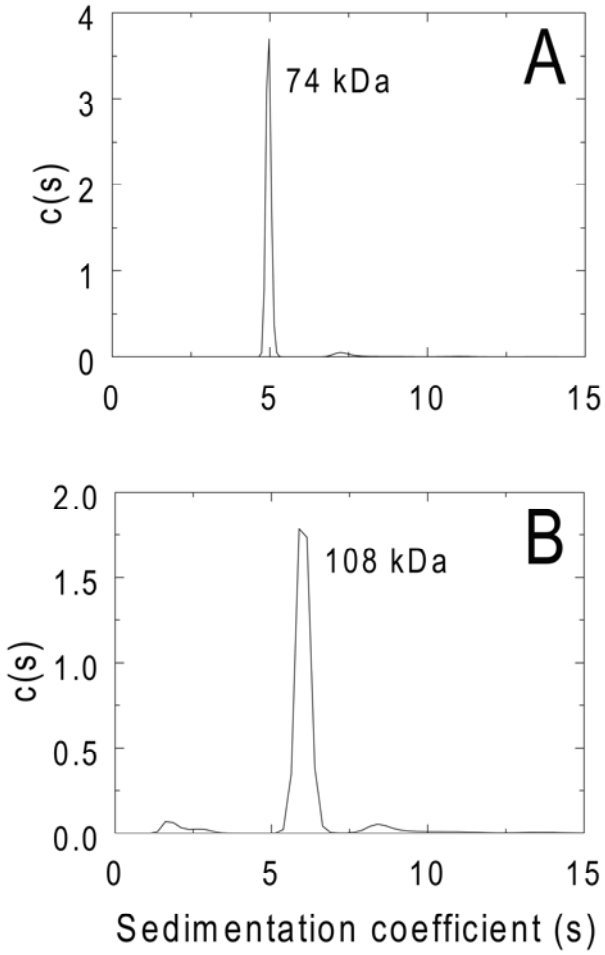

Figure 1S. Approximate molecular masses and sedimentation coefficient distributions (c(s)) from sedimentation velocity experiments. (A) c(s) distribution for Oregon Green-488-FPR-prothrombin (0.3 mg/mL). (B) c(s) distribution for a mixture of Oregon Green-488-FPR-prothrombin (4.2 μM) and VWbp(1-263) (4.2 μM).

Preliminary fluorescence equilibrium binding experiments

The following experimental results represent preliminary analyses of the binding of VWbp to native and active site-blocked (FPR-) ProT derivatives. The significant enhancement of affinity upon active site-inhibition made it impossible to use a single

experimental design for all the analogs, due to the necessity for a fluorescent reporter which bound in the same range of affinity as the targeted competitive ligand. For example, fluorescently-labeled ProT (Oregon Green-488-FPR-ProT) successfully reported high-affinity binding (K_D ~2 pM) of VWbp(1-263), but the relatively weak K_D of native ProT for VWbp(1-263) (K_D 2.5 μM) precluded its use as a competitive binding ligand. In contrast, the observation that VWbp could bind other proteolytic derivatives of ProT (e.g., Pre 1 and thrombin) with higher affinity allowed initial characterization of their affinities using similar experimental designs. Preliminary analysis of binding of VWbp(1-474) was also possible due to a change in the intrinsic (tryptophan) fluorescence of native ProT.

Competitive equilibrium binding of VWbp(1-263) to [OG]FPR-ProT and native/FPR-Pre 1

Single-point fluorescence measurements were taken of mixtures of [OG]FPR-ProT and VWbp(1-263) and varying concentrations of native Pre 1 (Fig. 2S *A*) or FPR-Pre 1 (Fig. 2S *B*). VWbp bound native Pre 1 with an ~280-fold weaker affinity (K_D 565

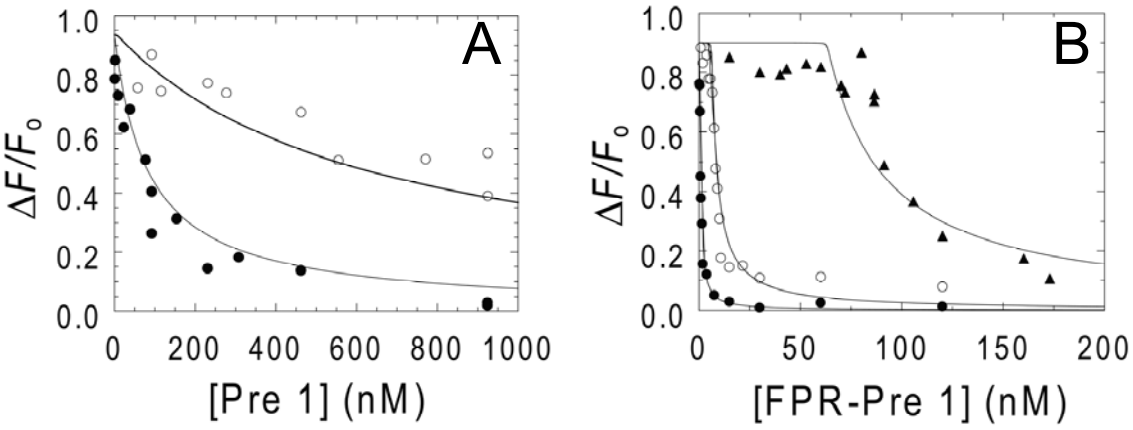

Figure 2S. Binding of VWbp(1-263) to 102 pM [OG]FPR-ProT and native or FPR-Pre 1. The fractional change in fluorescence ($\Delta F/F_o$) as a function of total Pre 1 concentration. (A) Native Pre 1 with 1 nM (●) and 7 nM (○) VWbp. (B) FPR-Pre 1 with 1 nM (●),7 nM (○), and 72 nM (▲) VWbp. The *lines* represent the simultaneous fit by the cubic competitive binding equation.

pM) than FPR-Pre 1 (K_D 2 pM), but the relatively weak K_D for native Pre 1 resulted in poorly-determined complex stoichiometry. In addition, an extended time was required to reach equilibrium in the native assays, which introduced the potential for proteolysis in the reaction mixtures. This indicated that native Pre 1 was not able to successfully compete with the fluorescently-labeled ProT analog, and as such, could not be investigated with this experimental design.

Competitive equilibrium binding of VWbp(1-263) and [5F]Hir(54-65) to FPR-ProT

Titrations of FPR-ProT were performed in the presence of [5F]Hir(54-65) and several set concentrations of VWbp(1-263) (Fig. 3S). Global analysis of the data resulted in excellent stoichiometry (0.96 ± 0.01), but very poor determination of the K_D for VWbp and FPR-ProT (0.80 ± 1.09 nM). Simulation of additional higher values for K_D (up to 10 nM) gave fit lines nearly identical to each other, indicating that the true affinity could not be determined. This was likely a result of the over 100-fold difference in affinity between VWbp and [5F]Hir(54-65) for FPR-ProT, which excluded the use of the labeled hirudin as a competitive ligand in this system.

Competitive equilibrium binding of VWbp(1-263) and [5F]Hir(54-65) to native or FPR-T

Titrations of either native T (Fig. S4A) or FPR-T (Fig. 4S *B*) were performed in the presence of [5F]Hir(54-65) and several fixed concentrations of VWbp(1-263). Global analysis of the data gave essentially indistinguishable affinities for the native (K_D 1.8 ± 0.9 nM) and FPR-blocked analog (K_D 750 ± 0.2 pM), and complex stoichiometries of about 1. This result was the first confirmation of the very high affinity of VWbp for the active enzyme, and revealed that competition with the fluorescently-labeled hirudin peptide could be successfully carried out with all of the native prothrombin derivatives.

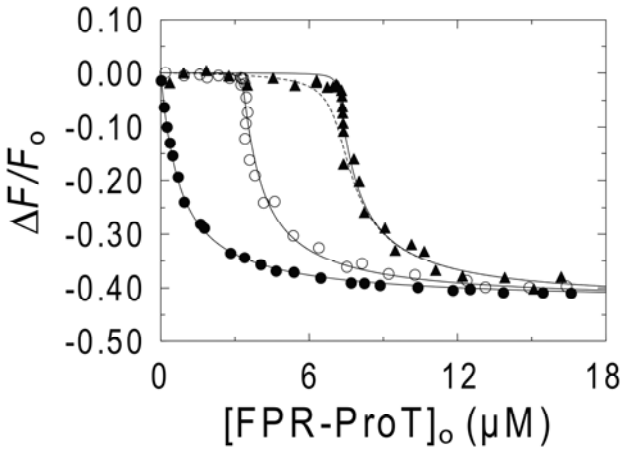

Figure 3S. Binding of VWbp(1-263) and 48 nM [5F]Hir(54-65) to FPR-ProT. The fractional change in fluorescence ($\Delta F/F_o$) as a function of total FPR-ProT concentration at 0 (●), 3.5 (○), and 7.5 μM (▲) VWbp. The *solid lines* represent the simultaneous fit by the cubic competitive binding equation, and the *dotted line* simulates a K_D of 10 nM.

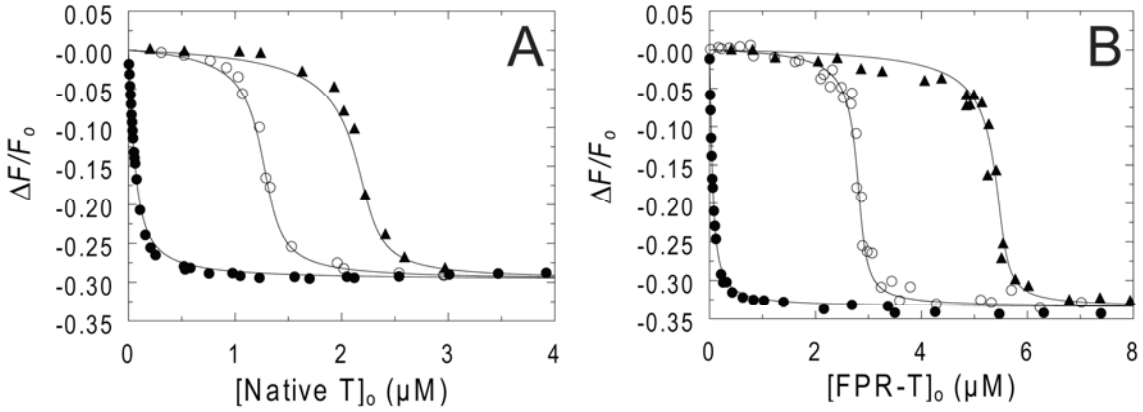

Figure 4S. Binding of VWbp(1-263) and 48 nM [5F]Hir(54-65) to native or FPR-T. The fractional change in fluorescence ($\Delta F/F_o$) as a function of total T concentration. (A) Native T with 0 (●), 1 (○), and 2 μM (▲) VWbp. (B) FPR-T with 0 (●), 3 (○), and 6 μM (▲) VWbp. The *lines* represent the simultaneous fit by the cubic competitive binding equation.

Direct equilibrium binding of VWbp(1-474) to native or FPR-ProT

ProT contains several tryptophan residues within its fragment and catalytic domains which fundamentally contribute to the intrinsic fluorescence of the protein with excitation at 295 nm. The structural changes associated with prothrombin activation and

membrane binding have been shown to affect the magnitude of the intrinsic tryptophan fluorescence (48-49), and preliminary observations with VWbp(1-474) demonstrated a concentration-dependent change in native ProT fluorescence upon binding of VWbp. Consequently, this experimental approach was used to determine the affinity of VWbp(1-474) for both native ProT (Fig. 5S *A*) and FPR-ProT (Fig. 5S *B*). Titrations with VWbp(1-474) and native ProT gave a relatively tight K_D (31 nM) compared to that of VWbp(1-263) in competitive binding assays with [5F]Hir(54-65) (K_D 2.5 μM), supporting kinetic data which showed higher activity of VWbp(1-474) with native ProT. A comparable titration with VWbp(1-474) and FPR-ProT revealed extremely tight binding of the ligand, but due to the experimental noise inherent in tryptophan fluorescence, simulation of multiple values for the K_D (1-15 nM) gave no indication of the true affinity value. Unfortunately, no change in tryptophan fluorescence was observed in mixtures of VWbp(1-263) and native ProT, preventing direct comparison of the two VWbp constructs and implying that a higher affinity interaction was needed to change the environment of the target tryptophan enough to affect the fluorescence.

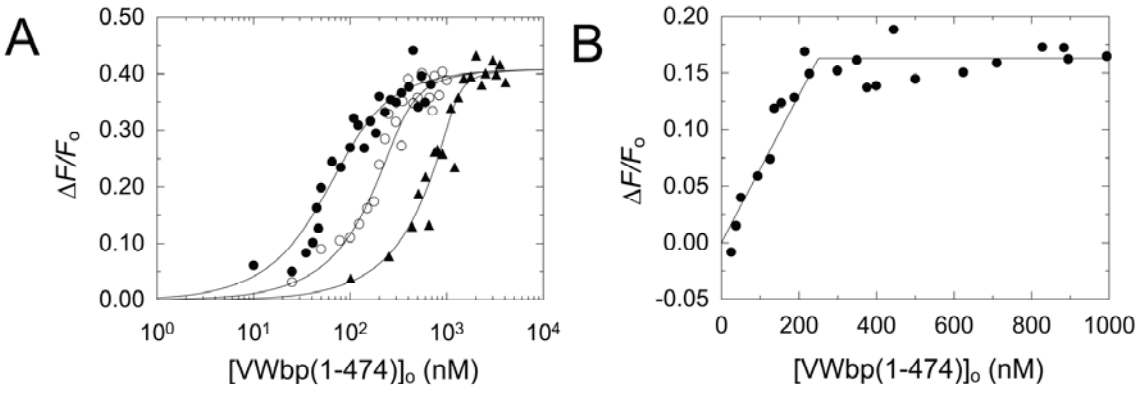

Figure 5S. Binding of VWbp(1-474) to native or FPR-Pre 1. The fractional change in fluorescence ($\Delta F/F_o$) at λ_{ex} = 295 nm and λ_{em} = 335 nm. (A) Increasing [VWbp] at 50 nM (●), 250 nM (○), and 1 μM (▲) native ProT. (B) Increasing [VWbp] at 250 nM (●) VWbp. The *lines* represent the simultaneous fit by the quadratic binding equation.

References

1. Goodey NM & Benkovic SJ (2008) Allosteric regulation and catalysis emerge via a common route. *Nature Chemical Biology* 4:474-482.

2. Bock PE, Panizzi P, & Verhamme IMA (2007) Exosites in the substrate specificity of blood coagulation reactions. *J. Thromb. Haemost.* 5 (Suppl. 1):81-94.

3. Huber R & Bode W (1978) Structural basis of the activation and action of trypsin. *Acc. Chem. Res.* 11:114-122.

4. Anderson PJ, Nesset A, & Bock PE (2003) Effects of activation peptide bond cleavage and fragment 2 interactions on the pathway of exosite I expression during activation of human prethrombin 1 to thrombin. *J. Biol. Chem.* 278(45):44482-44488.

5. Anderson PJ, Nesset A, Dharmawardana KR, & Bock PE (2000) Characterization of proexosite I on prothrombin. *J. Biol. Chem.* 275(22):16428-16434.

6. Monteiro RQ, Bock PE, Bianconi ML, & Zingali RB (2001) Characterization of bothrojaracin interaction with human prothrombin. *Protein Sci.* 10:1897-1904.

7. Doyle MF & Mann KG (1990) Multiple active forms of thrombin IV. Relative activities of meizothrombins. *J. Biol. Chem.* 265(18):10693-10701.

8. Verhamme IMA, Olson ST, Tollefsen DM, & Bock PE (2002) Binding of exosite ligands to human thrombin: Re-evaluation of allosteric linkage between thrombin exosites I and II. *J. Biol. Chem.* 277(9):6788-6798.

9. Petrera NS*, et al.* (2009) Long range communication between exosites 1 and 2 modulates thrombin function. *J. Biol. Chem.* 284(38):25620-25629.

10. Ye J, Liu L-W, Esmon CT, & Johnson AE (1992) The fifth and sixth growth factor-like domains of thrombomodulin bind to the anion-binding exosite of thrombin and alter its specificity. *J. Biol. Chem.* 267(16):11023-11028.

11. Dumas JJ, Kumar R, Seehra J, Somers WS, & Mosyak L (2003) Crystal structure of the GPIb(alpha)-thrombin complex essential for platelet aggregation. *Science* 301:222-225.

12. Celikel R*, et al.* (2003) Modulation of α-thrombin function by distinct interactions with platelet glycoprotein Ibα. *Science* 301:218-221.

13. Panizzi P*, et al.* (2006) Novel fluorescent prothrombin analogs as probes of staphylocoagulase-prothrombin interactions. *J. Biol. Chem.* 281:1169-1178.

14. Panizzi P*, et al.* (2006) Fibrinogen substrate recognition by staphylocoagulase-(pro)thrombin complexes. *J. Biol. Chem.* 281(2):1179-1187.

15. Kroh HK, Panizzi P, & Bock PE (2009) Von Willebrand factor binding-protein is a hysteretic conformational activator of prothrombin. *Proc. Natl. Acad. Sci. U. S. A.* 106(19):7786-7791.

16. Friedrich R*, et al.* (2003) Staphylocoagulase is a prototype for the mechanism of cofactor-induced zymogen activation. *Nature* 425:535-539.

17. Frieden C (1970) Kinetic aspects of regulation of metabolic processes: The hysteretic enzyme concept. *J. Biol. Chem.* 245(21):5788-5799.

18. Frieden C (1979) Slow transitions and hysteretic behavior in enzymes. *Annu. Rev. Biochem.* 48:471-489.

19. Bock PE, Olson ST, & Bjork I (1997) Inactivation of thrombin by antithrombin is accompanied by inactivation of regulatory exosite I. *J. Biol. Chem.* 272(32):19837-19845.

20. Bock P (1992) Active-site-selective labeling of blood coagulation proteinases with fluorescence probes by the use of thioester peptide chloromethyl ketones. I. Specificity of thrombin labeling. *J. Biol. Chem.* 267:14963-14973.

21. Carlisle TL, Bock PE, & Jackson CM (1990) Kinetic intermediates in prothrombin activation: Bovine prethrombin 1 conversion to thrombin by factor X. *J. Biol. Chem.* 265(35):22044-22055.

22. Kamath P & Krishnaswamy S (2008) Fate of membrane-bound reactants and products during the activation of human prothrombin by prothrombinase. *J. Biol. Chem.* 283(44):30164-30173.

23. Orcutt SJ & Krishnaswamy S (2004) Binding of substrate in two conformations to human prothrombinase drives consecutive cleavage at two sites in prothrombin. *J. Biol. Chem.* 279:54927-54936.

24. Bock PE (1992) Active-site-selective labeling of blood coagulation proteinases with fluorescence probes by the use of thioester peptide chloromethyl ketones II. Properties of thrombin derivatives as reporters of prothrombin fragment 2 binding and specificity of the labeling approach for other proteinases. *J. Biol. Chem.* 267(21):14974-14981.

25. Mac Sweeney A*, et al.* (2000) Crystal structure of gamma-chymotrypsin bound to a peptidyl chloromethyl ketone inhibitor. *Acta Crystallogr., Sect. D: Biol. Crystallogr.* D56:280-256.

26. Panizzi P, Friedrich R, Fuentes-Prior P, Bode W, & Bock PE (2004) The staphylocoagulase family of zymogen activator and adhesion proteins. *Cell. Mol. Life Sci.* 61:1-6.

27. Huang M*, et al.* (2003) Structural basis of membrane binding by Gla domains of vitamin K-dependent proteins. *Nature Structural Biology* 10(9):751-756.

28. Soriano-Garcia M, Park CH, Tulinsky A, Ravichandran KG, & Skrzypczak-Jankun E (1989) Structure of Ca^{2+} prothrombin fragment 1 including the conformation of the Gla domain. *Biochemistry* 28:6805-6810.

29. Soriano-Garcia M, Padmanabhan K, de Vos AM, & Tulinsky A (1992) The Ca^{2+} ion and membrane binding structure of the Gla domain of Ca-prothrombin fragment 1. *Biochemistry* 31:2554-2566.

30. Church FC, Lundblad RL, Noyes CM, & Tarvers RC (1985) Effect of divalent cations on the limited proteolysis of prothrombin by thrombin. *Arch. Biochem. Biophys.* 240(2):607-612.

31. Stevens WK, Cotes HCF, MacGillivray RTA, & Nesheim ME (1996) Calcium ion modulation of meizothrombin autolysis at Arg55-Asp56 and catalytic activity. *J. Biol. Chem.* 271(14):8062-8067.

32. Nesheim ME, Abbott T, Jenny R, & Mann KG (1988) Evidence that the thrombin-catalyzed feedback cleavage of fragment 1.2 at Arg154-Ser155 promotes the release of thrombin from the catalytic surface during the activation of bovine prothrombin. *J. Biol. Chem.* 263(2):1037-1044.

33. Anderson PJ & Bock PE (2003) Role of prothrombin fragment 1 in the pathway of regulatory exosite I formation during conversion of human prothrombin to thrombin. *J. Biol. Chem.* 278(45):44489-44495.

34. Bode W & Huber R (1976) Induction of the bovine trypsinogen-trypsin transition by peptides sequentially similar to the N-terminus of trypsin. *FEBS Lett.* 68(2):231-236.

35. Khan AR & James MNG (1998) Molecular mechanisms for the conversion of zymogens to active proteolytic enzymes. *Protein Sci.* 7:815-836.

36. Page MJ, MacGillivray RTA, & Di Cera E (2005) Determinants of specificity in coagulation proteases. *J. Thromb. Haemost.* 3:1-8.

37. Narayana SVL*, et al.* (1994) Structure of human factor D: A complement system protein at 2.0A resolution. *J. Mol. Biol.* 235:695-708.

38. Petrovan RJ & Ruf W (2002) Role of zymogenicity-determining residues of coagulation factor VII/VIIa in cofactor interaction and macromolecular substrate recognition. *Biochemistry* 41:9302-9309.

39. Olsen OH & Persson E (2008) Cofactor-induced and mutational activity enhancement of coagulation factor VIIa. *Cell. Mol. Life Sci.* 65:953-963.

40. Eigenbrot C & Kirchhofer D (2002) New insight into how tissue factor allosterically regulates factor VIIa. *Trends Cardiovasc. Med.* 12:19-26.

41. Perona JJ & Craik C, S. (1995) Structural basis of substrate specificity in the serine proteases. *Protein Sci.* 4:337-360.

42. Kettner C & Shaw E (1981) Inactivation of trypsin-like enzymes with peptides of argining chloromethyl ketone. *Methods Enzymol.* 80:826-842.

43. Vijayalakshmi J, Padmanabhan KP, Mann KG, & Tulinsky A (1994) The isomorphous structures of prethrombin2, hirugen-, and PPACK-thrombin: Changes accompanying activation and exosite binding to thrombin. *Protein Sci.* 3:2254-2271.

44. Petrovan RJ*, et al.* (1998) Autocatalytic peptide bond cleavages in prothrombin and meizothrombin. *Biochemistry* 37:1185-1191.

45. Esmon CT, Owen WG, & Jackson CM (1974) The conversion of prothrombin to thrombin II. Differentiation between thrombin- and factor Xa-catalyzed proteolyses. *J. Biol. Chem.* 249(2):606-611.

46. Downing MR, Butkowski RJ, Clark MM, & Mann KG (1975) Human prothrombin activation. *J. Biol. Chem.* 250(23):8897-8906.

47. Shi F, Hogg PJ, Winzor DJ, & Jackson CM (1998) Evidence for multiple enzyme site involvement in the modulation of thrombin activity by products of prothrombin proteolysis. *Biophys. Chem.* 75:187-199.

48. Stevens WK & Nesheim ME (1993) Structural changes in the protease domain of prothrombin upon activation as assessed by *N*-bromosuccinimide modification of tryptophan residues in prethrombin-2 and thrombin. *Biochemistry* 32:2787-2794.

49. Hof M (1998) Picosecond tryptophan fluorescence of membrane-bound prothrombin fragment 1. *Biochim. Biophys. Acta* 1388:143-153.

CHAPTER IV

EXPRESSION OF ALLOSTERIC LINKAGE BETWEEN THE SODIUM ION BINDING SITE AND EXOSITE I OF THROMBIN DURING PROTHROMBIN ACTIVATION

Heather K. Kroh*, Guido Tans[†], Gerry A. F. Nicolaes[†], Jan Rosing[†], and Paul E. Bock[*]

[*]Department of Pathology, Vanderbilt University, Nashville, TN 37232

[†]Department of Biochemistry, Cardiovascular Research Institute Maastricht, University Maastricht, 6200MD Maastricht, The Netherlands

(This research was originally published in the Journal of Biological Chemistry. Heather K. Kroh, Guido Tans, Gerry A. F. Nicolaes, Jan Rosing, and Paul E. Bock. Expression of allosteric linkage between the sodium ion binding site and exosite I of thrombin during prothrombin activation. 2007; 282(22):16095-16104.

Abstract

The specificity of thrombin for procoagulant and anticoagulant substrates is regulated allosterically by Na^+. Ordered cleavage of prothrombin (ProT) at Arg^{320} by the prothrombinase complex generates proteolytically active, meizothrombin (MzT), followed by cleavage at Arg^{271} to produce thrombin and fragment 1.2. The alternative pathway of initial cleavage at Arg^{271} produces the inactive zymogen form, the prethrombin 2 (Pre 2)-fragment 1.2 complex, which is cleaved subsequently at Arg^{320}. Cleavage at Arg^{320} of ProT or prethrombin 1 (Pre 1) activates the catalytic site and the precursor form of exosite I (proexosite I). To determine the pathway of expression of Na^+-(pro)exosite I linkage during ProT activation, the effects of Na^+ on the affinity of fluorescein-labeled hirudin-(54-65) ([5F]Hir-(54-65)(SO_3^-)) for the zymogens, ProT, Pre 1, and Pre 2, and for the proteinases, MzT and MzT-des-fragment 1 (MzT(-F1)) were quantitated. The zymogens showed no significant linkage between proexosite I and Na^+, whereas cleavage at Arg^{320} enhanced the affinities of MzT and MzT(-F1) for [5F]Hir-(54-65)(SO_3^-) 8-10 fold and 5-6-fold, respectively. MzT and MzT(-F1) showed kinetically different mechanisms of Na^+ enhancement of chromogenic substrate hydrolysis. The results demonstrate for the first time that MzT is regulated allosterically by Na^+. The results suggest that the distinctive procoagulant substrate specificity of MzT in activating factor V and factor VIII on membranes, and the anticoagulant, membrane-modulated activation of protein C by MzT bound to thrombomodulin are regulated by Na^+-induced allosteric transition. Further, the Na^+ enhancement in MzT activity and exosite I affinity may function in directing the sequential ProT activation pathway by accelerating thrombin formation from the MzT fast form.

Introduction

The blood coagulation proteinase, thrombin, is generated after cleavage of two peptide bonds in its zymogen precursor, prothrombin (ProT)[1], by the membrane-bound factor Xa-factor Va (prothrombinase) complex (1). The rate of thrombin generation from ProT catalyzed by factor Xa alone is accelerated ~300,000-fold by calcium ion-dependent assembly of factor Xa with its protein cofactor, factor Va. Factor Va in the prothrombinase complex directs the order of peptide bond cleavage in the activation pathway, resulting in sequential cleavage of ProT first at Arg^{320} in the catalytic domain to form the catalytically active intermediate, meizothrombin (MzT), followed by cleavage at Arg^{271} between the catalytic domain and ProT fragment 1.2 to produce the reaction products, thrombin and fragment 1.2 (2-7). In the absence of factor Va, the alternative, slower pathway of bond cleavage predominates, in which initial cleavage at Arg^{271} forms the inactive intermediate prethrombin 2 (Pre 2), bound noncovalently to fragment 1.2, followed by cleavage at Arg^{320} to form thrombin. Recent studies of the sequential pathway of ProT activation indicate that substrates are bound to prothrombinase in two alternate conformations that present the two peptide bonds sequentially to factor Xa for cleavage (7-14). Conformational changes accompanying catalytic site expression in the conversion of ProT to MzT direct the activation pathway by switching substrate bound to prothrombinase between alternate zymogen and proteinase conformations (8).

On conversion of ProT to thrombin, two electropositive surface sites, exosites I and II, become expressed on thrombin, which provide recognition sites for specific physiological substrates, inhibitors, and regulatory molecules (7, 15-18). Exosite I mediates fibrinogen and protease activated receptor-1 and -4 substrate interactions, fibrin binding, and binding of the COOH-terminal hirudin-(54-65) peptide (Hir-(54-65)(SO_3^-)). Exosite II binds heparin and the fragment 2 domain of ProT. Both exosites are involved in factor V and VIII activation, glycoprotein Ib binding, thrombomodulin

binding, and inactivation of thrombin by heparin cofactor II (15-18). The substrate specificity of MzT is different from that of thrombin, in that it exhibits ≤10% activity toward fibrinogen and ≤2% activity in activating platelets (19-20). MzT, however, is a potent procoagulant activator of factor V and factor VIII in reactions that are dependent on phospholipid membranes (21-22). MzT bound to thrombomodulin activates the anticoagulant, protein C, at a rate equal to or greater than thrombin. Protein C activation by thrombomodulin-bound MzT is also stimulated by membranes (19-20).

Exosite I interactions are allosterically linked to binding of a single sodium ion to thrombin (23-24). Binding of Na^+ converts thrombin from a "slow" to a "fast" form (25). The fast form has higher catalytic efficiency (k_{cat}/K_m) for the procoagulant substrates, fibrinogen and protease activated receptor-1, greater reactivity toward antithrombin, and increased amidolytic chromogenic substrate activity, notably towards *D*-Phe-Pro-Arg-*p*NA (15, 24). Alanine substitution mutagenesis and analysis of high resolution crystal structures of the fast and slow forms in their free states have identified four structural features critical to the allosteric transition to the fast form (23, 26-28): (a) alignment of residues stabilizing the Na^+ binding site; (b) a change in orientation of Asp^{189} in the primary substrate specificity site; (c) a shift in the Glu^{192} side chain that links a network of water molecules to Ser^{195}; and; (d) a change in Ser^{195} orientation, all of which optimize catalysis. Comparison of these structures with those of thrombin either inactivated with the transition state analog, *D*-Phe-Pro-Arg-CH_2Cl (FPR-CH_2Cl), or in which exosite I is occupied by the COOH-terminal hirudin peptide, hirugen (hirudin-(53-64)), show that thrombin adopts the fast conformation in these complexes (27, 29). Recent structural studies (30-31), consistent with kinetic studies of Na^+ binding (31-33), suggest that the catalytically active Na^+-free slow form is in equilibrium with a low level of an inactive thrombin in which the catalytic site and Na^+ site are occluded.

Previous studies of exosite I expression on ProT activation intermediates characterized a precursor form of exosite I on ProT (proexosite I), with a ~100-fold lower affinity for the model exosite I-specific ligand Hir-(54-65)(SO_3^-) (34-36). Removal of fragment 1 from ProT to form prethrombin 1 (Pre 1) is accompanied by a ~7-fold increase in proexosite I affinity (35). The further 11-20-fold increase in affinity, representing full exosite I expression, occurs in concert with expression of catalytic activity during formation of MzT and thrombin (35-36). Quantitative analysis of binding of the ProT activation fragments 2 and 1.2 to exosite II on Pre 2 and thrombin indicates that this exosite becomes unmasked upon cleavage at Arg^{271} and subsequent dissociation of the fragments (35-36). How linkage between the Na^+ site and (pro)exosite I is expressed during ProT activation has not been investigated.

In the present studies, fluorescein-labeled Hir-(54-65)(SO_3^-) ([5F]Hir-(54-65)(SO_3^-)) was used as a (pro)exosite I-specific probe to examine the linkage between Na^+ binding and (pro)exosite I affinity (34-37). The goal was to determine if Na^+ regulates the affinity of proexosite I for ProT, Pre 1, and Pre 2 zymogen forms, and the catalytically active intermediates of ProT and Pre 1 activation, MzT and meizothrombin des-fragment 1 (MzT(-F1)), respectively. The results demonstrate no significant effect of Na^+ on ProT, Pre 1, or Pre 2 proexosite I affinity for [5F]Hir-(54-65)(SO_3^-). Allosteric linkage between Na^+ binding and exosite I affinity occurred concomitantly with activation to MzT and MzT(-F1). The Na^+ enhancement of the rate of chromogenic substrate hydrolysis for MzT compared to MzT(-F1) and thrombin, however, followed a kinetically different mechanism. The results demonstrate for the first time that MzT and MzT(-F1) are allosterically regulated by Na^+-exosite I interactions, suggesting that the unique substrate specificity of MzT may be Na^+-regulated.

Experimental Procedures

Protein and Peptide Purification and Characterization

Human ProT, factor Xa, and thrombin were purified and characterized as described previously (38-39). Pre 1 was purified from products of ProT cleavage by thrombin (38). FPR-MzT(-F1) was prepared by activation of 20 μM Pre 1 with 2 units/ml (based on the manufacturers specifications) of purified ecarin from *Echis carinatus* venom (Sigma) in the presence of a 10-fold excess of FPR-CH_2Cl (40). FPR-MzT was prepared from ProT at the same reactant concentrations followed by chromatography on Resource Q (Amersham) in 20 mM sodium citrate buffer, pH 6.0. The column was washed with 10 ml of equilibration buffer, and eluted with a 50 ml NaCl gradient in the same buffer up to 0.5 M to remove ecarin. Pre 2 was purified from factor Xa-ProT activation reactions as described (36). The R155A substitution mutant of ProT ($ProT^{R155A}$) was prepared as described (21). Protein concentrations were determined by absorbance at 280 nm using the following absorption coefficients ($(mg/ml)^{-1}cm^{-1}$) and molecular weights (4, 41-42): ProT, $ProT^{R155A}$, and FPR-MzT, 1.47, 71,600; Pre 1 and FPR-MzT(-F1), 1.78, 49,900; Pre 2, 1.73, 37,000; and thrombin, 1.74, 36,600. [5F]Hir-(54-65)(SO_3^-) was prepared as described previously (37).

Fluorescence Titrations

Binding of [5F]Hir-(54-65)(SO_3^-) was measured by titrating the labeled peptide with the protein of interest and monitoring the change in fluorescence at 520 nm with excitation at 491 nm (4 nm or 8 nm band passes), using acrylic cuvettes coated with polyethylene glycol (PEG) 20,000. Fluorescence changes expressed as $(F_{obs}-F_o)/F_o=\Delta F/F_o$, as a function of total protein concentration were fit by the quadratic binding equation to obtain the maximum fluorescence change ($(F_{max}-F_o)/F_o=\Delta F_{max}/F_o$), and the dissociation constant (K_D), with the stoichiometric factor fixed at 1(37). Fluorescence

measurements were corrected for background signal by subtraction of a buffer blank, and for dilution, which was not more than 10%.

Exosite Linkage Analysis

The effect of Na^+ on binding of [5F]Hir-(54-65)(SO_3^-) to (pro)exosite I was characterized in fluorescence titrations with ProT species in 50 mM Tris-Cl, 110 mM NaCl or 110 mM Choline Cl (ChCl), 5 mM $CaCl_2$, 1 mg/ml PEG 8000, pH 7.4 at 25 ^oC. Linkage between Na^+ and [5F]Hir-(54-65)(SO_3^-) (H) binding to thrombin, MzT(-F1), and MzT (designated P) was analyzed according to the thermodynamic cycle in Scheme 1, where Na^+ binding affects the affinity of peptide binding and vice versa.

Scheme 1.

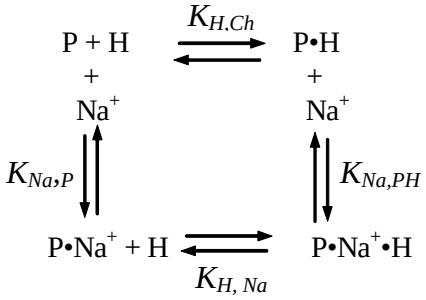

Because of the relatively small differences in fluorescence between titrations in NaCl and ChCl, it was not possible to determine accurately the dissociation constant for Na^+ binding from the Na^+ concentration dependence at a fixed thrombin concentration. Titrations in 110 mM NaCl and 110 mM ChCl were fit independently by the quadratic binding equation to obtain the maximum fluorescence change $\Delta F_{max,\ PH}/F_o$ and $K_{H,\ Ch}$ from the titration in ChCl, and $\Delta F_{max,\ PNaH}/F_o$ and $K_{H,\ Na}$ from the titration in the presence of NaCl.

Kinetic and Endpoint Fluorescence Titrations

To quantitate the effects of Na^+ on binding of [5F]Hir-(54-65)(SO_3^-) to exosite I on active MzT(-F1) and MzT^{R155A}, it was necessary to employ a kinetic approach to

separate the ecarin-catalyzed formation of MzT(-F1) and MzT^{R155A} from slower autocatalytic cleavages that process the products further (43). Experiments were performed for Pre 1 by measuring F_o for 20 nM [5F]Hir-(54-65)(SO_3^-), the instantaneous decrease in fluorescence on addition of Pre 1 due to peptide binding to (pro)exosite I, and the time dependence of the subsequent fluorescence decrease initiated by addition of 2 units/ml of ecarin. The ecarin-initiated fluorescence time-courses were fit by the sum of a single exponential decay and a straight line to determine the fluorescence endpoint corrected for any slow linear drift, and the results were expressed as $\Delta F/F_o$. For analysis of the progress curves, the integrated Michaelis-Menten equation was used to represent the ecarin (E)-catalyzed conversion of Pre 1 or ProT^{R155A} (C) into MzT(-F1) or MzT^{R155A} (P), respectively (*Scheme 2*). Comparison of this analysis with the integrated rate equation including competitive product inhibition showed no evidence for product inhibition with MzT(-F1), while including product inhibition for MzT^{R155A} improved the fit modestly.

Scheme 2. $E + C \underset{}{\overset{Km}{\longleftrightarrow}} E{\bullet}C \xrightarrow{V_{max}} E + P$

Under the experimental conditions used, the fluorescence change accompanying peptide (H) binding is not a linear function of the concentration of P or C. Moreover, these species compete for the peptide, and binding is accompanied by unequal fluorescence changes for the P•H and C•H complexes (*Scheme 3*). To analyze the time courses, the cubic competitive binding equation derived previously for Scheme 3 (44) in combination with the integrated Michaelis-Menten equation was used for nonlinear least-squares fitting. Fluorescence versus time data collected as a function of the concentration of C (Pre 1) in NaCl- or ChCl-containing buffers were analyzed with the

parameters determined independently for H ([5F]Hir-(54-65)(SO_3^-)) binding to C (Pre 1) fixed. The fitted parameters were the maximum fluorescence change for the

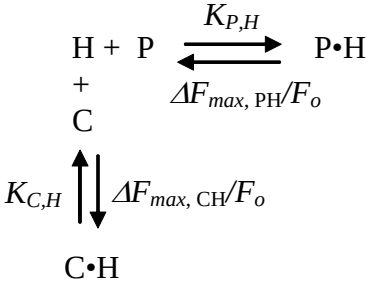

Scheme 3.

MzT(-F1)•[5F]Hir-(54-65)(SO_3^-) complex ($\Delta F_{max,\,PH}/F_o$), $K_{P,H}$, K_m, and V_{max}. The fluorescence and binding parameters determined from this analysis were compared to those obtained by fitting of the quadratic binding equation to the reaction endpoints as a function of C (Pre 1) concentration determined in a model-independent manner by the exponential fit described above. The same approaches were used in kinetic and endpoint titrations of the activation of $ProT^{R155A}$ to MzT^{R155A} by ecarin and FPR-MzT(-F1) from activation of Pre 1 in the presence of 24 μM FPR-CH_2Cl. The presence of 20 nM [5F]Hir-(54-65)(SO_3^-) in these reactions did not influence the results because ≤6 % of the total Pre 1 or $ProT^{R155A}$ was bound at any time, over the protein concentration range studied.

Pre 1 Activation Assay

Assays specific for MzT(-F1) were performed by modifications of the published methods (2, 5). This approach enables differential measurement of thrombin and MzT(-F1) based on the much faster rate of thrombin inactivation by antithrombin-heparin complex compared to MzT(-F1). Aliquots of activation reactions of Pre 1 in the buffers containing NaCl or ChCl initiated at 25 ^oC by addition of ecarin were quenched by dilution to 10 nM Pre 1 in 250 mM Hepes, 150 mM NaCl, 75 mM EDTA, 1 mg/ml PEG 8000, pH 7.70 (for NaCl reactions) or 250 mM Hepes, 590 mM NaCl, 75 mM EDTA, 1

mg/ml PEG 8000, pH 7.65 (for ChCl reactions) containing 50 nM antithrombin and 18 μg/ml heparin (Sigma) for exactly 30 s. An aliquot of the quenched reaction was diluted tenfold in 50 mM Hepes, 125 mM NaCl, 1 mM EDTA, 1 mg/ml PEG 8000, pH 7.4 containing 100 μM *D*-Phe-Pip-Arg-*p*NA, and the initial rate of chromogenic substrate hydrolysis was measured from the linear increase in absorbance at 405 nm. Thrombin was confirmed to be >99.9% inactivated during the 30 s quenching time. To correct for the differences in kinetic parameters of thrombin and MzT(-F1) and the small loss of MzT(-F1) during quenching, the rates obtained for Pre 1 fully activated by incubation with 2 units/ml ecarin for 60 min were measured as a function of time after quenching, relative to an equivalent concentration of thrombin. Extrapolation of the slow, linear decrease in MzT(-F1) activity with time due to antithrombin-heparin inactivation and possible autocatalytic thrombin formation to zero-time was taken to represent the total MzT(-F1) concentration. The extrapolated chromogenic substrate activity of MzT(-F1) relative to thrombin was determined to be 1.21 and 1.23 in the NaCl and ChCl experiments, respectively, and the correction for loss of MzT(-F1) activity was 10% and 6% in the NaCl and ChCl experiments, respectively

Na^+ Dependence of Chromogenic Substrate Hydrolysis

Initial rates of hydrolysis of 200 μM (saturating) *D*-Phe-Pip-Arg-*p*NA were measured at 25 ^oC as a function of Na^+ concentration using mixtures of buffers containing 110 mM NaCl or ChCl. These experiments measured the Na^+ dependence of k_{cat}, reflecting Na^+ binding to the enzyme-substrate complex. The initial rates at zero and saturating Na^+ concentration, and the apparent K_D for Na^+ binding were obtained by least-squares fitting of the hyperbolic titrations. To estimate the affinities of Na^+ for the free enzymes, k_{cat}, K_m, and K_i for product were determined by full progress curve analysis of *D*-Phe-Pip-Arg-*p*NA hydrolysis as a function of Na^+ concentration (45). Five progress curves at 5-15 μM substrate were fit simultaneously to obtain the kinetic

parameters. The K_D for Na^+ binding to thrombin and MzT(-F1) was obtained by fitting the hyperbolic dependence of k_{cat}/K_m on Na^+ concentration (45). In the case of MzT^{R155A} for which this was not possible, an estimate of the K_D for Na^+ binding to the free enzyme was obtained from the dependence of the observed K_m ($K_{m\ obs}$) on Na^+ concentration, where K_m was assumed to be equivalent to the dissociation constant for substrate binding. Equation 1 described by Segel (46) for the rapid equilibrium, nonessential activator mechanism was fit to the data to obtain K_m, K_{Na}, and α, which represents the linkage factor by which K_{Na} is changed by substrate binding.

$$K_{m\,obs} = K_m \frac{\left(1+\frac{[\mathrm{Na}]_o}{K_{Na}}\right)}{\left(1+\frac{[\mathrm{Na}]_o}{\alpha K_{Na}}\right)} \qquad \textbf{Eqn. 1}$$

Results

Na$^+$-exosite I Linkage for ProT Zymogen Forms

To assess the linkage between Na^+ binding and proexosite I, the effect of Na^+ on the affinity of proexosite I for the 5-fluorescein-labeled Tyr^{63}-sulfated hirudin-(54-65) peptide ([5F]Hir-(54-65)(SO_3^-)) was determined in fluorescence titrations in buffers containing 110 mM NaCl or 110 mM ChCl at constant 0.17 M ionic strength. As shown in Figure 1, ProT, Pre 1, and Pre 2 bound the peptide with virtually the same affinity in NaCl and ChCl. Although the titrations consistently showed a small increase in affinity by Na^+ (1.3-1.6-fold), this was within the experimental error of the binding parameters (Table I).

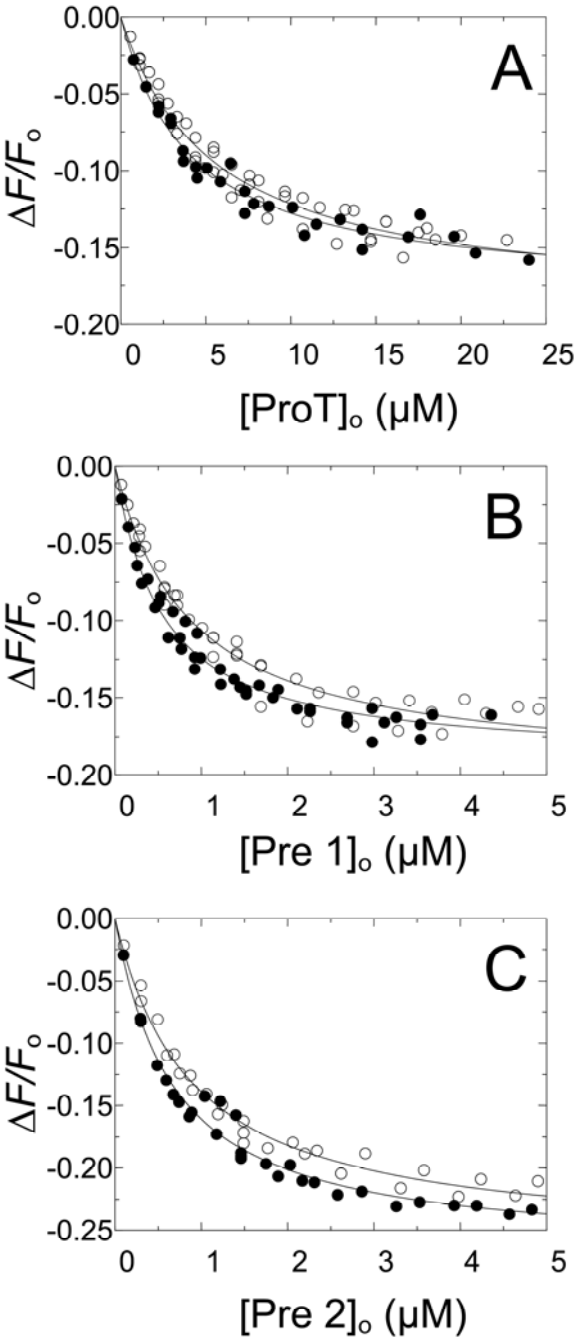

Figure 1. Effect of Na^+ on [5F]Hir-(54-65)(SO_3^-) binding to ProT zymogen forms. Changes in fluorescence ($\Delta F/F_o$) of 50 nM [5F]Hir-(54-65)(SO_3^-) as a function of the total concentrations of A, ProT (*[ProT]$_o$*), B, Pre 1 (*[Pre 1]$_o$*), and C, Pre 2 (*[Pre 2]$_o$*) are shown for experiments in buffers containing NaCl (●) or ChCl (○). The *solid lines* represent the nonlinear least-squares fits by the quadratic binding equation with the parameters listed in Table I. Titrations were performed and analyzed as described in "Experimental Procedures".

Na$^+$-exosite I Linkage for Thrombin and FPR-thrombin

As expected, thrombin affinity for [5F]Hir-(54-65)(SO_3^-) increased 5.6-fold from dissociation constants of 270 ± 20 nM in the absence of Na^+ to 48 ± 4 nM in NaCl (Fig. 2, Table I). Inactivation of thrombin with FPR-CH_2Cl virtually obliterated the effect of Na^+ on affinity and normalized the dissociation constants in the presence and absence of Na^+ to values indistinguishable from those of the fast form of native thrombin (Fig. 2, Table I).

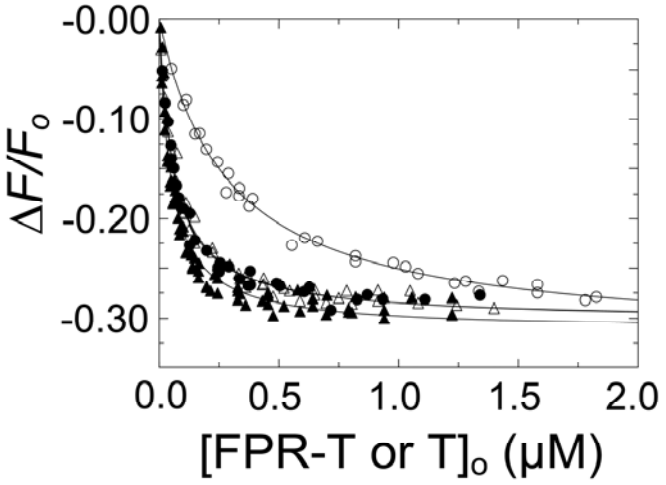

Figure 2. Effect of Na^+ on [5F]Hir-(54-65)(SO_3^-) binding to thrombin and FPR-thrombin. Titrations of the change in fluorescence ($\Delta F/F_o$) of 20 nM [5F]Hir-(54-65)(SO_3^-) as a function of total concentrations of FPR-thrombin or thrombin (*[FPR-T or T]$_o$*). Titrations with native thrombin in buffers containing NaCl (●) or ChCl (○), and FPR-thrombin in NaCl (▲) or ChCl (△). The *solid lines* represent the non-linear least-squares fit by the binding equation with the parameters listed in Table I. Titrations were performed and analyzed as described in "Experimental Procedures".

Analysis of Na$^+$-exosite I Linkage for MzT(-F1)

MzT and MzT(-F1) are unstable in their active forms as a result of autocatalytic cleavage (43). To characterize the effect of Na^+ on active MzT(-F1), a kinetic approach was used to quantitate [5F]Hir-(54-65)(SO_3^-) binding to MzT(-F1) during its generation by ecarin activation of Pre 1 (see "Experimental Procedures"). The integrated Michaelis-

Menten equation was used to calculate the full time-course of ecarin-catalyzed MzT(-F1) formation. The fluorescence change accompanying peptide binding is not a linear function of MzT(-F1) or Pre 1 concentration, and it was also necessary to account for the fluorescence changes due to competitive [5F]Hir-(54-65)(SO_3^-) binding to Pre 1 as its concentration decreased during the reaction. A binding equation for a model in which two ligands (Pre 1 and MzT(-F1)) bind competitively to a common fluorescent acceptor ([5F]Hir-(54-65)(SO_3^-)) with unequal fluorescence changes (44) was used to convert the fluorescence data into the concentrations of MzT(-F1) and Pre 1 with time. Figure 3 shows fluorescence traces in reaction mixtures containing NaCl or ChCl during activation of 1 μM Pre 1 by ecarin in the presence of 20 nM [5F]Hir-(54-65)(SO_3^-). The initial decrease in fluorescence corresponds to binding of the peptide to Pre 1 and the subsequent time-dependent decrease to generation of a product with a higher affinity for the peptide. To validate the experiments, a chromogenic substrate assay which enables quantitation of MzT(-F1) formation in the presence of thrombin was used to follow MzT(-F1) formation. Progress curves of MzT(-F1) generation in the absence and presence of Na^+ were in good agreement with the calculated progress curves (Fig. 3).

To confirm that the product of Pre 1 activation was MzT(-F1), SDS-gel time-courses were done under the same experimental conditions in the absence and presence of Na^+ (Fig. 4). The reduced samples showed the disappearance of Pre 1 and formation of the MzT(-F1) B-chain and fragment 2-A-chain. The nonreduced samples showed a single band representing Pre 1 and co-migrating MzT(-F1) for at least 20 min, corresponding to the longest activation reactions performed (Fig. 4). Traces of thrombin only appeared after 40 min incubation in the reaction mixture containing Na^+ as can be seen by the faint band around 36,000 molecular weight in Figure 4A. The results

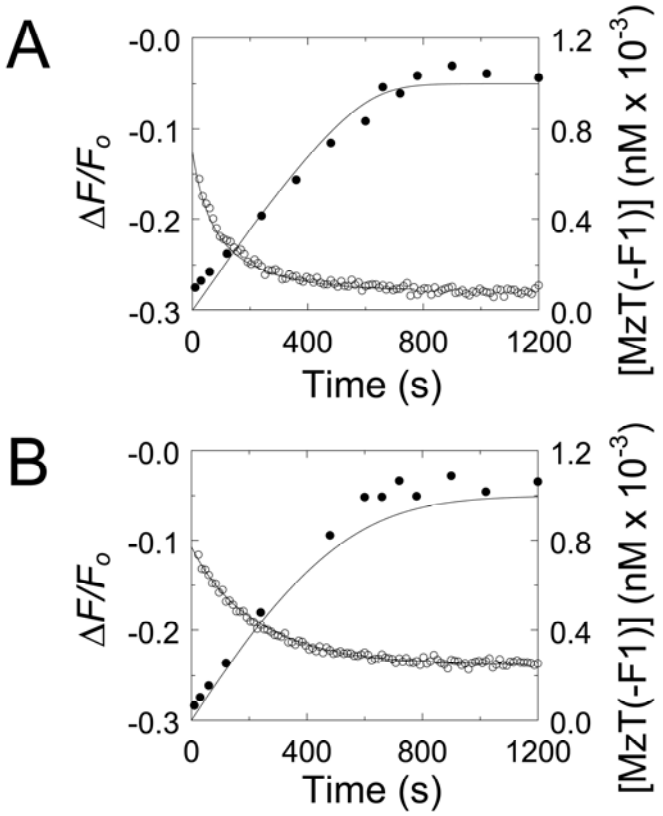

Figure 3. Time courses of [5F]Hir-(54-65)(SO_3^-) fluorescence changes and MzT(-F1) activity accompanying activation of Pre 1 by ecarin. A. The initial change in fluorescence ($\Delta F/F_o$) of 20 nM [5F]Hir-(54-65)(SO_3^-) on addition of 1 μM Pre 1 and the subsequent time-course of the fluorescence change initiated by 2 units/ml ecarin (○) are shown for a reaction in the presence of Na^+. The *solid line* represents is the nonlinear least-squares fit of the data by the model described in "Experimental Procedures" with the parameters obtained from the simultaneous analysis of the progress curves as a function of Pre 1 concentration listed in Table I. The time-course of MzT(-F1) formation ($[MzT(-F1)]_o$) measured by activity assays (●) is shown with the progress curve (*solid line*) calculated with the same parameters listed in Table I. B. Progress curves of the fluorescence change (○) and increase in MzT(-F1) concentration measured by activity (●) are shown for reactions in ChCl, with the other conditions as described in A. The *lines* represent the fits of the fluorescence data with the parameters determined from simultaneous analysis of progress curves in ChCl listed in Table I, and the calculated progress curve of MzT(-F1) formation using the same parameters. Fluorescence and activity measurements, and data analysis were performed as described under "Experimental Procedures".

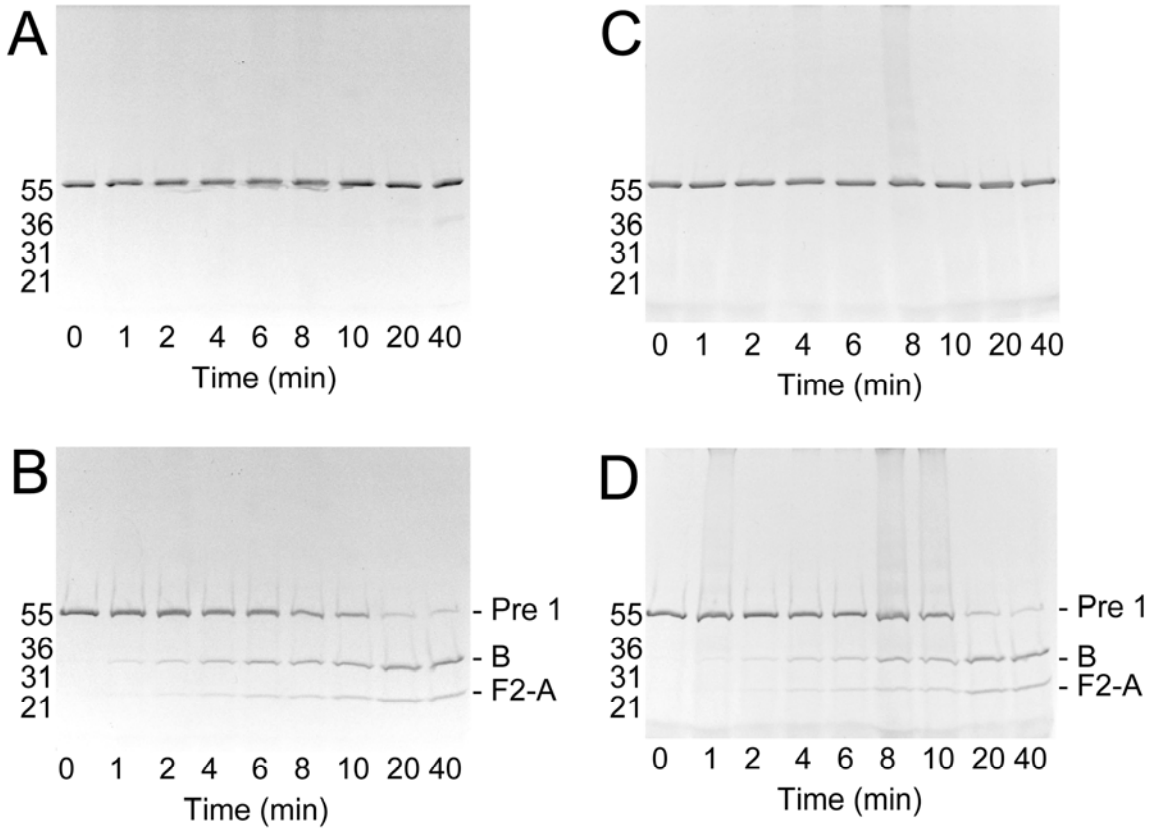

Figure 4. Time courses of Pre 1 activation monitored by SDS gel-electrophoresis. A and B. Activation of 1 μM Pre 1 initiated with 2 units/ml ecarin in buffer containing NaCl. Aliquots (~1 μg) were removed at the indicated reaction times, denatured under non-reducing (A) or reducing (B) conditions, and analyzed using 4-15% SDS gradient gels. Protein-stained bands corresponding to Pre 1, the MzT(-F1) B-chain (*B*), and fragment 2-A-chain (*F2-A*) are indicated for the reduced samples. Migration of molecular weight markers is indicated by the molecular weights in *thousands*. C and D. SDS gel-electrophoresis of non-reduced (C) and reduced (D) samples from Pre 1 activation in buffer containing ChCl as described in A and B. Reactions were performed as described under “Experimental Procedures”.

demonstrated that the observed fluorescence changes were well described by [5F]Hir-(54-65)(SO_3^-) binding with increased affinity for MzT(-F1), and that the results could be analyzed quantitatively.

Regulation of MzT(-F1) Exosite I Affinity by Na^+

Fluorescence-monitored time-courses at varied Pre 1 concentration in NaCl or ChCl (Fig. 5A and 5C) were fit simultaneously as described in "Experimental Procedures". The independently determined dissociation constant and maximum fluorescence change for [5F]Hir-(54-65)(SO_3^-) binding to Pre 1 (see Fig. 1) were fixed parameters, whereas K_m and V_{max} for the ecarin catalyzed reaction, the maximum fluorescence change, and the dissociation constant for labeled peptide binding to MzT(-F1) were fitted parameters. The K_m and V_{max} for MzT(-F1) formation were 128 ± 8 nM and 2.1 ± 0.03 nM/s in NaCl and 470 ± 60 nM and 2.9 ± 0.2 nM/s in ChCl. [5F]Hir-(54-65)(SO_3^-) bound to MzT(-F1) with a dissociation constant of 210 ± 5 nM in ChCl, which was decreased 5.1-fold to 41 ± 1 nM in NaCl, with indistinguishable changes in fluorescence (Table I).

Model-independent values for the affinity and fluorescence change maxima for MzT(-F1) were obtained by fitting of the quadratic binding equation to the reaction endpoints, representing a titration of [5F]Hir-(54-65)(SO_3^-) with MzT(-F1) (Fig. 5B and 5D). The parameters from this analysis were in excellent agreement with those obtained for the kinetic analysis, and indicated that the affinity of exosite I for [5F]Hir-(54-65)(SO_3^-) increased 5.7-fold in the presence of Na^+ (Table I).

Na^+-exosite I Linkage for FPR-MzT and FPR-MzT(-F1)

As was the case for FPR-thrombin, FPR-MzT and FPR-MzT(-F1) had essentially the same affinities for [5F]Hir-(54-65)(SO_3^-) determined in direct titrations in the absence and presence of Na^+ (Fig. 6). The dissociation constants corresponded closely to the

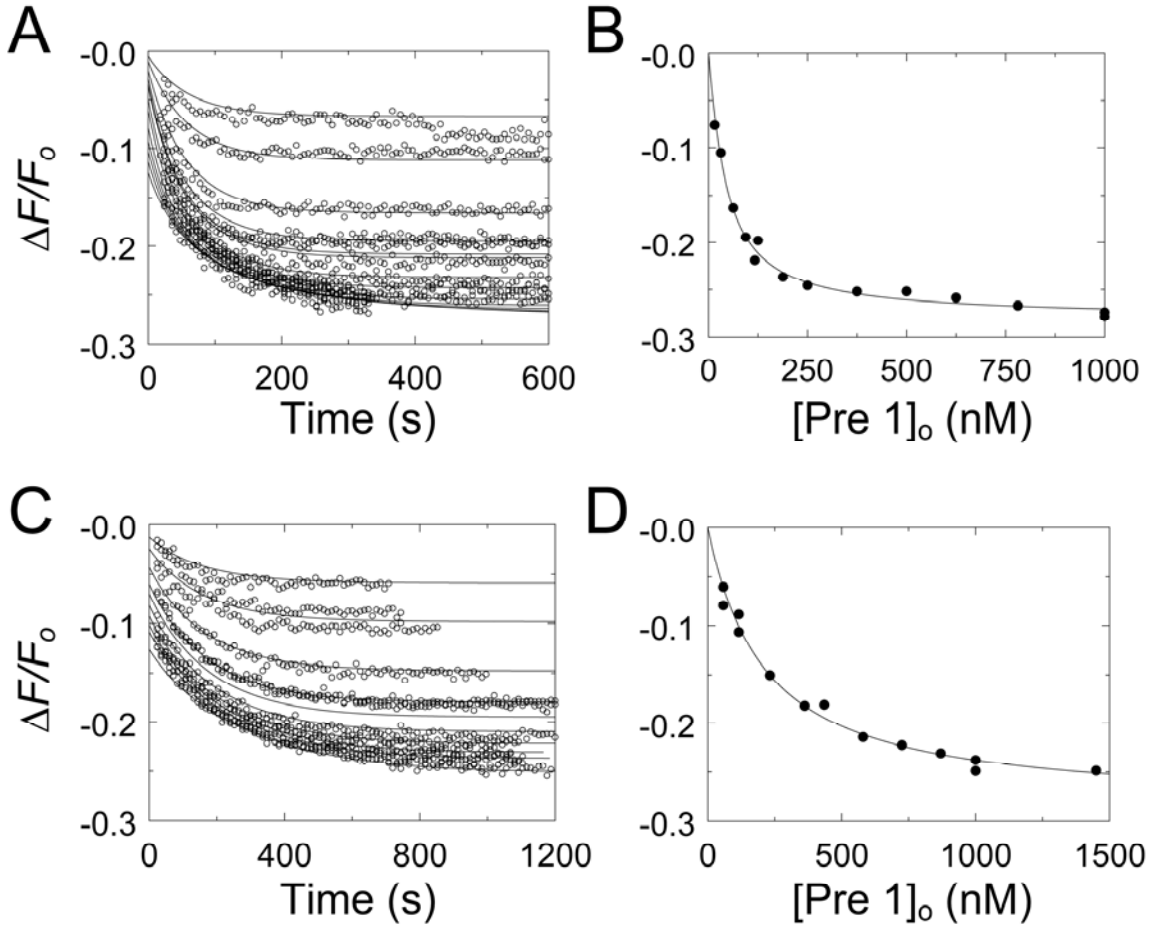

Figure 5. Kinetic and endpoint titrations of [5F]Hir-(54-65)(SO_3^-) binding to MzT(-F1) in the absence and presence of Na^+. A. Kinetic titration of fluorescence changes ($\Delta F/F_o$) of 20 nM [5F]Hir-(54-65)(SO_3^-) during activation of Pre 1 at concentrations ranging from 58 nM to 1000 nM, initiated by 2 units/ml ecarin in buffer containing NaCl (○). The *lines* represent the fit of the fluorescence data with the parameters listed in Table I. B. Analysis of the reaction endpoints as a function of the total Pre 1 concentration ($[Pre\ 1]_o$). The *line* represents the fit by the quadratic binding equation with the parameters listed in Table I. C. Kinetic titrations for activation of 116-1450 nM Pre 1 in buffer containing ChCl (○) otherwise as described in A, along with the simultaneous fit with the parameters listed in Table I. D. Endpoint titration for the reactions in buffer containing ChCl as described in B. Reactions were performed and analyzed as described in "Experimental Procedures".

affinity of the peptide for the Na^+-bound active MzT(-F1) and the thrombin fast form (Table I).

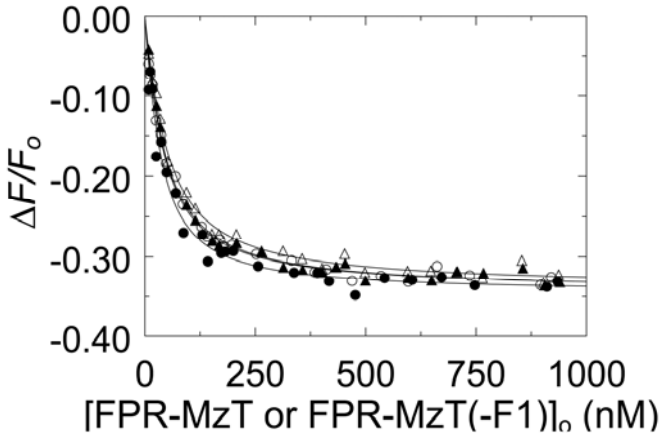

Figure 6. Effect of Na^+ on [5F]Hir-(54-65)(SO_3^-) binding to FPR-MzT and FPR-MzT(-F1). Titrations of the change in fluorescence (*$\Delta F/F_o$*) of 20 nM [5F]Hir-(54-65)(SO_3^-) in buffers containing NaCl (*closed symbols*) or ChCl (*open symbols*) as a function of the total concentrations of FPR-MzT (●, ○) and FPR-MzT(-F1) (▲, Δ) (*[FPR-MzT or FPR-MzT(-F1)]$_o$*). The *solid lines* represent the nonlinear least-squares fits of the titrations by the quadratic binding equation with the parameters listed in Table I. Titrations were performed and analyzed as described in "Experimental Procedures".

Effect of Na^+ on Exosite I of Active MzT

Intact, native MzT generated from ProT could not be studied because of rapid autocatalytic conversion to MzT(-F1) during ecarin activation (results not shown). A ProT mutant in which the fragment 1 cleavage site at Arg^{155} was substituted with Ala was activated to stable MzT^{R155A}, which allowed Na^+-exosite I linkage to be characterized. In direct titrations (not shown), $ProT^{R155A}$ bound [5F]Hir-(54-65)(SO_3^-) with K_D 1.9 ± 0.3 μM in ChCl and 1.1 ± 0.4 μM in NaCl. Results of kinetic titrations of MzT^{R155A} formation in Na^+ and Ch^+ are shown in Figure 7A and 7C, respectively. SDS-gel electrophoresis confirmed that MzT^{R155A} was the product of the reactions and was stable at concentrations and incubation times in excess of the experimental conditions (not shown). Full-length MzT^{R155A} behaved similarly to MzT(-F1), but with a few

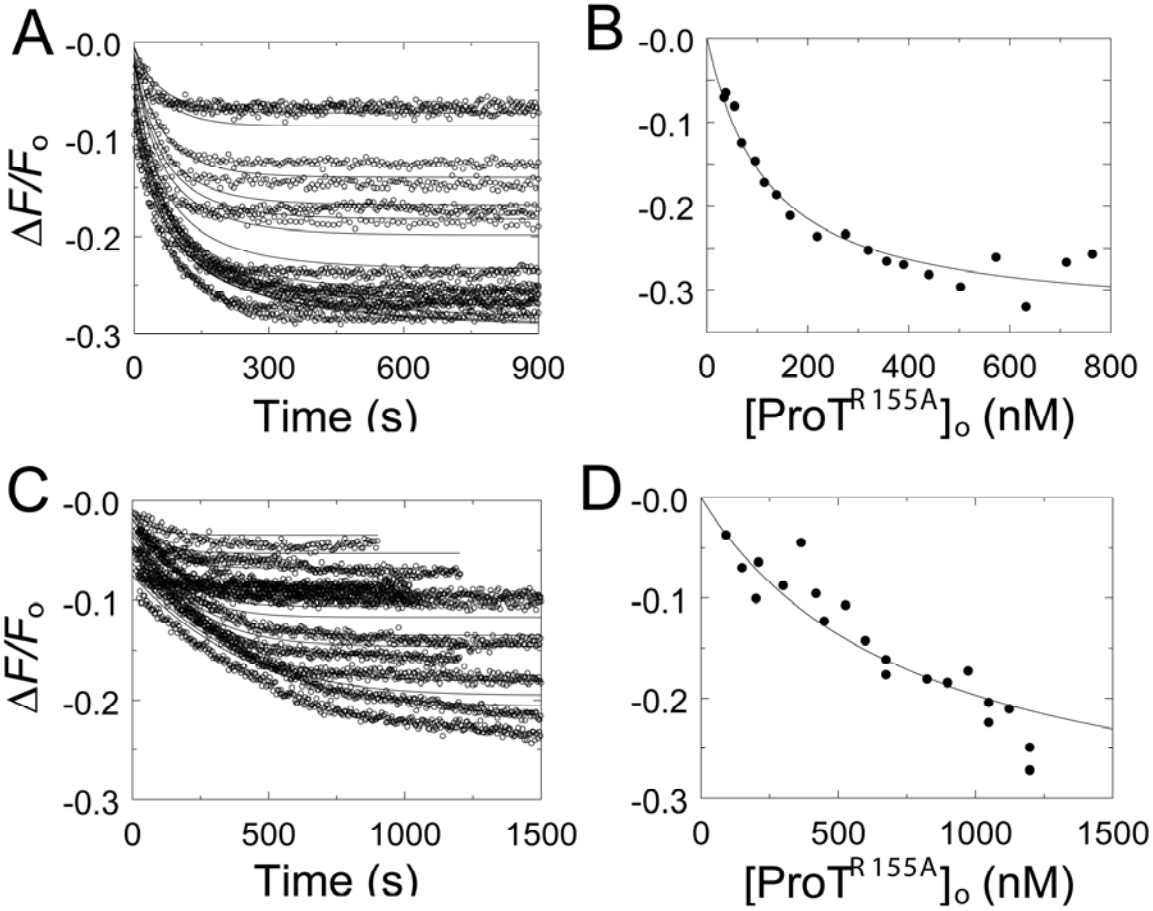

Figure 7. Kinetic and endpoint titrations of [5F]Hir-(54-65)(SO_3^-) binding to MzT^{R155A} in the absence and presence of Na^+. A. Kinetic titration of fluorescence changes ($\Delta F/F_o$) of 20 nM [5F]Hir-(54-65)(SO_3^-) during activation of $ProT^{R155A}$ at concentrations ranging from 28 to 760 nM, initiated by 2 units/ml ecarin in buffer containing NaCl (○). Thirteen reactions out of a total of 19 analyzed are shown. The *lines* represent the simultaneous fit of the fluorescence data with the parameters listed in Table I. B. Analysis of the reaction endpoints as a function of the total $ProT^{R155A}$ concentration ($[ProT^{R155A}]_o$). The *line* represents the fit by the quadratic binding equation with the parameters listed in Table I. C. Kinetic titrations for activation of 91-1198 nM $ProT^{R155A}$ in buffer containing ChCl (○) otherwise as described in A, along with the fit with the parameters listed in Table I. Twelve reactions out of a total of 21 analyzed are shown. D. Endpoint titration for the reactions in buffer containing ChCl as described in B except that the *line* represents the fit of the binding equation with $\Delta F_{max}/F_o$ fixed at -35%. Reactions were performed and analyzed as described in "Experimental Procedures".

distinguishing features. Unlike the results for MzT(-F1), the fit of the kinetics of MzT^{R155A} formation was improved modestly by including competitive product inhibition of ecarin. The fitted K_D for [5F]Hir-(54-65)(SO_3^-) binding to MzT^{R155A} was 81 ± 3 nM in NaCl and was 10-fold higher (830 ± 40 nM) in ChCl. The kinetic parameters for $ProT^{R155A}$ activation by ecarin in NaCl were V_{max} 2.1 ± 0.2 nM/s, K_m 110 ± 30 nM, and K_i 100 ± 50 nM, and were indistinguishable for V_{max}, K_m, and K_i, determined in ChCl at 2.0 ± 0.3 nM/s, 80 ± 40 nM, and 210 ± 160 nM, respectively. Analysis of the reaction endpoints for [5F]Hir-(54-65)(SO_3^-) binding to MzT^{R155A} in NaCl gave a K_D of 100 ± 30 nM (Fig. 7B). The endpoint results in ChCl could not be fit independently due to continued slow decreases in fluorescence at high ProT concentrations and long reaction times. Assuming an endpoint equivalent to that determined kinetically, gave a K_D of 770 ± 120 nM (Fig. 7D). Together, the results demonstrated slightly larger effects of Na^+ on the affinity of [5F]Hir-(54-65)(SO_3^-) for MzT^{R155A} (8 to 10-fold) compared to MzT(-F1) (5 to 6-fold).

Na^+ Binding Affinity Estimated from the Kinetics of Chromogenic Substrate Hydrolysis

To compare the apparent affinity of Na^+ for thrombin, MzT(-F1), and MzT^{R155A}, the initial rate of 200 μM (saturating) *D*-Phe-Pip-Arg-*p*NA hydrolysis was determined as a function of Na^+ concentration. Na^+ produced hyperbolic increases in rate of 4.9-fold, 3.1-fold, and 3.3-fold, from which apparent K_D*'s* of 12 ± 4, 9 ± 2, and 14 ± 4 mM were obtained for the substrate bound forms of thrombin, MzT(-F1), and MzT^{R155A}, respectively. The apparent affinities were the same and in reasonable agreement with the published K_D of 10 mM for Na^+ binding to the chromogenic substrate-thrombin complex at 25 ^oC, but at higher pH and ionic strength (25).

The K_D's for Na^+ binding to the free forms of thrombin and MzT(-F1) were estimated from the dependence of k_{cat}/K_m on Na^+ concentration (45). Despite the analysis of five progress curves at each Na^+ concentration, the error in the dissociation

constants was large (Fig. 8A). This was due to the necessity of fitting three parameters (k_{cat}, K_m, and K_i) to the progress curves and three parameters to k_{cat}/K_m as a function of Na^+ concentration (k_{cat}/K_m in the absence and at saturating Na^+, and K_D). The K_D's for thrombin and MzT(-F1) were both 26 ± 20 mM, roughly consistent with the value of 22 mM, determined at higher ionic strength and pH (25, 45). By contrast, k_{cat}/K_m for MzT^{R155A} increased linearly up to 110 mM NaCl. This was accompanied by a ~12-fold decrease in K_m, whereas this parameter decreased only ~2-3-fold for thrombin and MzT(-F1) (Fig. 8B). Analysis of the dependence of K_m on Na^+ concentration according to the nonessential activation mechanism as described in Experimental Procedures, gave an estimate of ~185 mM for the dissociation constant for Na^+ binding to free MzT^{R155A} and a linkage factor (α) of ~0.085, corresponding to a ~12-fold increase in Na^+ affinity at saturating substrate concentration. The value of αK_{Na} of ~16 mM from this analysis was in agreement with 14 ± 4 mM determined directly at saturating substrate concentration. The dependence of k_{cat} on Na^+ concentration for all of the enzymes was consistent with the directly measured dissociation constants for the substrate-saturated forms described above. The results demonstrated distinctly different kinetic behavior and a much higher K_D for Na^+ binding to MzT^{R155A}, which contains the fragment 1 domain, compared to thrombin and MzT(-F1) which do not.

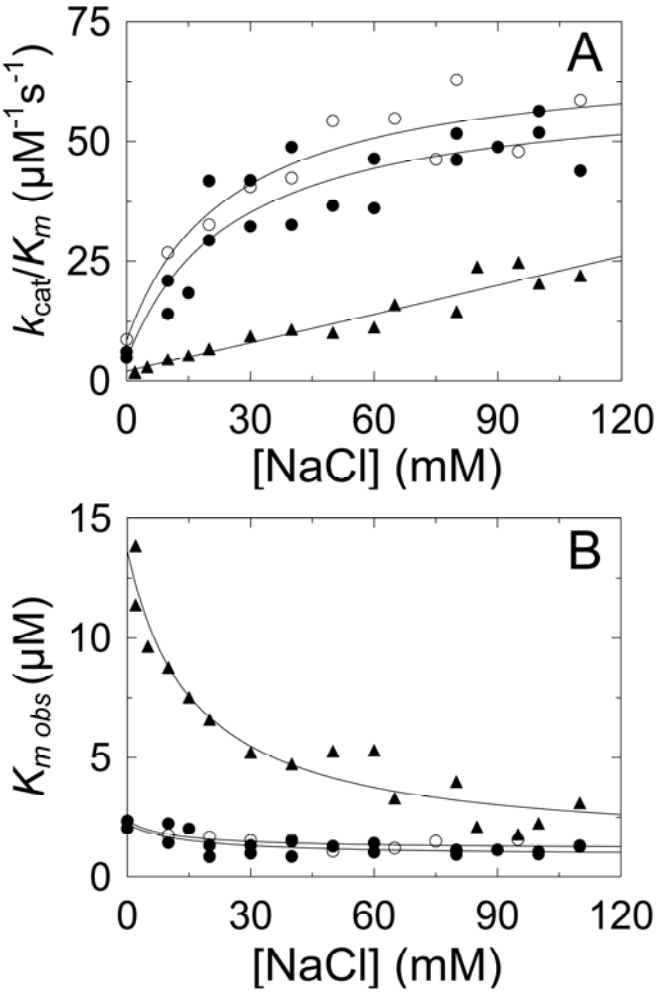

Figure 8. Effects of Na^+ on chromogenic substrate hydrolysis by thrombin, MzT(-F1), and MzT^{R155A}. A. Dependence of k_{cat}/K_m for *D*-Phe-Pip-Arg-*p*NA hydrolysis on Na^+ concentration for thrombin (●), MzT(-F1) (○), and MzT^{R155A} (▲). The *solid lines* for thrombin and MzT(-F1) represent the least squares fits of the data as described in Experimental Procedures, with indistinguishable K_D's for Na^+ binding of 26 ± 20 mM. The fit of a straight line is shown for MzT^{R155A}. B. Na^+ concentration dependence of the observed K_m ($K_{m\ obs}$) for hydrolysis of *D*-Phe-Pip-Arg-*p*NA by thrombin (●), MzT(-F1) (○), and MzT^{R155A} (▲). The *solid lines* represent the fits of Equation 1 with the parameters K_m, α, and K_{Na} of 2.2 μM, 0.39, and 34 mM for thrombin; 2.4 μM, 0.5, and 21 mM for MzT(-F1); and 14 μM, 0.085, and 185 mM for MzT^{R155A}. Experiments were performed and analyzed as described in "Experimental Procedures".

Table I
Summary of binding parameters

Dissociation constants are listed for binding of [5F]Hir-(54-65)(SO_3^-) to ProT and Pre 1 species in buffers containing 110 mM NaCl ($K_{H,\,Na}$), 110 mM ChCl ($K_{H,\,Ch}$), their ratio ($K_{H,\,Ch}/K_{H,\,Na}$), and the corresponding maximum fluorescence changes (($\Delta F_{max}/F_o)_{Na}$ and ($\Delta F_{max}/F_o)_{Ch}$). Results were obtained by direct, kinetic, and endpoint titrations as described under "Experimental Procedures".

Protein	Method	Dissociation Constant		$K_{H,\,Ch}/K_{H,\,Na}$	Fluorescence Change	
		$K_{H,\,Na}$ *(nM)*	$K_{H,\,Ch}$ *(nM)*		$(\Delta F_{max}/F_o)_{Na}$ *(%)*	$(\Delta F_{max}/F_o)_{Ch}$ *(%)*
ProT	Direct titration	4000±700	5400±900	1.4	-18±1	-19±1
$ProT^{R155A}$	Direct titration	1100±300	1900±300	1.7	-20±3	-20±2
Pre 1	Direct titration	510±70	830±140	1.6	-19±1	-20±1
Pre 2	Direct titration	640±90	850±120	1.3	-27±1	-26±1
Thrombin	Direct titration	48±4	270±20	5.6	-30±1	-32±1
FPR-thrombin	Direct titration	35±6	51±2	1.5	-31±1	-30±1
MzT(-F1)	Kinetic titration	41±1	210±5	5.1	-29±1	-29±1
MzT(-F1)	Endpoint titration	35±6	200±4	5.7	-28±1	-29±2
FPR-MzT(-F1)	Direct titration	26±5	34±3	1.3	-35±1	-34±1
FPR-MzT(-F1)	Kinetic titration	40±2			-32±1	
FPR-MzT(-F1)	Endpoint titration	40±20			-32±3	
MzT^{R155A}	Kinetic titration	80±3	830±40	10.4	-33±1	-35±2
MzT^{R155A}	Endpoint titration	100±30	770±120[a]	7.7	-34±5	-35[a]
FPR-MzT	Direct titration	35±4	41±5	1.2	-34±1	-34±1

[a] The K_D for peptide binding to MzT^{R155A} from the reaction endpoints in the absence of Na^+ was obtained by fixing $\Delta F_{max}/F_o$ at -35%

Discussion

Examination of the appearance of Na^+-exosite I linkage on ProT and its activation products supports the conclusion that proexosite I on ProT, Pre 1, and Pre 2 is not linked to Na^+ binding. Expression of linkage accompanies activation of the thrombin, MzT(-F1), and MzT catalytic sites by cleavage at Arg^{320}. Exosite I affinity and catalytic activity of MzT and MzT(-F1) are shown for the first time to be allosterically regulated by Na^+. The well-established coupling of protein substrate specificity to Na^+ binding for thrombin suggests that the distinctly different specificity of MzT will be regulated by the MzT slow form to fast form transition. Increasing MzT exosite I affinity and catalytic activity in the allosteric transition by Na^+ binding may also affect recognition of MzT as a substrate of the prothrombinase complex.

Linkage between Na^+ binding and exosite I affinity for [5F]Hir-(54-65)(SO_3^-) is expressed after cleavage at Arg^{320} of ProT and the ensuing conformational changes that activate the catalytic site and (pro)exosite I. The magnitudes of the effects of Na^+ on the enhancement of [5F]Hir-(54-65)(SO_3^-) affinity for exosite I on thrombin (5.6-fold) and MzT(-F1) (5.1-5.7-fold) were not significantly different, whereas MzT^{R155A} showed a slightly larger effect (7.7-10.4-fold). The 5.6-fold increase in affinity for thrombin is in reasonable agreement with previously reported values for acetyl-Hir-(55-65) (2-fold; (47)), Hir-(55-65) (2.3 and 6.4 fold; (24, 48)), and acetyl-Hir-(53-64) (5.4-fold; (32)), determined at different ionic strength, pH, and temperature.

The affinity of [5F]Hir-(54-65)(SO_3^-) for (pro)exosite I on the zymogen forms, ProT, $ProT^{R155A}$, Pre 1, and Pre 2 was consistently 1.3-1.7 fold higher in the presence of Na^+. This difference is well within the experimental error and may not be significant. As shown in the crystal structure of the Pre 2-hirugen complex, the Na^+ site is not properly formed on Pre 2 (49). On this basis, the results demonstrate that the absence of linkage between Na^+ and proexosite I is due to the inability of all zymogen forms to bind Na^+.

The conformational changes that complete the folding of the catalytic domain and formation of the catalytic site are necessary for expression of allosteric linkage.

In a recent structural analysis of human thrombin, crystal packing interactions were identified that have influenced interpretation of previous structures of the fast, slow, and inactive forms (31). The structure of the D102N thrombin mutant in the absence of Na^+ lacks crystal packing interactions, and is thought to represent more closely the inactive slow form in equilibrium with the active slow form and fast form. In the D102N thrombin structure, the catalytic site is blocked by large movements of Trp^{215} and Arg^{221a} to occlude the catalytic and primary specificity sites, while the guanidinium group of Arg^{187} occupies the Na^+ site (31). Rapid-reaction kinetic studies of Na^+ binding indicated that 23% of wild type thrombin is in the inactive slow form at 15 ºC, and that this form is not significantly populated at 37 ºC (31, 33). Presumably this form was also present at some level in the studies done here at 25 ºC, suggesting that binding of [5F]Hir-(54-65)(SO_3^-) to exosite I contains some contribution from inactive slow forms. Whether such inactive slow forms exist for MzT(±F1) is not known.

Inactivation of thrombin, MzT(-F1), and MzT with FPR-CH_2Cl virtually obliterated Na^+-exosite I linkage as probed by [5F]Hir-(54-65)(SO_3^-) binding affinity, and normalized all of the affinities to values indistinguishable from that of the fast form of thrombin. This is fully consistent with an analysis of the structures of the thrombin slow and fast forms, free and FPR-inactivated, which demonstrated that active site labeling locks thrombin in a fast form (26), and the essentially identical structures of FPR-thrombin and the Hir-(53-64)-thrombin complex (29). The Na^+ independence of the exosite I affinities is explained by binding of the transition state analog to the S1-$S4^2$ specificity sites, formation of a hemiketal with Ser^{195}, and subsequent alkylation of His^{57}. Although FPR-thrombin does bind Na^+ (26), the relaxation of Asp^{189} in the S1 site, Ser^{195}, and His^{57} to their conformations in the slow form in the absence of Na^+ cannot take place. It should be

noted that this finding does not compromise the conclusions of our previous studies of exosite I expression using FPR-inactivated thrombin and MzT(-F1) because, as shown here, these inactivated enzymes have affinities for the hirudin peptide essentially the same as the active fast forms. The affinities of MzT^{R155A} for the peptide, however, are 2-3-fold lower at 110 mM NaCl.

Kinetic analysis of Na^+ binding to MzT^{R155A} revealed a lower affinity compared to thrombin and MzT(-F1), which was associated with a larger decrease in K_m for the chromogenic substrate, and not significantly larger increases in k_{cat}. This unexpected behavior suggests that the presence of the fragment 1 domain attenuates affinity for Na^+ binding. The large effect of the presence of fragment 1 on the Na^+-dependent apparent substrate binding affinity may be due to steric or conformational differences affecting the active site or the Na^+ binding site, and indirectly exosite I. Further studies are needed to define the kinetic and molecular mechanism of MzT regulation by Na^+.

Although the mechanism of Na^+ regulation of MzT^{R155A} is not resolved, the results demonstrate for the first time that MzT(-F1) and MzT^{R155A} are Na^+-regulated proteinases exhibiting linkage to exosite I. Na^+ regulates the specificity of thrombin for procoagulant and anticoagulant substrates and effectors (15, 17-18, 23-24). The fast form has higher specificity (k_{cat}/K_m) than the slow form for the procoagulant substrates, fibrinogen and protease activated receptors, whereas relative to the fast form, the slow form is more specific for protein C activation (48). Compared to thrombin, MzT(±F1) has ≤10% activity toward fibrinogen and ≤2% activity in platelet activation despite having an active catalytic site and exosite I (19-20). Thrombin activates factor V in solution and factor V bound to phospholipid membranes in exosite I- and II-dependent reactions (22, 44, 50-52), whereas MzT activates factor V at a significant rate only when the substrate and enzyme are membrane-bound (21-22). It has been suggested that MzT may play an important procoagulant role as a specific physiological activator of membrane-bound

factor V during initiation of blood coagulation (21-22). Based on the present results, and the observation that factor V activation is catalyzed more efficiently by the thrombin fast form (52), MzT-catalyzed factor V activation is predicted to be regulated by Na^+. The dissociation constant for Na^+ binding to thrombin under physiological conditions is 110 mM, indicating an equilibrium of 60% fast and 40% slow forms (25, 53-54). The K_D for Na^+ binding to MzT^{R155A} at 37 ºC was not determined for the reasons cited above, but depending on the temperature dependence of Na^+ binding, MzT may be similarly poised for Na^+ regulation physiologically.

In the thrombin-thrombomodulin complex, the slow form of thrombin becomes a potent anticoagulant proteinase due in part to the loss of specificity for fibrinogen and other procoagulant substrates, whereas the capacity for protein C activation is greatly increased (15-18, 48, 55). Activation of protein C by MzT and MzT(-F1) is also stimulated by thrombomodulin to rates comparable to thrombin, and even faster rates when MzT is bound to phospholipid membranes (19-20). This has been suggested to represent an important physiological role for MzT as an anticoagulant (19-20). The present studies suggest that, like thrombin, Na^+-bound and free forms of MzT may exhibit higher procoagulant and anticoagulant activities, respectively.

ProT activation is dependent on expression of exosites on factor Xa in the factor Xa-Va-membrane complex that mediate a substrate recognition mechanism consisting of initial exosite binding and a subsequent conformational change engaging the catalytic site in peptide bond cleavage (7-14). Other studies support the hypothesis that (pro)exosite I on ProT also contributes to substrate recognition by mediating productive ProT binding and/or affecting the subsequent conformational change through interactions with the ProT binding site on factor Va in the prothrombinase complex (56-59). ProT activation catalyzed by prothrombinase proceeds sequentially, with initial cleavage at Arg^{320} to form MzT, followed by cleavage at Arg^{271} to generate thrombin and

fragment 1.2 (2-7). Recent studies of the activation pathway support a mechanism in which substrates in the zymogen and proteinase states bind in alternate conformations that direct sequential cleavage at the two activation sites (8). The ProT zymogen is positioned for optimal cleavage at Arg^{320}, whereas the product, MzT in the proteinase conformation ratchets to a different bound conformation for cleavage at Arg^{271}. On the basis of the evidence for the role of (pro)exosite I in substrate recognition through factor Va (56-59), and the differential expression of the exosite on ProT zymogen and proteinase forms (35-36), expression of exosite I on MzT may contribute to ratcheting of the bound substrate for presentation of Arg^{271} for cleavage. The present studies show that the chromogenic substrate activity and affinity of MzT exosite I are enhanced by Na^+, suggesting that coupling of Na^+ binding and exosite I expression upon cleavage at Arg^{320} may contribute to recognition of this substrate. Previous studies of the role of Na^+ on the rate of Pre 1 activation in the absence of membranes by the Na^+-insensitive factor Xa mutant, Y225P, also lacking the γ-carboxyglutamic acid domain, showed a 10-fold enhancement by Na^+, which was correlated with a modest increase in affinity for factor Va (60). On the other hand, with wild-type factor Xa assembled into prothrombinase the Na^+ enhancement was only <1.5-fold (60). Whether Na^+ affects the rate of MzT cleavage by prothrombinase remains an open question.

Acknowledgements

We thank Sarah Stuart for excellent technical assistance, and Dr. Ingrid Verhamme for comments on the manuscript.

Footnotes

*Supported by NIH Heart, Lung, and Blood Institute grant HL038779 to P. E. B., and the Edmond Hustinx Foundation, Cardiovascular Research Institute Maastricht, Department of Biochemistry, University Maastricht. This work was also supported by VIDI grant no. 916-046-330 from the Dutch Organization for Scientific Research to G. A. F. N. H. K. K. was supported by NIH Training Grant HL 07751.

[1.] Abbreviations used are: ProT, prothrombin; Pre 1, prethrombin 1; Pre 2, prethrombin 2; F1, fragment 1; MzT, meizothrombin; MzT(-F1), meizothrombin-des-fragment 1; T, thrombin; FPR-CH_2Cl, *D*-Phe-Pro-Arg-CH_2Cl; Hir-(54-65)(SO_3^-), Gly-Asp-Phe-Glu-Glu-Ile-Pro-Glu-Glu-Tyr(SO_3^-)-Leu-Gln; [5F]Hir-(54-65)(SO_3^-), Hir-(54-65)(SO_3^-) labeled at the amino terminus with 5-carboxy(fluorescein); hirugen, hirudin-(53-64); PEG, polyethylene glycol; *p*NA, *p*-nitroaniline.

[2.] Schechter-Berger (61) notation referring to the residues of a substrate (from the NH_2-terminal end) as …P4-P3-P2-P1-P1'-P2'… with the scissile bond at P1-P1'.

References

1. Mann KG, Nesheim ME, Church WR, Haley P, & Krishnaswamy S (1990) Surface-dependent reactions of the vitamin K-dependent enzyme complexes. *Blood* 76(1):1-16.

2. Rosing J, Zwaal RF, & Tans G (1986) Formation of meizothrombin as intermediate in factor Xa-catalyzed prothrombin activation. *J. Biol. Chem.* 261(9):4224-4228.

3. Krishnaswamy S, Mann KG, & Nesheim ME (1986) The prothrombinase-catalyzed activation of prothrombin proceeds through the intermediate meizothrombin in an ordered, sequential reaction. *J. Biol. Chem.* 261(19):8977-8984.

4. Krishnaswamy S, Church WR, Nesheim ME, & Mann KG (1987) Activation of human prothrombin by human prothrombinase. Influence of factor Va on the reaction mechanism. *J. Biol. Chem.* 262(7):3291-3299.

5. Tans G, Janssen-Claessen T, Hemker HC, Zwaal RF, & Rosing J (1991) Meizothrombin formation during factor Xa-catalyzed prothrombin activation. Formation in a purified system and in plasma. *J. Biol. Chem* 266(32):21864-21873.

6. Rosing J & Tans G (1988) Meizothrombin, a major product of factor Xa-catalyzed prothrombin activation. *Thromb. Haemost.* 60(3):355-360.

7. Krishnaswamy S (2005) Exosite-driven substrate specificity and function in coagulation. *J. Thromb. Haemost.* 3(1):54-67.

8. Bianchini EP, Orcutt SJ, Panizzi P, Bock PE, & Krishnaswamy S (2005) Ratcheting of the substrate from the zymogen to proteinase conformations directs the sequential cleavage of prothrombin by prothrombinase. *Proc. Natl. Acad. Sci. U. S. A* 102(29):10099-10104.

9. Krishnaswamy S & Betz A (1997) Exosites determine macromolecular substrate recognition by prothrombinase. *Biochemistry* 36(40):12080-12086.

10. Boskovic DS & Krishnaswamy S (2000) Exosite binding tethers the macromolecular substrate to the prothrombinase complex and directs cleavage at two spatially distinct sites. *J. Biol. Chem.* 275(49):38561-38570.

11. Betz A & Krishnaswamy S (1998) Regions remote from the site of cleavage determine macromolecular substrate recognition by the prothrombinase complex. *J. Biol. Chem.* 273(17):10709-10718.

12. Wilkens M & Krishnaswamy S (2002) The contribution of factor Xa to exosite-dependent substrate recognition by prothrombinase. *J. Biol. Chem.* 277(11):9366-9374.

13. Orcutt SJ, Pietropaolo C, & Krishnaswamy S (2002) Extended interactions with prothrombinase enforce affinity and specificity for its macromolecular substrate. *J. Biol. Chem.* 277(48):46191-46196.

14. Orcutt SJ & Krishnaswamy S (2004) Binding of substrate in two conformations to human prothrombinase drives consecutive cleavage at two sites in prothrombin. *J. Biol. Chem.* 279(52):54927-54936.

15. Page MJ, Macgillivray RT, & Di Cera E (2005) Determinants of specificity in coagulation proteases. *J. Thromb. Haemost.* 3(11):2401-2408.

16. Huntington JA (2005) Molecular recognition mechanisms of thrombin. *J. Thromb. Haemost.* 3(8):1861-1872.

17. Bode W (2005) The structure of thrombin, a chameleon-like proteinase. *J. Thromb. Haemost.* 3(11):2379-2388.

18. Bode W (2006) Structure and interaction modes of thrombin. *Blood. Cells Mol. Dis.* 36(2):122-130.

19. Doyle MF & Mann KG (1990) Multiple active forms of thrombin. IV. Relative activities of meizothrombins. *J. Biol. Chem.* 265(18):10693-10701.

20. Cote HC*, et al.* (1994) Characterization of a stable form of human meizothrombin derived from recombinant prothrombin (R155A, R271A, and R284A). *J. Biol. Chem.* 269(15):11374-11380.

21. Tans G*, et al.* (1994) Activation of Human Factor V by Meizothrombin. *J. Biol. Chem.* 269(23):15969-15972.

22. Bukys MA*, et al.* (2006) The structural integrity of anion binding exosite I of thrombin is required and sufficient for timely cleavage and activation of factor V and factor VIII. *J. Biol. Chem.* 281(27):18569-18580.

23. Di Cera E (2004) Thrombin: a paradigm for enzymes allosterically activated by monovalent cations. *C. R. Biol.* 327(12):1065-1076.

24. Di Cera E, Dang QD, & Ayala YM (1997) Molecular mechanisms of thrombin function. *Cell. Mol. Life Sci.* 53(9):701-730.

25. Wells CM & Di Cera E (1992) Thrombin is a Na(+)-activated enzyme. *Biochemistry* 31(47):11721-11730.

26. Pineda AO*, et al.* (2004) Molecular dissection of Na+ binding to thrombin. *J. Biol. Chem.* 279(30):31842-31853.

27. Pineda AO, Savvides SN, Waksman G, & Di Cera E (2002) Crystal structure of the anticoagulant slow form of thrombin. *J. Biol. Chem.* 277(43):40177-40180.

28. Prasad S*, et al.* (2004) Residue Asp-189 controls both substrate binding and the monovalent cation specificity of thrombin. *J. Biol. Chem.* 279(11):10103-10108.

29. Vijayalakshmi J, Padmanabhan KP, Mann KG, & Tulinsky A (1994) The isomorphous structures of prethrombin2, hirugen-, and PPACK-thrombin: changes accompanying activation and exosite binding to thrombin. *Protein Sci.* 3(12):2254-2271.

30. Carrell CJ, Bush LA, Mathews FS, & Di Cera E (2006) High resolution crystal structures of free thrombin in the presence of K(+) reveal the molecular basis of monovalent cation selectivity and an inactive slow form. *Biophys. Chem.* 121(3):177-184.

31. Pineda AO*, et al.* (2006) Crystal Structure of Thrombin in a Self-inhibited Conformation. *J. Biol. Chem.* 281(43):32922-32928.

32. Lai MT, Di Cera E, & Shafer JA (1997) Kinetic pathway for the slow to fast transition of thrombin. Evidence of linked ligand binding at structurally distinct domains. *J. Biol. Chem.* 272(48):30275-30282.

33. Bah A, Garvey LC, Ge J, & Di Cera E (2006) Rapid kinetics of Na(+) binding to thrombin. *J. Biol. Chem.* 281(52):40049-40056.

34. Anderson PJ, Nesset A, Dharmawardana KR, & Bock PE (2000) Characterization of proexosite I on prothrombin. *J. Biol. Chem.* 275(22):16428-16434.

35. Anderson PJ & Bock PE (2003) Role of prothrombin fragment 1 in the pathway of regulatory exosite I formation during conversion of human prothrombin to thrombin. *J. Biol. Chem.* 278(45):44489-44495.

36. Anderson PJ, Nesset A, & Bock PE (2003) Effects of activation peptide bond cleavage and fragment 2 interactions on the pathway of exosite I expression during activation of human prethrombin 1 to thrombin. *J. Biol. Chem.* 278(45):44482-44488.

37. Bock PE, Olson ST, & Björk I (1997) Inactivation of thrombin by antithrombin is accompanied by inactivation of regulatory exosite I. *J. Biol. Chem.* 272(32):19837-19845.

38. Bock PE (1992) Active-site-selective labeling of blood coagulation proteinases with fluorescence probes by the use of thioester peptide chloromethyl ketones. I. Specificity of thrombin labeling. *J. Biol. Chem.* 267(21):14963-14973.

39. Bock PE, Craig, P. A., Olson, S. T., and Singh, P. (1989) Isolation of Human Blood Coagulation a-factor Xa by Soybean Trypsin Inhibitor-sepharose Chromatography and its Active-site Titration with Fluorescein Mono-p-guanidinobenzoate. *Arch. Biochem. Biophys.* 273:375-388.

40. Bock PE (1992) Active-site-selective labeling of blood coagulation proteinases with fluorescence probes by the use of thioester peptide chloromethyl ketones. II. Properties of thrombin derivatives as reporters of prothrombin fragment 2 binding and specificity of the labeling approach for other proteinases. *J. Biol. Chem.* 267(21):14974-14981.

41. Fenton JW, 2nd, Fasco MJ, & Stackrow AB (1977) Human thrombins. Production, evaluation, and properties of alpha-thrombin. *J. Biol. Chem.* 252(11):3587-3598.

42. Mann KG, Elion J, Butkowski RJ, Downing M, & Nesheim ME (1981) Prothrombin. *Methods Enzymol.* 80 Pt C:286-302.

43. Petrovan RJ*, et al.* (1998) Autocatalytic peptide bond cleavages in prothrombin and meizothrombin. *Biochemistry* 37(5):1185-1191.

44. Dharmawardana KR, Olson ST, & Bock PE (1999) Role of regulatory exosite I in binding of thrombin to human factor V, factor Va, factor Va subunits, and activation fragments. *J. Biol. Chem.* 274(26):18635-18643.

45. Di Cera E, Hopfner KP, & Dang QD (1996) Theory of allosteric effects in serine proteases. *Biophys. J.* 70(1):174-181.

46. Segel IH (1993) *Enzyme Kinetics: Behavior and Analysis of Rapid Equilibrium and Steady-State Enzyme Systems, pp. 227-228* (John Wiley & Sons, Inc., New York).

47. Ayala YM*, et al.* (1995) Thermodynamic investigation of hirudin binding to the slow and fast forms of thrombin: evidence for folding transitions in the inhibitor and protease coupled to binding. *J. Mol. Biol.* 253(5):787-798.

48. Dang OD, Vindigni A, & Di Cera E (1995) An allosteric switch controls the procoagulant and anticoagulant activities of thrombin. *Proc. Natl. Acad. Sci. U. S. A.* 92(13):5977-5981.

49. Zhang E & Tulinsky A (1997) The molecular environment of the Na+ binding site of thrombin. *Biophys. Chem.* 63(2-3):185-200.

50. Dharmawardana KR & Bock PE (1998) Demonstration of exosite I-dependent interactions of thrombin with human factor V and factor Va involving the factor Va heavy chain: analysis by affinity chromatography employing a novel method for active-site-selective immobilization of serine proteinases. *Biochemistry* 37(38):13143-13152.

51. Esmon CT & Lollar P (1996) Involvement of thrombin anion-binding exosites 1 and 2 in the activation of factor V and factor VIII. *J. Biol. Chem.* 271(23):13882-13887.

52. Myles T, Yun TH, Hall SW, & Leung LL (2001) An extensive interaction interface between thrombin and factor V is required for factor V activation. *J. Biol. Chem.* 276(27):25143-25149.

53. Guinto ER & Di Cera E (1996) Large heat capacity change in a protein-monovalent cation interaction. *Biochemistry* 35(27):8800-8804.

54. Griffon N & Di Stasio E (2001) Thermodynamics of Na+ binding to coagulation serine proteases. *Biophys. Chem.* 90(1):89-96.

55. Esmon CT, Esmon NL, & Harris KW (1982) Complex formation between thrombin and thrombomodulin inhibits both thrombin-catalyzed fibrin formation and factor V activation. *J. Biol. Chem.* 257(14):7944-7947.

56. Anderson PJ, Nesset A, Dharmawardana KR, & Bock PE (2000) Role of proexosite I in factor Va-dependent substrate interactions of prothrombin activation. *J. Biol. Chem.* 275(22):16435-16442.

57. Beck DO, Bukys MA, Singh LS, Szabo KA, & Kalafatis M (2004) The contribution of amino Acid region asp695-tyr698 of factor v to procofactor activation and factor va function. *J. Biol. Chem.* 279(4):3084-3095.

58. Arocas V*, et al.* (1998) Inhibition of thrombin-catalyzed factor V activation by bothrojaracin. *Thromb. Haemost.* 79(6):1157-1161.

59. Chen L, Yang L, & Rezaie AR (2003) Proexosite-1 on prothrombin is a factor Va-dependent recognition site for the prothrombinase complex. *J. Biol. Chem.* 278(30):27564-27569.

60. Rezaie AR & He X (2000) Sodium binding site of factor Xa: role of sodium in the prothrombinase complex. *Biochemistry* 39(7):1817-1825.

61. Schechter I & Berger A (1967) On the size of the active site in proteases. I. Papain. *Biochem. Biophys. Res. Commun.* 27(2):157-162.

CHAPTER V

SIGNIFICANCE AND FUTURE PATHWAYS

Summary of research

The preceding studies described the molecular mechanisms involved in the activation of ProT by the staphylococcal exoprotein VWbp, as well as some of the allosteric processes that are important for ligand recognition and regulation of substrate hydrolysis by the active ProT·VWbp complex. First and foremost, VWbp can now be classified as one of the few proteins identified which function as non-proteolytic zymogen activators. The unique process of conformational induction of the active site of the proenzyme is dependent upon both sequence mimicry in the NH_2-terminus of the activator and high-affinity interactions with crucial regions of the zymogen activation domain. In addition, hysteretic, substrate-dependent regulation of this activity provides a second level of specificity for recognition of the physiological thrombin substrate, fibrinogen, by the ProT·VWbp complex. Potential steric and allosteric opposition provided by the small fragment domains of ProT further controls the activity of VWbp, but this effect may be mitigated *in vivo* by secondary autocatalysis which results in progressive loss of the fragment domains. Proteolytic activation of the zymogen, and to an even greater extent, occupation of the active site by a highly-specific substrate, also enhances the affinity of VWbp for ProT and its derivatives. The role of anion-binding (pro)exosite I and its activation state in the interaction of ProT and VWbp is very similar to that seen during the physiological pathway of ProT activation, where formation of a competent active site (such as in MzT) is linked to a high-affinity exosite expression, as well as other allosteric sites like the sodium binding site. Taken together, these findings reveal a pattern of ligand and substrate recognition with VWbp that shows a strong

mechanistic resemblance to the normal pattern of thrombin activity, but the overall specificity of which is substantially constrained by structural alterations due to the presence of the activator itself.

Significance of the Mechanism of Activation of ProT by VWbp

VWbp is only the third protein so far that has been demonstrated mechanistically to be a conformational activator of a zymogen. The model of non-proteolytic activation through exploitation of the linkage between the canonical NH_2-terminal binding cleft and the actual activation domain has been examined using tight-binding substrates and NH_2-terminal peptide mimetics (1), but it was not until recently (with SC) that any clear structural proof of this concept was established (2). The ability of SC and streptokinase (SK) to bind their cognate zymogens and induce functional active sites, despite the vast differences in secondary and tertiary structure between the two activators, underscores the essential role of their NH_2-terminal residues in the mechanism of activation. Corresponding mutational analysis of VWbp revealed strict dependence of its activity upon the initial Val-Val residues, comparable to that found with both SC and SK (2, 3), which firmly places VWbp into the class of bacterial non-proteolytic zymogen activators. In addition to their reliance upon the NH_2-terminal insertion mechanism, these three bacterial proteins also produce other subtle functional differences in the complexes they form, compared to the analogous proteinases. Even though they all induce an active site within the zymogen, the enzymatic specificity of the active site is not necessarily equivalent with respect to all of the potential substrates. Either plasminogen or plasmin in complex with SK demonstrates the ability to convert other molecules of plasminogen to plasmin (4), whereas free plasmin lacks this capacity. SC in complex with ProT retains high specificity for several thrombin substrates, including fibrinogen, but it also imparts resistance to macromolecular thrombin inhibitors and protein substrates which

normally interact with the active site (5). Nearly identical limitation of substrates and resistance to inhibition is seen with VWbp, particularly in the inability of ProT·VWbp to activate a number of other thrombin-cleavable coagulation factors. The pattern of changes in substrate and inhibitor specificity indicates that the conformational changes involved in folding of the zymogen activation domains do not exactly mirror those that follow proteolytic activation. These differences may stem from direct interactions of the bacterial activators with the activation domain, as well as global conformational shifts in the zymogen, and the restricted specificity likely represents the foundation for the true function of the activator proteins in manipulating the host coagulation and fibrinolytic systems. Although conformational, NH_2-terminus-dependent activation of zymogens has only been experimentally demonstrated for these few exoproteins, identification of several SC-homologous activators (the ZAAPs) from staphylococci and streptococci suggests that other exoproteins may also be able to directly interact with blood coagulation zymogens (6). As such, non-proteolytic activation of host enzymes could be a valid mechanistic approach for bacteria during infection.

In addition to the distinctive conformational mechanism of activation of ProT, VWbp also demonstrates strict regulation of its activity by way of additional cofactor requirements for complete zymogen activation. While SC alone is able to bind ProT with very high affinity and induce a fully functional active site, VWbp recognizes the zymogen with a comparatively low affinity, resulting in incomplete activation of ProT in equimolar mixtures with VWbp. The behavior of VWbp in complex with ProT is consistent with a kinetically slow, hysteretic step in the ultimate conversion of zymogen ProT to the conformationally activated form. The proposed hysteretic kinetic model for VWbp-mediated activation of ProT includes a crucial slow and unfavorable equilibrium between inactive and active forms of the ProT·VWbp complex, produced by a suboptimal interaction between the two proteins which likely results in partial NH_2-terminal insertion

or folding of the activation domain. Association of a tight-binding substrate with the induced active site stabilizes the fully-active complex, increasing the rate of substrate hydrolysis through a positive change in the conformational equilibrium. Based on what is known about cooperative linkage between NH_2-terminal insertion and the active site, this outcome in the presence of a substrate would not be unexpected, but the rate at which it occurs indicates the true uniqueness of the hysteretic kinetic mechanism of VWbp. By definition, hysteresis in enzyme kinetics occurs when a system has a slow response to a sudden stimulus that changes the biochemical conditions, which includes processes such as slow isomerization of an enzyme or displacement of one ligand by another (7). Only upon addition of substrate does the inactive-active equilibrium of the ProT·VWbp complex shift towards the active form, with a slow observable rate. As a result, the kinetic process actually requires two cofactors for ProT activation, both VWbp and a substrate, an unusual characteristic in the relatively small field of hysteretic enzymes and the first example of hysteresis in serine proteinase zymogen activation.

Allostery and Thrombin Specificity

Despite the fact that other thrombin ligands can induce small conformational changes in the enzyme to affect its activity, the activity of VWbp with ProT could be characterized as the definitive allosteric interaction. There are many examples of ligands that can allosterically change the activity of thrombin, such as binding of thrombomodulin, which allows thrombin to recognize and cleave protein C, and hirudin-mediated alteration of the active site to generally inhibit thrombin activity (8, 9). One or both of exosites I and II are typically involved in binding of the various thrombin ligands, and any allosteric effects are, in general, targeted toward specific alterations in substrate recognition. We have shown that formation of the proteinase active site and exosite I is allosterically linked to binding of a sodium ion, a process known to influence the pro- and

anti-coagulant substrate specificity of different sodium-bound forms of thrombin (10). Identical regulation by sodium has been recently identified for MzT(-F1) (11), and ProT in complex with SC also demonstrates sodium-dependent effects on activity (12). VWbp likely exhibits analogous behavior with ProT in the presence of sodium, an indication of how effectively these activators can exploit the normal regulatory mechanisms of thrombin.

Although VWbp also modifies the substrate profile of the ProT complex, seemingly restricting it to fibrinogen and small tripeptide substrates, VWbp most significantly differs in the magnitude of change it induces in the zymogen. Complete conformational activation of ProT by VWbp relies on manipulation of multiple interactions between the NH_2-terminus of the activator and critical residues involved in folding of the activation domain, as well as direct exosite and active site contact. Not only does VWbp bind directly to (pro)exosite I, it also interacts with the NH_2-terminal binding cleft (and potentially the nearby autolysis loop); the COOH-terminal half of VWbp may also specifically interact with the ProT fragment domains or activation domain. Through these interactions with VWbp, the catalytic site and substrate-specificity cleft can be completely converted to a thrombin-like configuration, an effect that can be triggered by only one other known ligand—SC. The proteinase substrate also acts as a cofactor in this process through stabilization of the active site, connecting with the activating conformational changes initiated by VWbp to produce a potent procoagulant complex. The cooperativity between VWbp and substrate in inducing an enzymatically active complex actually mirrors other rare examples of cofactor-induced enzyme activation. Analogous conversion from a partially activated to fully competent enzyme form occurs in the factor VIIa-tissue factor complex, where initial proteolytic “activation” of factor VIIa results in a protein with very low enzymatic activity. It is only upon binding of its cofactor, tissue factor, that the active site of factor VIIa properly folds, allowing the serine

proteinase to recognize and hydrolyze its target substrates, factors IX and X (13). Similarly, substrate cofactors are required during activation of complement protease factor D, where only binding of a specific substrate relieves steric distortion within the active site of the enzyme (14). The behavior of VWbp in complex with ProT resembles both of these cofactor-dependent mechanisms, with VWbp itself serving as a cofactor in induction of an "inactive" ProT form that is converted to a fully functional complex upon binding of a substrate to the active site. Due to the clear role of cofactors in temporally and spatially regulating the activity of factor VIIa and complement factor D, it is reasonable to speculate that the cofactor requirements for formation of active ProT*·VWbp would also be a primary influence on complex activity. This is in clear contrast to the more straightforward mechanisms of activation demonstrated by SC and SK, where direct and rapid interaction of the activator alone with the zymogen results in an active species. The complexity exhibited by VWbp in activation of ProT, in particular the substrate-dependent hysteretic changes in complex conformation, sets VWbp apart mechanistically, even within the very small class of non-proteolytic zymogen activators. Whether VWbp or SC has the dominant mechanistic characteristics of other ZAAPs is not established, although preliminary studies of SfbX suggest a hysteretic mechanism (Jonathan Creamer, Ph.D., personal communication).

The Role of von Willebrand Factor in Hemostasis

Specific association with one or more adhesion or extracellular matrix proteins is one of the most significant characteristics of many exoproteins in both the MSCRAMM and SERAM families, but only a relatively small number of bacterial products have been shown to have a pathological function for these interactions. Studies on cell-surface localized proteins such as ClfA and FnBP showed moderate success in linking protein expression to bacterial colonization in *in vivo* models of infection (15, 16), but secreted

factors may have more indirect or synergistic effects that make correlation with a specific disease difficult. Neither VWbp nor SC has had a significant role assigned to their COOH-terminal adhesion protein binding motifs, apart from basic specificity for VWF (VWbp) or fibrinogen (SC). The promiscuity of interactions displayed by proteins such as fibrinogen creates an intricate meshwork of potential protein or cellular targets for bacterial factors. Hence, the capacity of bacterial exoproteins for binding adhesive molecules remains an important area of investigation in both biochemical systems and animal models of human diseases.

The contribution of VWF to the progression of infectious vascular disease has not been examined as frequently as more ubiquitous adhesion proteins like fibrinogen and fibronectin, despite its unique roles in mediating platelet function and thrombus formation. VWF is a large (~250 kDa) glycoprotein which forms disulfide-bonded multimers up to 20,000 kDa in size, and it is either secreted by endothelial cells, from which the plasma population of VWF originates, or stored in intracellular cytoplasmic granules (Weibel-Palade bodies) for later induced secretion (17). Release of VWF from endothelial cells can be triggered by several agonists common to coagulation and inflammatory responses, including thrombin and fibrin (18), resulting in increased local concentrations of the adhesion protein. The first major function of VWF is to tether free platelets to the subendothelium following an injury, a process that depends upon binding of two of the type A structural domains of VWF (A1 and A3; Figure 1) to several different forms of collagen found in exposed extracellular matrices (19). Conformational changes within VWF are induced by this interaction and the shear force of blood flow, exposing regions of the protein that can interact with two different targets on the platelet surface: the GPIbα-IX-V receptor complex and the integrin $\alpha_{IIb}\beta_3$ (20). These actions are most significant in high shear rate environments, such as small arteries and capillaries, where other adhesion proteins cannot bind platelets with sufficient force to arrest the movement

of the cells. Initial adhesion occurs through the GPIbα component of the platelet receptor, which allows the platelets to roll across the surface of the exposed matrix. Once the momentum is reduced, secondary interactions between $\alpha_{IIb}\beta_3$ and a specific Arg-Gly-Asp (RGD) sequence in VWF activates the platelets and enhances affinity and subsequent aggregation of platelets at the site of injury. The second role for VWF in thrombus formation is to serve as a carrier protein for blood clotting factor VIII, a cofactor in factor X activation by factor IXa. Association of factor VIII with the residues near the A3 domain of VWF serves to stabilize the coagulation factor by increasing its half-life in circulation and protecting it from inactivating proteolysis by activated protein C (21). As a result of these vital roles, quantitative deficiencies or defects in VWF multimerization can have wide-spread consequences for hemostasis, ranging from relatively minor bleeding phenotypes to the severe symptoms of hemophilia A (17).

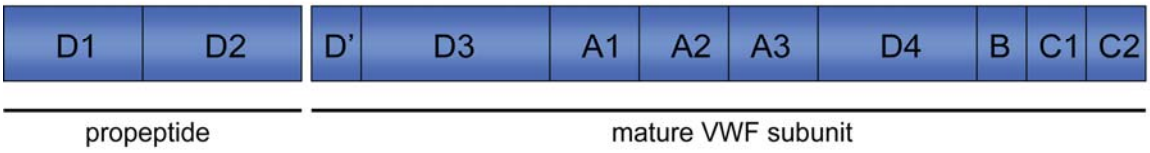

Figure 1. Domain organization of VWF propeptide and mature protein. Adapted from (19).

Recognition of von Willebrand Factor by Pathogens

In view of the multiple functions of VWF in the vasculature, what would be the potential benefit for a bacterial pathogen to secrete an exoprotein that recognizes VWF? Secretion of proteins from the Weibel-Palade bodies of aortic endothelial cells has been shown to be upregulated by components of bacterial cell walls, including lipoteichoic acid from gram-positive organisms (22). Release of several vascular mediators, including VWF, is triggered by recognition of the pathogen by the Toll-like receptor 2,

which has a role in the innate immune response. Subsequent vascular inflammation could then set the stage for a number of pathologic responses, from both the endogenous host systems and the bacteria themselves. Studies have also been performed with several species of bacteria to examine any direct involvement of VWF in altering pathological coagulation or hemostasis. Platelet aggregation by one clinical strain of *Streptococcus sanguis*, an oral bacterium that is often linked with infective endocarditis, was initially linked to a VWF-independent interaction with GPIbα (23). Later reports contest this conclusion by demonstrating that plasma from patients with von Willebrand's disease could not support platelet activation by certain other strains of *S. sanguis*, suggesting a role for VWF in platelet activity, perhaps through noncanonical interactions with other platelet receptors (24). *Staphylococcus aureus* directly interacts with VWF in solution, as well as VWF adsorbed to surfaces, providing this species with multiple adhesive targets in an intravascular environment (25). *S. aureus* expresses the surface-localized receptor protein A, or Spa, which directly binds VWF (26), and this protein has been shown to be a major determinant of bacterial adhesion to immobilized platelets at high shear rates (27, 28). In general, binding of VWF by bacteria could allow localization to newly-exposed subendothelium, as well as pre-existing platelet-rich thrombi. Regulation of expression of VWF-specific receptors, such as protein A, would influence the mechanisms of cellular adhesion at different bacterial growth cycles (29), consequently affecting the time- and flow-dependent pattern of dissemination. The multimeric and multi-domain structure of VWF also presents numerous binding sites for simultaneous interactions with cellular receptors and other extracellular matrix proteins, all of which could also control bacterial colonization.

VWbp: A Bifunctional Staphylococcal Exoprotein

As a secreted protein, VWbp could use its interaction with VWF to not only localize fibrin deposition to VWF-rich areas of the vasculature, but also directly alter the function of VWF. VWF contains a number of different domains that can be classified into several homologous types. The A1-A2-A3 domains are responsible for interactions with many of the VWF ligands, such as GPIbα, and the multimerization site for VWF is located immediately before the A1 domain. There are smaller groups of B and C domains, and larger D-type domains which govern factor VIII and collagen recognition (30). Exposure of varying binding sites in the domains, dependent on shear rate and secondary binding of other ligands, is known to induce different functions for VWF, and bacterial proteins could exploit similar mechanisms to manipulate the adhesive properties of VWF. Protein A contains four or five repeat domains, each individually forming a three-helical bundle structure which recognizes the A1 domain of VWF; contact between these two proteins could potentially block binding of GPIbα and collagen (VWF), as well as the Fc region of IgG (protein A), significantly changing the specificity of both proteins (31). The domain specificity of a cell-surface receptor from *Staphylococcus lugdenensis*, which also recognizes VWF, has not been fully defined, but no sequence homology with protein A has been uncovered (32). A specific binding site for VWbp on VWF has not been identified, and the disordered 26-residue region within the COOH-terminus of VWbp that is responsible for binding of VWF shares no sequence (or structural) homology with these other known bacterial VWF ligands. As such, the possible consequences of the VWbp-VWF interaction are presently unknown. The fact that VWbp can bind to VWF under static conditions (33) indicates that either binding occurs through a region of VWF that is accessible in its globular, unextended form, or that VWbp can change the conformation of VWF to expose cryptic binding sites. If binding of VWbp can reveal regions of VWF that are only normally exposed at high

shear flow or after binding of collagen, this would enhance the platelet-binding functions of VWF in low shear environments to produce abnormal platelet aggregation and activation. A combination of increased platelet-induced thrombus growth with escalating fibrin deposition from procoagulant zymogen-activator complexes would have the potential to quickly occlude smaller vessels or cause harmful embolisms.

The multiple functions of exoproteins like VWbp and SC may play synergistic roles in bacterial colonization and protection of *S. aureus* from the host immune response. Fibrin elicits the activation of endothelial cells, prompting direct engulfment of bacteria by host cells, and fibrin clots also serve as a physical barrier to pathogen-recognizing cells of the innate and adaptive systems (34). *S. aureus* can not only survive phagocytosis, but it can also use the host cells themselves as a line of defense against antibody and complement molecules. Any mechanisms that lead to increased fibrin deposition and recognition would be beneficial, but the overall effect of these processes on the life cycle of the bacteria would be determined by the specificity and localization of the different fibrin receptors. During a blood-borne *S. aureus* infection, the bacteria would produce at least two secreted factors that recognize fibrinogen, SC and VWbp, as well as several cell-surface proteins, the most significant of which is ClfA. Binding of free fibrinogen by surface receptors would cover the bacteria in a non-antigenic coating of host proteins, essentially making the pathogens invisible to the immune cells. In addition, existing transient deposits of fibrin in the vasculature would support initial localization of the bacteria through receptors such as ClfA.

In concert with the bacterial surface proteins, secreted factors like VWbp may contribute to more widespread dissemination of the bacteria during an infection. If VWbp can recognize both free and immobilized VWF, it could bind the adhesion protein at any presented opportunity. Transient sites of injury, with exposed endothelium, would be obvious targets of the procoagulant ProT·VWbp complex, and succeeding fibrin

formation and platelet activation would offer protection to the spreading pathogen. In turn, VWbp could also interact with the portion of VWF present in the plasma and be transported to distant sites in the vasculature, quickly setting up a base of fibrin for subsequent thrombus development. Once a favorable site is established, surface receptors on the bacteria would allow bacterial recognition and localization. This may be an important mechanism at low bacterial densities, because VWbp is secreted during the exponential growth phase. Besides the ability to initiate thrombus growth, VWbp is also able to affect the innate immune response through autocatalytic cleavage of the fragment domains of ProT·VWbp. Fragments 1 and 2 have been shown to stimulate the chemokine receptors on neutrophils, modulating migration of the cells (35). Release of the fragment domains could either desensitize the immune cells to other stimuli or induce chemotaxis, depending on the signaling microenvironment. Furthermore, it is important to note that the COOH-terminal half of VWbp contributes to both VWF recognition and ProT affinity, and this region seems to be quite sensitive to cleavage. Contact of VWbp with VWF could provide protection from proteolysis, stabilizing higher affinity interactions between ProT and VWbp and enhancing the procoagulant activity of the ProT·VWbp complex.

VWbp and Staphylococcal Pathology

There are a considerable number of pathologies which could be produced by an intravascular staphylococcal infection, ranging from minor vasculitis to severe hematogenous pneumonia. The expression of a plethora of staphylococcal proteins which recognize adhesion proteins underlines the importance of extracellular matrix in establishing and propagating bacterial colonization of the host. Vulnerable areas of the vasculature, such as congenitally dysfunctional heart valves or narrowed arteries with high shear flow rates, are susceptible targets for bacterial adhesion because of host

repair processes which rely on proteins such as fibrinogen and VWF to protect injured endothelium. Exogenous surfaces such as prosthetic heart valves and intravenous catheters are even more at risk for bacterial contamination, due to the propensity of adhesion proteins to adsorb to artificial surfaces.

The staphylococcal pathology most clearly associated with uncontrolled fibrin deposition is a condition called infective endocarditis. This often-fatal infection of the heart valves can be produced by many species of bacteria, but in recent years, staphylococcal species have become a predominant cause of endocarditis of normal heart valves (36, 37). Several steps are needed to support colonization of a heart valve, including disruption of the endothelial cell surface, association of bacteria with the activated surface, and protection of adherent bacteria to maintain propagation (38). Once a valve is colonized, a vegetative growth composed of fibrin, platelets, and bacteria progressively builds up on the surface, diminishing the function of the valve (Figure 2). The involvement of the coagulation cascade in this process is clear, and many species of pathogenic bacteria can sustain fibrin production through triggering the release of tissue factor from endothelial cells. Many of the staphylococcal exoproteins could play a role in the development of endocarditis through their adhesion protein interactions, but *S. aureus* is unique in that it can specifically produce thrombin-like activity through expression of VWbp and SC.

Based on its recognized interactions with ProT, fibrinogen, and VWF, VWbp is a likely candidate for involvement in the virulence of *S. aureus* infective endocarditis. Exposure of subendothelium would be common in areas of high shear stress, such as heart valves, along with transient deposition of VWF and platelets. As an ideal stage for VWbp activity, the injured endothelial surface of the heart valve could quickly become colonized by bacteria through fibrin deposition mediated by VWbp and, eventually, SC. The connection between procoagulant exoproteins and endocarditis had been previously

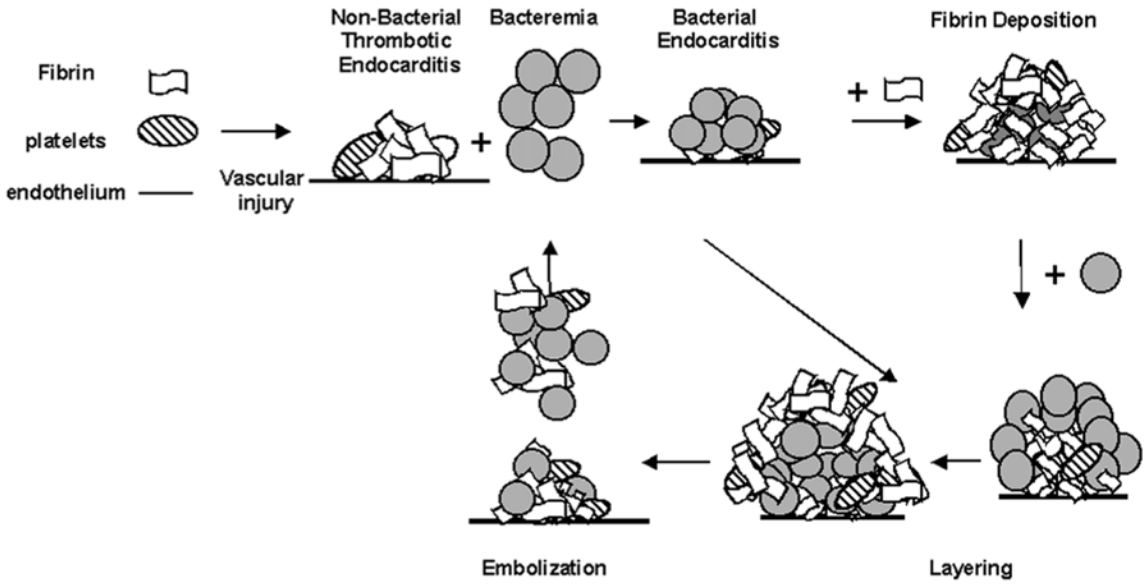

Figure 2. Development of vegetative growths during bacterial infective endocarditis. The presence of coagulase-positive *S. aureus* can exacerbate transient lesions on heart valves, leading to enhanced fibrin deposition and thrombus growth.

examined in several rat models of staphylococcal endocarditis, using *S. aureus* strains which had the SC gene specifically knocked out (39, 40). No clear correlation was found between expression of SC and disease progression, but these studies were performed before the gene for VWbp was identified. If the *S. aureus* strains used in these experiments still expressed a procoagulant protein like VWbp, a significant alteration in overall pathology may not be detected. The animal models also focused on relatively narrow windows during the progression of the disease, further limiting the conclusions of the studies.

As a new potential virulence factor for *S. aureus*, it is important to understand the contribution of VWbp to not only altered hemostatic function during an infection, but also bacterial localization and propagation throughout the time-course of the disease. With the increased prevalence of methicillin- and vancomycin-resistant strains of *S. aureus*, multiple therapeutic approaches will eventually be needed for effective treatment of

staphylococcal infections. Awareness of the synergistic roles between the myriad of proteins expressed by *S. aureus* is essential for the development of therapies targeted towards the molecular mechanisms involved in bacterial survival and dissemination.

References

1. Bode W & Huber R (1976) Induction of the bovine trypsinogen-trypsin transition by peptides sequentially similar to the N-terminus of trypsin. *FEBS Lett.* 68(2):231-236.

2. Friedrich R*, et al.* (2003) Staphylocoagulase is a prototype for the mechanism of cofactor-induced zymogen activation. *Nature* 425:535-539.

3. Wang S, Reed GL, & Hedstrom L (1999) Deletion of Ile1 changes the mechanism of streptokinase: Evidence for the molecular sexuality hypothesis. *Biochemistry* 38:5232-5240.

4. Boxrud PD & Bock PE (2004) Coupling of conformational and proteolytic activation in the kinetic mechanism of plasminogen activation by streptokinase. *J. Biol. Chem.* 279(35):36642-36649.

5. Kawabata S-I*, et al.* (1987) Structure and function relationship of staphylocoagulase. *J. Protein Chem.* 6(1):17-32.

6. Panizzi P, Friedrich R, Fuentes-Prior P, Bode W, & Bock PE (2004) The staphylocoagulase family of zymogen activator and adhesion proteins. *Cell. Mol. Life Sci.* 61:1-6.

7. Frieden C (1979) Slow transitions and hysteretic behavior in enzymes. *Annu. Rev. Biochem.* 48:471-489.

8. Adams TE & Huntington JA (2006) Thrombin-cofactor interactions: Structural insights into regulatory mechanisms. *Arterioscler. Thromb. Vasc. Biol.* 26:1738-1745.

9. Bock PE, Panizzi P, & Verhamme IMA (2007) Exosites in the substrate specificity of blood coagulation reactions. *J. Thromb. Haemost.* 5 (Suppl. 1):81-94.

10. Di Cera E (2008) Thrombin. *Mol. Aspects Med.* 29:203-254.

11. Papaconstantinou ME, Gandhi PS, Chen Z, Bah A, & Di Cera E (2008) Na^+ binding to meizothrombin desF1. *Cell. Mol. Life Sci.* 65(22):3688-3697.

12. Panizzi PR & Bock PE (2006) Identification and characterization of a sodium ion binding site on the staphylocoagulase-prothrombin complex. *Blood (ASH Annual Meeting Abstracts)* 108:Abstract 1700.

13. Eigenbrot C & Kirchhofer D (2002) New insight into how tissue factor allosterically regulates factor VIIa. *Trends Cardiovasc. Med.* 12:19-26.

14. Narayana SVL*, et al.* (1994) Structure of human factor D: A complement system protein at 2.0A resolution. *J. Mol. Biol.* 235:695-708.

15. Hauck CR & Ohlsen K (2006) Sticky connections: extracellular matrix protein recognition and integrin-mediated cellular invasion by *Staphylococcus aureus*. *Curr. Opin. Microbio.* 9:5-11.

16. Higgins J, Loughman A, van Kessel KPM, van Strijp JAG, & Foster TJ (2006) Clumping factor A of *Staphylococcus aureus* inhibits phagocytosis by human polymorphonuclear leucocytes. *FEMS Microbiol. Lett.* 258:290-296.

17. Sadler JE (1998) Biochemistry and genetics of von Willebrand factor. *Annu. Rev. Biochem.* 67:395-424.

18. Ribes JA, Francis CW, & Wagner DD (1987) Fibrin induces release of von Willebrand factor from endothelial cells. *J. Clin. Invest.* 79:117-123.

19. Ruggeri ZM (2001) Structure of von Willebrand factor and its function in platelet adhesion and thrombus formation. *Best Practice & Research Clinical Haematology* 14(2):357-379.

20. Ruggeri ZM (2003) Von Willebrand factor, platelets, and endothelial cell interactions. *J. Thromb. Haemost.* 1:1335-1342.

21. Fay PJ (2004) Activation of factor VIII and mechanisms of cofactor action. *Blood Reviews* 18:1-15.

22. Into T*, et al.* (2007) Pathogen recognition by Toll-like receptor 2 activates Weibel-Palade body exocytosis in human aortic endothelial cells. *J. Biol. Chem.* 282:8134-8141.

23. Kerrigan SW*, et al.* (2002) A role for glycoprotein Ib in *Streptococcus sanguis*-induced platelet aggregation. *Blood* 100:509-516.

24. McNicol A, Eyer E, Jackson EC, & Israels SJ (2007) A role for von Willebrand factor in *Streptococcus sanguis*-induced platelet activation. *Thromb. Haemostasis* 98:1382-1384.

25. Herrmann M*, et al.* (1997) Interaction of von Willebrand factor with *Staphylococcus aureus*. *J. Infect. Dis.* 176:984-991.

26. Hartleib J*, et al.* (2000) Protein A is the von Willebrand factor binding protein on *Staphylococcus aureus*. *Blood* 96:2149-2156.

27. George NPE, Wei Q, Shin PK, Konstantopoulos K, & Ross JM (2006) *Staphylococcus aureus* adhesion via Spa, ClfA, and SdrCDE to immobilized platelets demonstrates shear-dependent behavior. *Arterioscler. Thromb. Vasc. Biol.* 26:2394-2400.

28. George NPE, Konstantopoulos K, & Ross JM (2007) Differential kinetics and molecular recognition mechanisms involved in early versus late growth phase *Staphylococcus aureus* cell binding to platelet layers under physiological shear conditions. *J. Infect. Dis.* 196:639-646.

29. Shenkman B*, et al.* (2001) Adherence properties of *Staphylococcus aureus* under static and flow conditions: Roles of *agr* and *sar* loci, platelets, and plasma ligands. *Infect. Immun.* 69(7):4473-4478.

30. Sadler JE (1991) von Willebrand Factor. *J. Biol. Chem.* 266(34):22777-22780.

31. O'Seaghdha MN*, et al.* (2006) *Staphylococcus aureus* protein A binding to von Willebrand factor A1 domain is mediated by conserved IgG binding regions. *FEBS J.* 273:4831-4841.

32. Nilsson M*, et al.* (2004) A von Willebrand factor-binding protein from *Staphylococcus lugdunensis*. *FEMS Microbiol. Lett.* 234:155-161.

33. Bjerketorp J*, et al.* (2002) A novel von Willebrand factor binding protein expressed by *Staphylococcus aureus*. *Microbiology* 148:2037-2044.

34. Foster TJ (2005) Immune evasion by staphylococci. *Nature Reviews Microbiology* 3:948-958.

35. Mariano-Oliveira A, De Freitas MS, Monteiro RQ, & Barja-Fidalgo C (2008) Prothrombin fragments containing kringle domains induce migration and activation of human neutrophils. *Int. J. Biochem. Cell Biol.* 40:517-529.

36. Becker RC, DiBello PM, & Lucas FV (1987) Bacterial tissue tropism: an in vitro model for infective endocarditis. *Cardiovasc. Res.* 21:813-820.

37. Mylonakis E & Calderwood SB (2001) Infective endocarditis in adults. *N. Engl. J. Med.* 345(18):1318-1330.

38. Sullam PM, Drake TA, & Sande MA (1985) Pathogenesis of endocarditis. *Am. J. Med.* 78 (suppl 6B):110-115.

39. Baddour LM, Tayidi MM, Walker E, McDevitt D, & Foster TJ (1994) Virulence of coagulase-deficient mutants of *Staphylococcus aureus* in experimental endocarditis. *J. Med. Microbiol.* 41:259-263.

40. Moreillon P*, et al.* (1995) Role of *Staphylococcus aureus* coagulase and clumping factor in pathogenesis of experimental endocarditis. *Infect. Immun.* 63(12):4738-4743.